

---

[All ETDs from UAB](#)

[UAB Theses & Dissertations](#)

---

2020

## Deficiency Of Tumor Suppressor Merlin Induces Metabolic Reprogramming In Breast Cancer

Mateus Mota

*University of Alabama at Birmingham*

Follow this and additional works at: <https://digitalcommons.library.uab.edu/etd-collection>



Part of the [Medical Sciences Commons](#)

---

### Recommended Citation

Mota, Mateus, "Deficiency Of Tumor Suppressor Merlin Induces Metabolic Reprogramming In Breast Cancer" (2020). *All ETDs from UAB*. 867.

<https://digitalcommons.library.uab.edu/etd-collection/867>

This content has been accepted for inclusion by an authorized administrator of the UAB Digital Commons, and is provided as a free open access item. All inquiries regarding this item or the UAB Digital Commons should be directed to the [UAB Libraries Office of Scholarly Communication](#).

DEFICIENCY OF TUMOR SUPPRESSOR MERLIN INDUCES METABOLIC  
REPROGRAMMING IN BREAST CANCER

by

MATEUS S.V. MOTA

LALITA SHEVDE-SAMANT  
JOANNE MURPHY-ULLRICH  
RAJEEV SAMANT  
RALPH SANDERSON  
SUNIL SUDARSHAN

A DISSERTATION

Submitted to the graduate faculty of The University of Alabama at Birmingham,  
in partial fulfillment of the requirements for the degree of  
Doctor of Philosophy

BIRMINGHAM, ALABAMA

2020

Copyright by  
Mateus S. V. Mota  
2020

# DEFICIENCY OF TUMOR SUPPRESSOR MERLIN INDUCES METABOLIC REPROGRAMMING IN BREAST CANCER

MATEUS S. V. MOTA

GRADUATE BIOMEDICAL SCIENCES: CANCER BIOLOGY

## ABSTRACT

The tumor suppressor Merlin is encoded by Neurofibromin 2 (*NF2*) gene. Merlin is predominantly located in the cell cortex where regulates cell proliferation by mediating cell contact-dependent growth inhibition. Metastatic breast cancer tissues presented with a remarkable loss of Merlin protein, revealing clinical relevance of Merlin. In order to examine the cellular effect of Merlin deficiency, breast cancer cell lines were silenced for *NF2*. Additionally, to assess the impact of Merlin loss at the organismal level, a mammary-specific *NF2* knockout mouse mammary tumor model was engineered. Merlin deficiency induced a metabolic shift from mitochondrial oxidative phosphorylation to aerobic glycolysis. Furthermore, Merlin deficiency resulted in accumulation of reactive oxygen species (ROS) as a consequence of defective redox management and increased expression of ROS-producing enzymes. These two outcomes of Merlin deficiency in breast cancer cells yield novel insight into Merlin's functions beyond its recognized role in halting cell proliferation through abolishing mitogenic pathways. Mechanistically, the research demonstrates how Merlin deficiency compromises redox homeostasis and alters cellular bioenergetics in breast cancer. This expands the knowledge about Merlin functions as a tumor suppressor and contributes to the identification of potential therapeutic targets to overcome aberrant behaviors enhanced by Merlin deficiency.

Keywords: Merlin, cancer, glycolysis, STAT3, Nrf2, NOX

## DEDICATION

I dedicate this dissertation to my parents Cristina and Ednilson Mota. They didn't have the opportunity to go to college but have paved the way so their son could get the highest academic degree. I will forever be grateful for the unconditional support both of you have provided throughout the years. This achievement is OURS! Thank you!

## ACKNOWLEDGEMENTS

Pursuing a career in science is definitely not an easy task; however, this journey becomes less burdensome when we are surrounded by colleagues that uplift us. And I can say I have met the best people for my PhD training. I would like to start by thanking Dr. Lalita Shevde-Samant for her effective mentorship. I have grown so much professionally in these past five years and your guidance has undoubtedly shaped my skills and made me understand what is expected from a scientist.

I also thank the committee members, Dr. Joanne Murphy-Ullrich, Dr. Rajeev Samant, Dr. Ralph Sanderson, and Dr. Sunil Sudarshan for their invaluable advices. I definitely had a very challenging dissertation committee and this has made me more confident and prepared for the next step in my career.

As we spend so much time in the laboratory, our lab mates represent a big part of this training. You guys made this sometime arduous, difficult process into a more enjoyable and positive moment. I would like to specially extend my appreciation to Brandon Metge for being always willing to help and dedicate his time. You are a co-mentor to all of us !

Last but not least, thank you to the UAB community for being my home in these past 5 years !

## TABLE OF CONTENTS

	<i>Page</i>
ABSTRACT .....	iii
DEDICATION .....	v
ACKNOWLEDGMENTS .....	vi
LIST OF TABLES .....	ix
LIST OF FIGURES .....	x
INTRODUCTION .....	1
Neurofibromin 2 ( <i>NF2</i> ) gene and Merlin protein .....	1
Molecular structure .....	1
Role as a tumor suppressor .....	2
Transcriptional regulation of <i>NF2</i> .....	3
Translational regulation of Merlin .....	4
Molecular implications of <i>NF2</i> /Merlin deficiency .....	5
Effect of Merlin deficiency in cancer .....	6
Mesothelioma.....	7
Brain cancer .....	8
Thyroid cancer .....	9
Colorectal cancer .....	9
Liver cancer .....	10
Pancreatic cancer .....	11
Melanoma .....	12



Merlin and breast cancer .....	12
Proteasomal degradation of Merlin.....	12
Induction of WNT signaling in Merlin-deficient breast cancer cells .....	14
Merlin and the hallmarks of cancer .....	15
From cell proliferation to metastasis .....	15
Cancer metabolism.....	17
Aerobic glycolysis .....	17
Glutamine addiction.....	19
Redox imbalance.....	20
Metabolic impact of Merlin deficiency in breast cancer .....	22
MERLIN REGULATES SIGNALING EVENTS AT THE NEXUS OF DEVELOPMENT AND CANCER .....	23
DEFICIENCY OF TUMOR SUPPRESSOR MERLIN FACILITATES METABOLIC ADAPTATION BY CO-OPERATIVE ENGAGEMENT OF SMAD-HIPPO SIGNALING IN BREAST CANCER .....	50
MERLIN DEFICIENCY ALTERS THE REDOX MANAGEMENT PROGRAM IN BREAST CANCER .....	84
DISCUSSION .....	118
FUTURE DIRECTIONS .....	124
LIST OF REFERENCES .....	129
APPENDICES .....	137
A: DEFICIENCY OF TUMOR SUPPRESSOR MERLIN FACILITATES METABOLIC ADAPTATION BY CO-OPERATIVE ENGAGEMENT OF SMAD-HIPPO SIGNALING IN BREAST CANCER - Supplementary material .....	137
B: MERLIN DEFICIENCY ALTERS THE REDOX MANAGEMENT PROGRAM IN BREAST CANCER - Supplementary material .....	141
C: Extended animal material and methods .....	146
D: Institutional Animal Care and Use Committee (IACUC) notice of approval.	154
E: Reprints approval forms .....	156

LIST OF TABLE

<i>Table</i>	<i>Page</i>
1. Effect of Merlin deficiency in cancer .....	6

## LIST OF FIGURES

<i>Figure</i>	<i>Page</i>
1. Molecular structure of Merlin.....	1
2. Role as a tumor suppressor .....	3
3. Proteasomal degradation of Merlin in breast cancer.....	14
4. Merlin and the hallmarks of cancer .....	15
5. STAT3 signaling upregulates the expression of NADPH oxidase enzymes in Merlin-deficient cells .....	121
6. Inhibition of TGF- $\beta$ reduces NADPH oxidase expression .....	125
7. Merlin-deficient breast cancer cells have increased 18-FDG uptake .....	126
MERLIN REGULATES SIGNALING EVENTS AT THE NEXUS OF DEVELOPMENT AND CANCER	
1. Merlin regulates different developmental signaling pathways .....	48
2. Merlin depletion negatively impacts embryonic development and tissue maintenance .....	49
DEFICIENCY OF TUMOR SUPPRESSOR MERLIN FACILITATES METABOLIC ADAPTATION BY CO-OPERATIVE ENGAGEMENT OF SMAD-HIPPO SIGNALING IN BREAST CANCER	
1. Loss of Merlin is concordant with the loss of SMAD7 in breast cancer .....	77
2. Merlin deficiency leads to the co-operative activation of YAP/TAZ/SMAD signaling.....	79
3. Loss of Merlin induces bioenergetics alterations in breast cancer cells .....	80
4. Merlin keeps a check on cellular metabolism and glycolysis mediators .....	81

5. UCA1 directs cell metabolism towards aerobic glycolysis through AKT and STAT3 activation in Merlin-deficient cells .....82

6. STAT3 inhibition preferentially impacts Merlin-deficient cells .....83

**MERLIN DEFICIENCY ALTERS THE REDOX MANAGEMENT PROGRAM IN BREAST CANCER**

1. Merlin deficiency modulates a redox signaling signature .....113

2. ROS clearance attenuates migratory and invasion phenotypes in NF2-deficient cells .....114

3. Merlin-deficient breast cancer cells display a dysfunctional anti-oxidant system .....115

4. Merlin deficiency upregulates proteins from the pro-oxidative NOX family .....116

5. Genetically-engineered oncogene-driven Merlin deficient mammary tumors harbor elevated oxidative stress .....117

## INTRODUCTION

### NEUROFIBROMIN 2 (*NF2*) GENE AND MERLIN PROTEIN

#### Molecular structure

The human Neurofibromin 2 (*NF2*) gene is located on chromosome 22 and contains 17 exons. *NF2* encodes a 70-kDa protein that has over 50% sequence homology with the cytoskeletal Ezrin/Radixin/Moesin (ERM) protein family and is therefore named **Moesin-Ezrin-Radixin-Like Protein (Merlin)**. Alternative splicing of *NF2* mRNA generates a number of Merlin isoforms with isoform 1 (595 amino acids), being the most predominant. Merlin's protein structure comprises the N-terminal,  $\alpha$ -helix and C-terminal domains (1, 2). The phosphorylation sites at Serine 10 (Ser10), Threonine 230 (Thr230), Serine 315 (Ser315), and Serine 518 (Ser518) determine stability and activation of Merlin. Like many cytoskeleton-associated proteins, Merlin's N-terminal region has a specific domain, referred as **Four-point one, ERM (FERM)**, responsible for its binding to the cytoplasmic portion of transmembrane receptors (Fig. 1). While the C-terminal domain in most FERM-containing proteins binds to the actin cytoskeleton, Merlin's interaction with actin is mediated by the N-terminal FERM domain (1, 2).

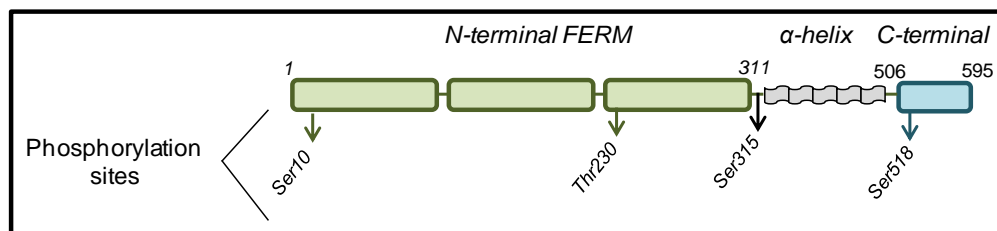


**Figure 1: Molecular structure of Merlin.** Merlin comprises an N-terminal FERM,  $\alpha$ -helix, and C-terminal domains. With 595 amino acids, the phosphorylation sites at Threonine 230 (Thr230), Serine 315 (Ser315), and Serine 518 (Ser518) are crucial for Merlin's activation and protein stability.

### **Role as a tumor suppressor**

Merlin is mainly localized to the cell cortex where it conveys extracellular inputs to ultimately modulate cellular behaviors. Merlin has a very dynamic protein conformation that is determined by the phosphorylation status of its Ser518 residue in the C-terminal domain. This is directly related to Merlin's tumor suppressor role in inducing contact-dependent growth inhibition. In high cell density conditions, there is increased cadherin-associated cell-cell adhesion that inhibits p21-activated kinase (PAK). In addition, there is accumulation of hyaluronic acid, a component of the extracellular matrix, which binds to CD44 receptors and activates MYPT1 phosphatase. These events dephosphorylate Merlin's Ser518 residue, resulting in the close physical proximity of the N-terminal FERM and C-terminal domains based on ERM protein analogy. In this closed, active structure, Merlin downregulates the activity of classical mitogenic signaling, including Rho GTPases, mTOR, EGFR, PDGFR and PI3K/AKT, and concomitantly activates the Hippo tumor suppressor pathway. Additionally, Merlin is also present in the nucleus where it hinders the binding between DCAF1 substrate adaptor and CRL4 ubiquitin ligase (CRL4<sup>DCAF1</sup>) (1-3), known for inducing the activation of oncogenic transcription factors by ubiquitinating chromatin-associated factors, such as histones and transcription coactivators (Fig. 2A). The restraint of these combined events result in growth arrest and regulates cell proliferation.

On the other hand, proliferative cues, such as integrins and receptor tyrosine kinases, activate Rho GTPases Cdc42 and Rac, that in turn, activate PAK. Along with cyclic AMP-protein kinase A (PKA), PAK phosphorylates the Ser518 residue, hindering the binding between the N-terminal FERM and C-terminal domains and giving Merlin an open structure (Fig. 2B) (1-3). In this new conformation Merlin loses its capacity to downregulate mitogenic signals and to activate Hippo pathway, thereby failing to induce contact-dependent growth inhibition.

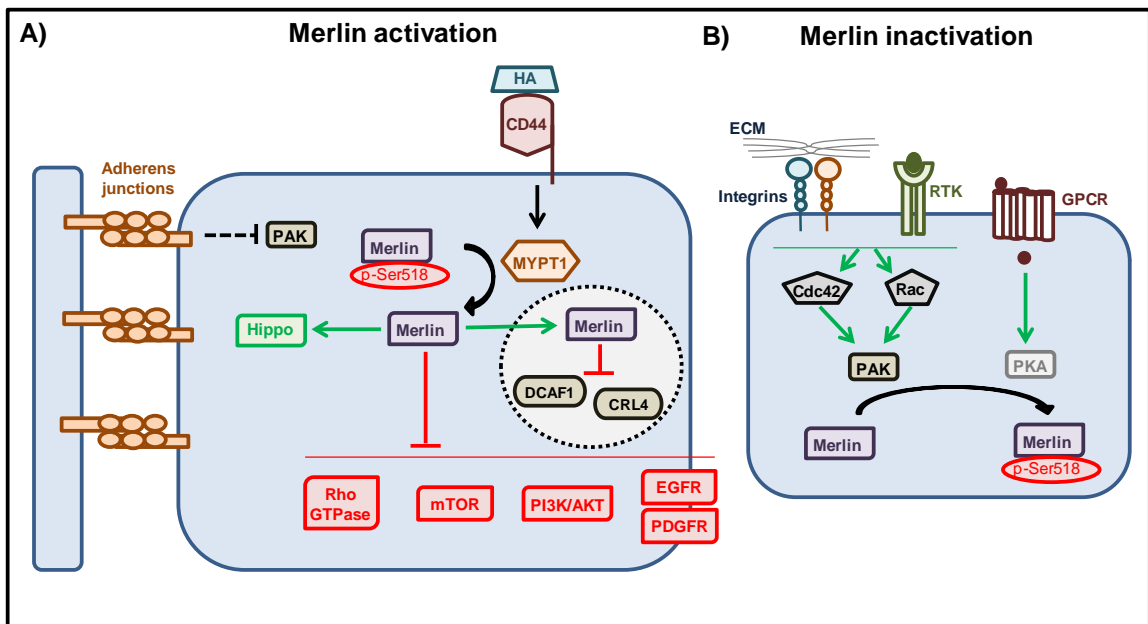


**Figure 2: Role as a tumor suppressor.** (A) Dephosphorylation of Ser518 by MYPT1 phosphatase and inhibited PAK activates Merlin. This results in the activation of Hippo pathway and repression of mitogenic pathways, such as Rho GTPase, mTOR, PI3K/AKT, EGFR, PDGFR, and CRL4<sup>DCAF1</sup>; (B) Under proliferation condition, Merlin is inactivated by phosphorylation of Ser518 mediated by PAK and PKA.

### Transcriptional regulation of *NF2*

The expression of *NF2* gene is transcriptionally downregulated by loss of heterozygosity (LOH), characterized by frequent deletion of the chromosomal region

22q12, locus of *NF2* gene. In addition, point mutations, such as frameshift and nonsense, are the most common inactivation mechanisms of *NF2*. These mutations result in the insertion of a premature stop codon and generation of a truncated, non-functional version of Merlin protein (4-6). *NF2* can also be posttranscriptionally inactivated as a result of gene splicing, such as in the splice variant lacking exons 2, 3, and 4. These exons form the N-terminal region of Merlin and their absence negatively affects the integrity of the FERM domain. Thus, this FERM-defective Merlin isoform is unable to exert its tumor suppressor function (7).

Interestingly, some tumors do not harbor detectable genetic *NF2* alteration or LOH events. It is now known that *NF2* can be silenced by epigenetic modification, such as methylation, revealing an alternative mechanism of inactivation of *NF2* (5). For instance, increased DNA methyltransferase 1 (DNMT1) expression hypermethylates and silences *NF2* (8). Additionally, microRNAs (miR) contribute to epigenetic silencing of *NF2*. MiRs are small, non-coding RNAs that bind to and mainly destroy messenger RNA (mRNA), silencing its respective gene expression (9). Functional luciferase assay showed that miR-146b-p3 directly targets the 3'-UTR of *NF2*, causing posttranscriptional inactivation of *NF2* (10). Overall, silencing of *NF2* is mediated by both, genetic and epigenetic modifications.

### **Translational regulation of Merlin**

Studies have found that *NF2* transcript is either not altered or, its alteration is not the only cause leading to malfunction of Merlin in many pathological conditions. This likely indicates a regulation at the protein level of Merlin. For instance, the oncogene protein kinase C-potentiated phosphatase inhibitor-17 kDa (CPI-17) is a phosphatase



inhibitor that inhibits MYPT phosphatase that contributes to Merlin's Ser518 dephosphorylation and activation. CPI-17 levels are significantly increased in many cancers with normal *NF2* (11). Therefore, although the expression of *NF2* and levels of Merlin are not altered in such cases, Ser518 phosphorylation of Merlin due to increased CPI-17 curbs the tumor suppressor function of Merlin. In addition, constitutive activation of PAK is another mechanism that contributes to extensive phosphorylation of Merlin's Ser518 residue, leading to Merlin inactivation regardless of normal gene expression and protein levels. Indeed, the inhibition of PAK reduces such phosphorylation pressure upon Merlin (12). In all, regulation at the post-translational level also affects the activation and tumor suppressor function of Merlin.

### **MOLECULAR IMPLICATIONS OF *NF2*/MERLIN DEFICIENCY**

Tissue homeostasis requires a well-coordinated program involving cell proliferation and growth arrest. As a critical mediator in inhibiting cell proliferation due to cell:cell contact, Merlin acts as classical tumor suppressor abolishing tissue overgrowth (1-3, 13). Notably, *in vivo* studies with mice harboring total loss of *NF2* showed that lack of *NF2* is lethal at embryonic day 7 (E7) (14). This observation has instigated the analysis of the role of Merlin in regulating developmental signaling pathways which are also dysregulated in diseases marked by aberrant cell proliferation such as cancer. In the published review "Merlin regulates signaling events at the nexus of development and cancer" of my authorship, I discuss the role of Merlin in impacting classical developmental- and cancer-associated pathways, including the Hippo, WNT/ $\beta$ -catenin, TGF- $\beta$ , receptor tyrosine kinase (RTK), Notch, and Hedgehog signaling pathways.

## EFFECT OF MERLIN DEFICIENCY IN CANCER

Many investigations have demonstrated how deficiency of *NF2*/Merlin promotes the onset and progression of many diseases. Neurofibromatosis type 2, a benign tumor condition in the nervous system, was the first pathological condition to be associated with alterations of *NF2*/Merlin (4, 5). However, lack of functional *NF2*/Merlin was also detected in malignant mesothelioma (6, 15, 16) which sparked investigations on other types of cancer. It is now recognized that the establishment and progression of brain (8, 17, 18), thyroid (10, 19), colorectal (20), liver (7, 21), pancreatic (22), melanoma (23), and breast (24-26) cancers are also promoted by dysfunctional *NF2*/Merlin (Table 1). The deficiency of *NF2*/Merlin triggers activation of several mechanisms that enhance malignant attributes and promote tumor survival.

CANCER TYPE	EFFECT
<b>Mesothelioma</b>	<i>Elevation of PAK-dependent cyclin D1 expression</i> <i>Upregulation of FAK activity</i>
<b>Brain</b>	<i>Promotion of STAT3 signaling by the YAP/TEAD2/miR-296-3p node</i> <i>Upregulation of cIAP1/2 caspase inhibitor and cyclin E anti apoptotic protein</i> <i>Upregulation of WNT signaling</i>
<b>Thyroid</b>	<i>Upregulation of YAP/TAZ-induced mutant Ras</i> <i>Activation of Rac1-PAK1 signaling</i> <i>Promotion of MAPK/ERK signaling</i>
<b>Colorectal</b>	<i>Increase of WNT and EGFR signaling</i>
<b>Liver</b>	<i>Increase of WNT and EGFR signaling</i> <i>Activation of stemness-related genes</i>
<b>Pancreatic</b>	<i>Activation of FOXM1-WNT signaling</i>
<b>Melanoma</b>	<i>Inactivation of Hippo pathway</i>

**Table 1: Effect of Merlin deficiency in cancer**

## Mesothelioma

Mesothelioma is a type of cancer of the lining of the abdomen, heart, and lungs, with the latter being the most common, mainly caused by exposure to asbestos fibers. Mesothelioma is the most studied type of cancer regarding *NF2*/Merlin alterations with at least 40% of patients harboring loss of chromosome 22q12 region or *NF2* point mutations (5, 6). The high proliferation characteristic of mesothelioma is attributed in part due to elevated PAK-dependent expression of cyclin D1 that promotes CDK4 kinase activity and entry into S phase. Reexpression of Merlin in mesothelioma cells repressed PAK activity and consequently inhibited cyclin D1 expression. This blocked cell proliferation by arresting mesothelioma cells at G1 phase (16).

Mesothelioma is a rapidly progressive malignancy due to its elevated tumor cell migration and invasion abilities. The cytoplasmic enzyme focal adhesion kinase (FAK) is involved in cell adhesion, promotes migration and invasion, and is upregulated in many cancers, including mesothelioma. Merlin negatively regulates FAK activity by hindering its phosphorylation and compromising its catalytic activity. Merlin may inhibit FAK phosphorylation by forming an inhibitory complex mediated by NHERF (Na<sup>+</sup>/H<sup>+</sup> exchanger regulatory factor), a protein adapter, common to both, Merlin and FAK. It is also possible that Merlin negatively regulates Rho GTPase/PAK-dependent FAK activity (27). Since Merlin is deficient in mesothelioma, the regulation of FAK is also compromised. Indeed, *in vitro* studies showed that restoration of Merlin in mesothelioma cell lines diminished FAK phosphorylation and reduced cell motility and invasiveness (27). Moreover, the identification of FAK upregulation in light of Merlin deficiency in mesothelioma opens new venues for therapeutic strategies. For instance, pleural

mesothelioma with low Merlin expression is more sensitive to FAK inhibitors both in *in vitro* and *in vivo* systems (28).

### **Brain cancer**

Expression of *NF2* and levels of Merlin were decreased in high-grade gliomas. This resulted in overproliferation and inhibition of apoptosis of glioma cell lines and increased subcutaneous and intracranial growth of human Merlin-deficient glioma cells in a xenograft mouse model. Reexpression of Merlin weakened all these malignant behaviors (17).

As in Neurofibromatosis type 2 disorder, epigenetic modifications also contribute to *NF2* silencing in brain cancer. MiRs can have a tumor promoter role in cancer biology (9) and this function in relation to Merlin status is also demonstrated in gliomas. Merlin activates the Mst1/2-LATS1/2 kinase cascade of the Hippo pathway, resulting in the phosphorylation of YAP/TAZ transcription co-activator and its retention in the cytoplasm for degradation. When this phosphorylation mark fails, YAP/TAZ translocates to the nucleus where it forms a transcriptional complex with its DNA-binding partner TEAD, and activates tumor-promoting targets (3). Malfunction of Hippo signaling due to lack of Merlin enables YAP/TEAD2 to induce the expression of miR-296-3p in glioblastoma (GBM) cells. MiR-296-3p silences *STAT5* expression and disengages its inhibitory phosphorylation and activation control on STAT3. Therefore, STAT3 oncogene addiction (29), known for contributing to invasion of many tumors, is promoted via the YAP/TEAD2/miR-296-3p node in Merlin-deficient GBM cells (18). Lau et al. 2008 have also shown that YAP/TAZ activates the expression of cIAP1/2 caspase inhibitor and

cyclin E anti-apoptotic protein in GBM, inhibiting apoptosis and promoting tumor growth (17).

Furthermore, WNT signaling is also enhanced in Merlin-deficient glioma cells and contributes to cell survival and tumor growth. Restoration of Merlin was able to suppress the WNT pathway by downregulating the expression of FZD1 receptor, required for the initiation of WNT signaling, while concomitantly upregulating the expression of DKK1/3, a negative WNT regulator (17). In conclusion, unrestrained signaling of both YAP/TAZ and WNT pathways contribute to increased growth and progression of Merlin-deficient, high-grade glioma cells.

### **Thyroid cancer**

The lack of normal Merlin function disrupts the Hippo pathway's restraint on YAP, that in turn induces the expression of mutant Ras in thyroid cancer. Defective Merlin also results in the activation of Rac1 GTPase, which in turn activates PAK1. Mutant Ras and Rac1-PAK1 signaling phosphorylate and activate c-RAF and MEK effectors, enhancing ERK transcriptional activity. Therefore, loss of Merlin has a profound positive effect on activation of the MAPK/ERK pathway in thyroid cancer by failing to restrain mutant Ras activation and inhibit Rac1-PAK1 through YAP/TEAD suppression (19).

### **Colorectal cancer**

Inactivation of *NF2* was seen in 20% of cases of sporadic colorectal cancer. These tumors showed high histological grade and were larger than five centimeters in size, suggesting low Merlin levels as an unfavorable prognostic factor in colorectal cancer. WNT and EGFR signaling are enhanced in colorectal cancer and Merlin loss likely

contributes to activation of these pathways (20). Following WNT activation, phosphorylation of specific sites in cytoplasmic  $\beta$ -catenin drives its translocation to the nucleus. This process is facilitated by the Rac1-JNK2 axis that phosphorylates  $\beta$ -catenin on Ser191 and Ser605. Mutation of both phosphorylation sites significantly reduces nuclear  $\beta$ -cate accumulation, reflecting their importance for the WNT signaling (30). Considering that Merlin inhibits Rac1 (3), increased activation of WNT targets in *NF2*-inactivated colorectal cancer cells may be the result of sustained Rac1-JNK2-induced phosphorylation of  $\beta$ -catenin.

One of the intracellular responses of Merlin to extracellular conditions is to limit the availability of receptor tyrosine kinase (RTK). Merlin plays a role in the reorganization of cell membrane domains that compartmentalizes RTKs into endosomes for lysosomal degradation or recycling, downregulating RTK signaling (31). Therefore, lack of Merlin is likely contributing to elevated EGFR signaling in colorectal cancer cells that, in cooperation with unchecked WNT signaling, is potentially driving tumor dedifferentiation and growth in Merlin-deficient colorectal cancer.

### **Liver cancer**

*Nf2* inactivation in differentiated hepatocytes was not sufficient to derail proliferation and cause cancer. However, all mice carrying *NF2* deletion in the liver progenitor compartment showed abnormal bile duct cells and hepatocytes, developing cholangiocellular and hepatocellular carcinoma, respectively. This indicates an early function of *NF2*/Merlin in liver organogenesis resulting in long-term cancer. Further investigations identified increased EGFR signaling in *NF2*-deficient liver progenitor

cells; and pharmacological inhibition of EGFR signaling was able to diminish aberrant proliferation (21).

A dysfunctional isoform of Merlin with defective FERM domain was detected in liver cancer. This isoform was identified to lose its ability to bind to ERM proteins and  $\beta$ -catenin on the inner side of the cell membrane, becoming predominantly located in the cytoplasm (7). This results in loss of regulation of ERM proteins, and subsequent WNT-dependent tumor proliferation and CD44- and Rac1- induced migration (32, 33). Moreover, the expression of many stemness-related genes, including SOX2, OCT4, KIF4, c-Myc, and Nanog, was upregulated in liver cancer cells containing this FERM-defective isoform of Merlin. These events cumulatively caused uncontrolled cell migration and invasion, facilitating pulmonary metastases in mouse models of liver cancer (7).

### **Pancreatic cancer**

Defective Merlin function in PDAC also contributes to the overactivation of WNT/ $\beta$ -catenin (22). Activation of WNT signaling disassembles the  $\beta$ -catenin destruction complex. This stabilizes cytoplasmic  $\beta$ -catenin that translocates to the nucleus. The FOXM1 transcription factor was reported to directly bind to cytoplasmic  $\beta$ -catenin and facilitate its nuclear transport and activation of target genes (34). Merlin negatively regulates levels of FOXM1 by promoting its ubiquitination and degradation, hindering the traffic of  $\beta$ -catenin into the nucleus. Therefore, in *NF2*-inactivated PDAC, the FOXM1/ $\beta$ -catenin node is a promising therapeutic target to inhibit aberrantly activated WNT signaling and consequently limit the development and progression of PDAC (22).

## **Melanoma**

Merlin deficiency in melanoma illustrates the basic concept of Merlin activating the Hippo pathway and controlling cell proliferation. Deficiency of Merlin leads to upregulated proliferation, migration, and invasion of melanoma cells. In addition, these attributes are observed in immunocompromised xenograft models where Merlin-deficient melanoma cells exhibit a high rate of subcutaneous growth. It is proposed that the activation of MST1/2, the first kinase of the Hippo cascade, is compromised due to inadequate Merlin function. This results in deficient Hippo signaling and uncontrolled cell proliferation in melanoma (23).

## **MERLIN AND BREAST CANCER**

### **Proteasomal degradation of Merlin**

The first investigations of *NF2* in breast cancer dates back to the 90's. These early studies did not find significant alterations in *NF2*, such as inactivating mutations or chromosomal deletion of 22q12 (35, 36). Therefore, it was concluded that *NF2* did not play a role in the development of breast malignancy which discouraged further investigations. However, we now know that malignant tissues with normal expression of *NF2* can be epigenetically silenced by methylation (5, 8). In addition, posttranslational modifications, such as constitutive Ser518 phosphorylation, inactivate Merlin function (11, 12).

In agreement with previous investigations, a recent study by our laboratory did not detect defective expression of *NF2* transcript in tissue samples from a cohort of 75 invasive breast cancer patients compared with normal breast tissue. However, a



significant decrease in the levels of Merlin protein was seen in 75% of cases by IHC staining, suggesting posttranslational degradation of Merlin. Notably, this reduction was increasingly more prominent as cases were stratified from grade I to grade III. Additionally, levels of Merlin were not detected in a separate group of metastatic breast cancer samples, indicating a negative correlation between levels of Merlin and advanced breast cancer (24).

In order to mimic the loss of Merlin *in vitro* for further investigation of cellular and molecular implications supporting breast cancer, *NF2* was silenced in Merlin-expressing non-metastatic breast cancer cell lines. These engineered Merlin-deficient cells showed increased motility, migration, and invasion abilities. Moreover, these cells had higher proliferation rates and rapid tumor growth in a xenograft mouse model. In contrast, restoration of Merlin dampened malignant behavior of a highly aggressive and metastatic breast cancer cell line (24). Overall, these analyses suggest Merlin functions as more than just relevant tumor suppressor that reduces the aggressiveness of breast cancer.

Further studies found that elevated AKT signaling induced by osteopontin, a secreted phosphoglycoprotein highly expressed in advanced breast cancer, caused Merlin elimination in breast cancer. As a kinase, AKT directly phosphorylates Merlin on threonine 230 and serine 315 residues. These phosphorylation events block the interaction between the N-terminal FERM and C-terminal domains, inhibiting the tumor suppressor function of Merlin. In addition to these post-translational modifications, Merlin is ubiquitinated and undergoes proteasomal degradation (Fig. 3). Thus, elevated OPN expressed by breast cancer cells directs post-translational modifications on Merlin, leading to its elimination (24). In conclusion, this study confirmed (i) lack of alteration of

*NF2* transcripts and (ii) uncovered a posttranslational mechanism that leads to Merlin degradation in breast cancer.

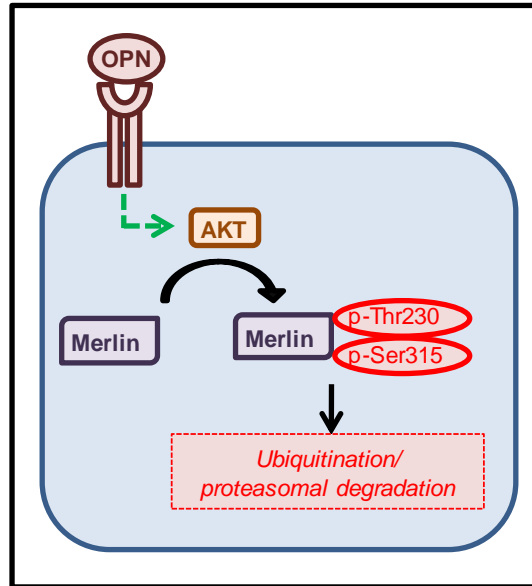


**Figure 3: Proteasomal degradation of Merlin in breast cancer.** Merlin's Thr230 and Ser315 sites are phosphorylated by OPN-induced AKT signaling. This compromises the association between the N-terminal FERM and C-terminal domains and destabilize Merlin that undergoes ubiquitin-proteasome degradation.

### Induction of WNT signaling in Merlin-deficient breast cancer cells

Membrane-bound  $\beta$ -catenin associates with  $\alpha$ -catenin and E-cadherin, forming adherens junctions. The formation of cell adherens junctions is crucial for the cell contact-growth inhibition by Merlin. Analysis by co-immunoprecipitation shows that Merlin physically interacts with  $\beta$ -catenin, the WNT pathway effector, and restricts its localization to the cell membrane. Thus, Merlin controls the availability of free cytoplasmic  $\beta$ -catenin that otherwise would be directed to the nucleus to activate WNT targets involved in stemness, tumor progression, and survival (25).

## MERLIN AND THE HALLMARKS OF CANCER

The hallmarks of cancer are a set of characteristics acquired during malignant transformation that enable cells to overproliferate and ultimately metastasize (37). After reviewing the deleterious impact of Merlin deficiency from being lethal in *NF2*-deleted embryonic stages to its impact on tumor formation and progression in differentiated tissues, Merlin is undoubtedly implicated in many malignant behaviors (Fig. 4).

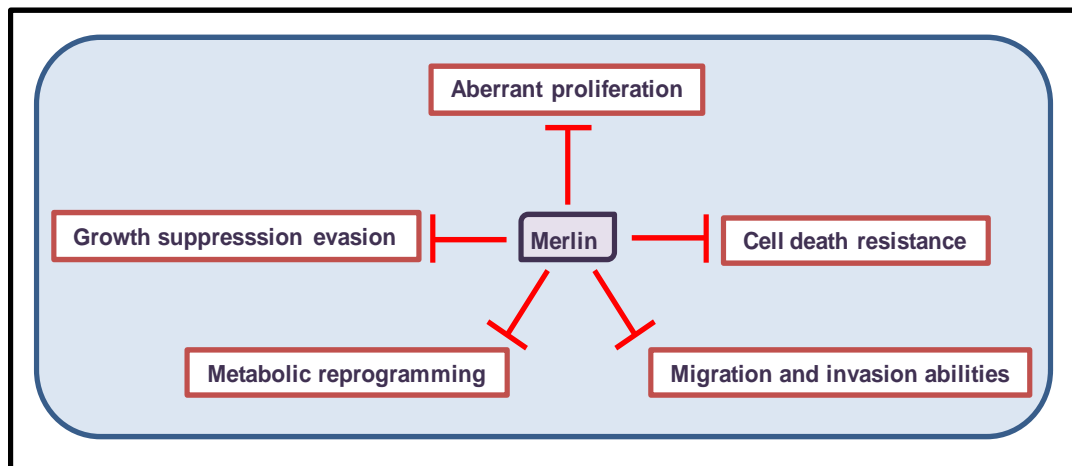


**Figure 4: Merlin and the hallmarks of cancer.** Merlin regulates many hallmarks of cancer, including aberrant proliferation, growth suppression evasion, cell death resistance, migration and invasion abilities and metabolic reprogramming.

### From cell proliferation to metastasis

Merlin stops aberrant proliferation, the first hallmark of cancer, by activating the Hippo pathway and inhibiting the activity of PDGF and EGF receptors for example (2, 3, 37). Thus, deficiency of Merlin already equips cells with the basic trait required for tumor formation. At the same time, this can be interpreted as Merlin-deficient cells becoming unresponsive to growth suppression mechanisms (37), once Merlin-associated contact-growth inhibition is lost.

Malignant cells also develop resistance to cell death. Enhanced signaling of the PI3K/AKT-mTOR node prevents cells from undergoing apoptosis and autophagy (37). Despite being regulated by PI3K/AKT, Merlin also regulates AKT signaling. The phosphorylation function of PI3K is elevated when bound to the long isoform of PI3K enhancer (PIKE-L). Merlin binds to PIKE-L and disrupts its interaction with PI3K, attenuating PI3K activity (38). One of the targets of PI3K/AKT signaling is the serine/threonine mTOR kinase (39). Thus, deficiency of Merlin favors may induce mTOR signaling in a PI3K/AKT-dependent manner. However, increased function of mTORC1 independent of PI3K/AKT signaling is reported in an *NF2*-deficient context, suggesting alternative mechanisms of the regulation of mTOR pathway by Merlin.

Chronic proliferative cells spread uncontrollably and show increased motility, a key component of the metastatic process (37). It is likely that migration and invasion abilities are promoted in Merlin-deficient cells once they are no longer responsive to commands that inhibit their expansion. The epithelial-to-mesenchymal transition (EMT) is a crucial step in this process, and lack of Merlin resulted in the downregulation of epithelial signatures, such as E-cadherin and Keratin 8, and upregulation of mesenchymal ones, such as N-cadherin, metalloproteinase 2, Snail 2, Twist1, and ZEB. Direct evidence of Merlin's involvement in this cell behavior was confirmed when restoring Merlin resulted in a switch in the expression of these signatures (26). In conclusion, loss of Merlin enhances survival, motility and invasion of tumor cells all of which are important phenotypic characteristics that support acquisition of metastatic potential.

## **Cancer metabolism**

The acquired malignant traits of sustained overproliferation, EMT transition, migration, and invasion, that facilitate metastasis, require higher energy expenditure. Thus, it is unlikely that pre-malignant and malignant cells utilize the same bioenergetic and biosynthetic processes of their normal counterparts. It is now known that cancer cells draw upon distinct metabolic strategies to support their malignant behavior, such as a switch to aerobic glycolysis and increased uptake of glutamine. In addition, cancer cells benefit from an intracellular oxidative milieu where ROS act as second messengers activating tumor-promoting pathways (39-41). The establishment of an oxidative tumor microenvironment also favors tumor survival by inducing stromal cells to emit growth signals and immune cells to secrete pro-tumor cytokines. These events enhance tumor cell proliferation, migration, and invasion phenotypes.

## **Aerobic glycolysis**

The first observation of reprogramming of energy metabolism in cancer cells was demonstrated by altered glucose catabolism. In oxygenated milieu, glucose is converted into pyruvate through glycolysis in the cytoplasm of normal cells. Pyruvate translocates to the mitochondria where it is processed into acetyl-CoA by pyruvate dehydrogenase (PDH) and enters the tricarboxylic acid (TCA) cycle generating NADH and FADH<sub>2</sub>, the substrates of oxidative phosphorylation (OXPHOS) in the inner mitochondrial membrane electron transport chain. However, in low oxygen-supplied situations, pyruvate dehydrogenase kinase (PDK) phosphorylates and inhibits PDH function, and lactate dehydrogenase (LDH) converts pyruvate into lactate, characterizing anaerobic glycolysis (39, 42, 43). While OXPHOS generates approximately 36 mol ATP/glucose, anaerobic

glycolysis ATP yield/glucose is around 2mol. Interestingly, tumor cells mainly convert glucose into lactate, even in well-oxygenated conditions. This phenomenon is referred as Warburg effect, named after the scientist who first observed this phenomenon, or “aerobic glycolysis” (39).

The discovery of aerobic glycolysis in cancer cells sparked the interest in cancer metabolism. Considering that malignant cells need a high input of energy, it first seemed contradictory to rely on a metabolic system that generates considerably lower amounts of ATP. However, aerobic glycolysis allows the generation of many metabolic intermediates that constitute nucleosides and amino acids that are crucial for the synthesis of macromolecules and organelles (39, 44). For instance, glucose is first converted to glucose-6-phosphate (G6P) after entering the cell. G6P can be diverted to the pentose phosphate pathway where it serves as the substrate to generate NADPH and ribose-5-phosphate, a precursor to DNA and RNA. In addition, other glycolytic intermediates, such as fructose-6-phosphate and glycerol-3-phosphate are used as substrates in the biosynthesis of hexosamine and amino acids serine and glycine, respectively (40).

The process of aerobic glycolysis is faster than OXPHOS which may compensate for the disadvantage in terms of ATP production. Moreover, reprogrammed cells show increased expression of glucose transporters (GLUTs) which enable higher glucose uptake compared to normal cells. The expression of GLUT1 and its translocation to the cell surface is driven by the PI3K/AKT pathway (40). Signals from PI3K/AKT pathway also stimulate the activity of hexokinase, which phosphorylates glucose into G6P, and phosphofructokinase. In addition, Ras GTPase also plays a role in glucose consumption by upregulating GLUT1. The c-myc transcription factor also contributes to aerobic

glycolysis by activating the expression of PDK1, LDH-A, and monocarboxylate transporter (MCT1), that export lactate into the extracellular milieu. In addition, WNT/ $\beta$ -catenin signaling also upregulates the expression of PDK1 and MCT1. Furthermore, it is well known that tumors frequently dwell in a hypoxic environment leading to the stabilization of HIF-1 $\alpha$  and the expression of HIF-1 target genes, including PDK1 and LDH-A (40, 45).

The increased consumption of glucose is an indicator of poor prognosis in cancer and is exploited as an imaging tool in positron emission tomography (PET). By administration of a glucose analog containing the radionuclide fluorine-18 (18F-fluorodeoxyglucose), glucose uptake can be monitored and used in cancer diagnosis, staging, and responsiveness to treatment (40).

### **Glutamine addiction**

Many tumor cells are also addicted to glutamine uptake as it serves as a nitrogen donor for the biosynthesis of nucleotides (purine and pyrimidine), glucosamine-6-phosphate, and non-essential amino acids (44). c-myc is the main activator of glutamine transporters, such as ASCT2 and SN2, and enzymes involved in the conversion of glutamine into glutamate, such as glutaminase 1, phosphoribosyl pyrophosphate synthetase, and carbamoyl-phosphate synthetase 2 (40). Glutamate feeds the TCA cycle and is also part of the cystine antiporter xCT system where cells uptake one molecule of cystine and export one molecule of glutamate. Intracellular cystine is processed into cysteine which is a substrate for the *de novo* synthesis of reduced glutathione (GSH), a major cellular antioxidant co-factor (46).

Similar to elevated glucose uptake, higher consumption of glutamine is a poor prognosis indicator. This phenomenon has been captured by PET using a modified glutamine containing the radionuclide fluorine-18 (18F-labeled glutamine). This glutamine analog is useful in situations where the use of 18F-fluorodeoxyglucose is not recommended due to normal glucose uptake, such as in the brain (40).

### **Redox imbalance**

Another aspect of cancer metabolism is the accumulation and harness of intracellular reactive oxygen species (ROS) to promote malignant behavior and foster a pro-tumor microenvironment (47-50). ROS are oxygen-containing chemical species primarily generated by OXPHOS in the mitochondrion (51). Electrons from NADH and FADH<sub>2</sub> are transferred through a series of protein complexes at the inner mitochondrial membrane to be finally accepted by molecular oxygen (O<sub>2</sub>) in the mitochondrial matrix. However, this electron transport chain can go awry with electrons leaking and partially reducing O<sub>2</sub> into superoxide (O<sub>2</sub><sup>•-</sup>) - the first form of ROS - in the intermembrane space and matrix of the mitochondrion. The resultant O<sub>2</sub><sup>•-</sup> is rapidly converted into hydrogen peroxide (H<sub>2</sub>O<sub>2</sub>) by superoxide dismutase 1 (SOD1) and SOD2 in the mitochondrial intermembrane space and matrix, respectively (49, 51).

Knowing that cancer cells use less mitochondrial OXPHOS for glucose catabolism, additional mechanisms are likely in charge of ROS accumulation in tumor cells. Indeed, the expression of the NADPH oxidase (NOX) family, comprised of seven isoforms, NOX 1-5, Dual oxidase 1 (DUOX1), and DUOX2, is frequently upregulated in many malignancies and is the main source of ROS generation in cancer. These enzymes generate O<sub>2</sub><sup>•-</sup> or H<sub>2</sub>O<sub>2</sub> by transferring electrons across membranes from NADPH to O<sub>2</sub>



(52). Lastly,  $\beta$ -oxidation of fatty acids in peroxisomes and enzymatic reactions by cyclooxygenase, xanthine oxidase, and Fenton reaction can also result in ROS generation (53).

ROS were long thought to be just by-products of cell mechanisms and are well-known for causing damage to DNA, proteins and lipids when in high amounts. However, the activity of ROS is not limited to its deleterious effect; in low-to-moderate levels, ROS can regulate various cell behaviors. Although  $O_2^{\cdot-}$  is unstable and poorly diffusible through cell membranes,  $H_2O_2$  is relatively stable, can diffuse freely and thus acts as a second messenger altering protein functions and modulating cell signaling pathways. ROS promote proliferation, differentiation, transcriptional regulation and proteome degradation (54, 55).

In order to keep ROS levels under a certain threshold, cells have developed different antioxidant mechanisms. The glutathione peroxidase (Gpx) and peroxiredoxins (Prxs) enzymes are main effectors in the conversion of  $H_2O_2$  into  $H_2O$  and  $O_2$ . In addition, thioredoxin (Trx) and glutaredoxin (Grx) are crucial for the reduction of oxidized macromolecules, such as proteins. The antioxidant activity of Gpx and Grx relies on the use of GSH as an antioxidant cofactor. Although GSH can be *de novo* synthesized, its oxidized form, glutathione disulfide (GSSG), can be reduced in a reaction mediated by glutathione reductase (GR) with NADPH as an electron donor. Oxidized Prxs can be reduced by Trx, and oxidized Trx can, in turn, be reduced in a thioredoxin reductase (Trxd)/NADPH-dependent manner (56). Therefore, there is a well-coordinated and intricate antioxidant signaling to ensure that ROS are maintained at acceptable threshold.

Untargeted metabolomics of Merlin-deficient breast cancer cells revealed lower levels of GSH-containing metabolites, further confirmed by decreased amounts of intracellular GSH. Knowing that GSH functions as a major antioxidant cofactor, it was not surprising to find greater accumulation of ROS in these Merlin-deficient cells. This evidence suggested that Merlin is likely playing a role in the maintenance of redox systems in breast cancer cells (26).

### **METABOLIC IMPACT OF MERLIN DEFICIENCY IN BREAST CANCER**

Signaling activity of pathways involved in aerobic glycolysis, such as PI3K/AKT, Ras GTPase, and WNT/ $\beta$ -catenin, are also enhanced in *NF2*/Merlin-deficient cancer cells. This suggests that metabolic aspects are likely perturbed upon Merlin deficiency. In addition, a diminished pool of GSH levels in the context of Merlin deficiency supports the hypothesis that *NF2*/Merlin is intimately involved in cell metabolism. In the published article “Deficiency of tumor suppressor Merlin facilitates metabolic adaptation by co-operative engagement of SMAD-Hippo signaling in breast cancer” of my authorship, I showed that deficiency of Merlin in breast cancer induces a metabolic shift toward aerobic glycolysis in a TGF- $\beta$ /Hippo signaling-dependent manner. Furthermore, in a separate study communicated for peer-review, I show that ROS management mechanisms dependent on Nrf2/GSH signaling are disrupted in Merlin-deficient cells simultaneous with upregulation of NOX enzymes cumulatively contributing to increased ROS levels.

MERLIN REGULATES SIGNALING EVENTS AT THE NEXUS OF  
DEVELOPMENT AND CANCER

by

MATEUS MOTA AND LALITA A SHEVDE

*Cell Communication and Signaling*

Copyright

2020

by

Authors according to the BMC License Agreement

Format adapted for dissertation

## **Abstract**

### **Background**

In this review, we describe how the cytoskeletal protein Merlin, encoded by the Neurofibromin 2 (NF2) gene, orchestrates developmental signaling to ensure normal ontogeny, and we discuss how Merlin deficiency leads to aberrant activation of developmental pathways that enable tumor development and malignant progression.

### **Main body**

Parallels between embryonic development and cancer have underscored the activation of developmental signaling pathways. Hippo, WNT/ $\beta$ -catenin, TGF- $\beta$ , receptor tyrosine kinase (RTK), Notch, and Hedgehog pathways are key players in normal developmental biology. Unrestrained activity or loss of activity of these pathways causes adverse effects in developing tissues manifesting as developmental syndromes. Interestingly, these detrimental events also impact differentiated and functional tissues. By promoting cell proliferation, migration, and stem-cell like phenotypes, deregulated activity of these pathways promotes carcinogenesis and cancer progression. The NF2 gene product, Merlin, is a tumor suppressor classically known for its ability to induce contact-dependent growth inhibition. Merlin plays a role in different stages of an organism development, ranging from embryonic to mature states. While homozygous deletion of Nf2 in murine embryos causes embryonic lethality, Merlin loss in adult tissue is implicated in Neurofibromatosis type 2 disorder and cancer. These manifestations, cumulatively, are reminiscent of dysregulated developmental signaling.

## **Conclusion**

Understanding the molecular and cellular repercussions of Merlin loss provides fundamental insights into the etiology of developmental disorders and cancer and has the potential, in the long term, to identify new therapeutic strategies.

## **Background**

The human Neurofibromin 2 (NF2) gene is located on chromosome 22, contains 17 exons, and directs the synthesis of a 70-kDa protein named NF2 or Merlin. High NF2 expression was initially observed in the nervous system, more specifically in Schwann cells, meninges, and ependyma, and to some extent in the lens and nerves as well. Merlin regulates cell behavior by integrating extracellular cues with intracellular responses and acts as a classical tumor suppressor. Functionally, Merlin inhibits tumorigenesis by inducing contact-dependent growth inhibition [1].

Merlin shares more than 50% sequence homology with the Ezrin/Radixin/Moesin (ERM) family of proteins, and indeed, its nomenclature represents an acronym for “Moesin-Ezrin-Radixin-Like Protein” (Merlin). In general, the N-terminal region of cytoskeleton-associated proteins, such as the 4.1 and ERM families, contains a unique module denominated as the 4.1, ERM (FERM) domain. The FERM family of proteins, including Merlin, are mainly located near the cell membrane where they bind to cytoplasmic tails of transmembrane receptors and to actin filaments through their N-terminal FERM and C-terminal domains, respectively. However, Merlin does not bind actin via its C-terminal domain; instead its interaction with actin is mediated via the FERM domain [2]. Merlin mediates contact-dependent growth inhibition in its closed form, characterized by the binding between its N-terminal FERM and C-terminal

domains. This is induced by anti-mitogenic signals, such as cadherin-dependent cell-cell adhesion and CD44-dependent MYPT1 phosphatase, that keep Serine 518 (Ser518) at Merlin's C-terminal domain dephosphorylated. However, promotogenic signals initiated by integrins and receptor tyrosine kinases activate Rho family of GTPases, such as Cdc42 and Rac, which in turn activate p21-activated kinase (PAK). PAK phosphorylates Ser518, disrupting the binding between the N-terminal FERM and C-terminal domains. In this now open structure, the tumor suppressor role of Merlin is inhibited. Merlin's phosphorylation and inactivation are also promoted by cyclic AMP-protein kinase A (PKA) signaling and by AKT-dependent phosphorylation and ubiquitination, which cause proteasome-mediated degradation of Merlin [3].

Mutations in NF2 causatively result in Neurofibromatosis type 2, an autosomal dominant disorder mainly associated with benign tumors in the nervous system, such as bilateral vestibular schwannomas, meningiomas, and ependymomas [2]. Although lack of functional NF2/Merlin activity was initially investigated in Neurofibromatosis type 2 disorder, Merlin deficiency is recognized in malignant tumors, including mesothelioma, prostate cancer, melanoma, glioma, and breast cancer [2]. The onset and progression of cell proliferative disorders are intimately connected to deregulation of cell signaling pathways that govern developmental processes. Therefore, the association of NF2/Merlin malfunction with both benign and malignant disease, suggests that Merlin likely regulates cell signaling associated with developmental programs. Hippo, WNT/ $\beta$ -catenin, TGF- $\beta$ , receptor tyrosine kinase (RTK), Notch, and Hedgehog signaling pathways are the main coordinators of developmental biology [4]. In this review, we discuss how, in a spatiotemporal-dependent manner, Merlin may contribute to either activation or

inhibition of developmental pathways in order to maintain cell integrity, tissue organization, and adequate overall development. Much of the current knowledge describing a possible role for Merlin in regulating components of these pathways comes from the impact of NF2/Merlin deficiency on the activity of these developmental biology-associated signaling events that impinge upon a malignant phenotype.

### **Merlin's role in developmental processes**

Many steps of development consist in a sequence of well-coordinated events involving cell proliferation and differentiation, resulting in an organized and functional tissue. Normal embryo patterning is important before and during gastrulation, a crucial early stage of vertebrate embryogenesis, which results in the formation of the germ layers that will support organogenesis [5]. Early studies interrogating the role of Nf2 in vivo discovered that homozygous Nf2 mutation in murine embryos is lethal, with developmental failure occurring by embryonic days 6.5 and 7. Merlin presented as a crucial component in the organization of extraembryonic structure. The extraembryonic ectoderm of homozygous Nf2-mutated embryos failed to develop into an epithelial tissue, compromising their orientation and elongation. These irregular-shaped mutant embryos had impaired production of mesoderm, failed to gastrulate, and became embryonically inviable [6]. Recognizing Merlin's role in inducing contact dependent growth inhibition, it is reasonable to infer that Merlin controls cell proliferation of the extraembryonic compartment and further contributes to an optimal gastrulation process.

Merlin's anti-proliferative activity continues to be critical even after gastrulation phase and is crucial for the fusion of epithelial tissue, such as in the transition from neural plate to a neural tube in vertebrate embryos. For instance, a nerve cell-specific Nf2

knockout mouse model under the control of Nestin promoter exhibited neural tube defects such as encephalocele and exencephaly [7]. Furthermore, although heterozygous Nf2 knockout embryos are viable, the mice usually develop tumors, such as osteosarcomas, fibrosarcoma, and hepatocellular carcinoma, with high metastatic rate to the lungs and liver [8].

Dysregulated signaling activity of pathways known for instructing embryonic development, such as Hippo, WNT/ $\beta$ -catenin, TGF- $\beta$ , receptor tyrosine kinases, Notch, and Hedgehog usually leads to cell overproliferation and consequently lack of differentiation and functionality, resulting in abnormal embryonic formation and malignancies in developed tissues [4]. Undoubtedly, regulation of cell proliferation at either the embryonic or mature stage is imperative to the development and maintenance of an organism. Therefore, Merlin may be orchestrating these developmental signaling pathways to assure well-coordinated proliferation events, justifying its indispensable roles in preventing both failure of embryonic development and tumorigenesis.

Controlled cell proliferation is at the core of many embryonic developmental phases. For instance, proliferation of epithelial or endothelial cells into tubules, a developmental program termed branching morphogenesis, is a fundamental step in the formation of several mammalian organs, such as kidney, lung, pancreas, and mammary gland [9]. Furthermore, cell cycle progression is associated with cell polarity, a characteristic that is crucial for the establishment of an organized and functional tissue in metazoans. For instance, planar-cell polarity (PCP) is established orthogonally to apical-basal polarity and is responsible for cell behavior across the plane of the tissue. PCP defines the dorsoventral and anteroposterior body axes in vertebrates and invertebrates



and is required for tissue patterning, vertebrate gastrulation, and neural tube closure [10, 11]. By controlling cell proliferation and adhesion, Merlin is instrumental for induction of cell polarity and together with the establishment of PCP, ensures epithelial tissue function in the skin and kidney for example [12, 13]. Overall, Merlin presents as a promising regulator of cell proliferation and organization through its association with developmental signaling pathways.

### **Merlin and developmental signaling pathway**

#### **Hippo signaling pathway**

First described as a regulator of imaginal disc growth in fruit flies (*Drosophila melanogaster*) by inducing cell-cycle arrest and apoptosis, the Hippo signaling pathway was later associated with organ growth restriction [14]. Hippo was also found to be involved in neuroepithelial cell differentiation in the optic lobe and dendrite morphogenesis in sensory neurons of *Drosophila* larvae [15]. Merlin, in cooperation with the transducer protein Kibra, is a classical activator of Hippo signaling and regulates the organization of embryonic and adult tissues/organs [3]. Merlin/Kibra serves as a scaffolding complex that localizes Hippo-associated Mst and Lats kinases to the cell membrane. Lats phosphorylates YAP/TAZ co-activators, resulting in their retention in the cytoplasm and degradation by the proteasome system. Lack of Hippo signaling results in translocation of YAP/TAZ to the nucleus and binding to TEAD transcription factors, which activate the expression of genes usually involved in tissue growth [14]. Merlin also supports Hippo activation by directly associating with  $\alpha$ -catenin and facilitating its binding to 14-3-3 protein for cytoplasmic sequestration of YAP/TAZ. Furthermore, although predominantly a cytoskeletal protein, Merlin can translocate to the nucleus,

bind to DCAF1, a substrate adaptor of the CRL4-E3 ubiquitin ligase, and inhibit overall activity of CRL4DCAF1 ligase. By ubiquitinating histones and other chromatin-associated factors, the CRL4DCAF1 ligase system facilitates the activation of some YAP/TAZ targets [3]. Thus, Merlin relies on different mechanisms to tightly control YAP/TAZ transcriptional function (Fig. 1A).

Abnormal YAP/TAZ activity due to Hippo deficiency contributes to tumorigenesis, cancer progression, and metastasis with most striking cases observed in breast cancer where Hippo dysregulation is necessary for disease progression and can be detected in up to 70% of advanced cases [16]. Interestingly, Merlin loss has been correlated with increased grade in breast cancer which might justify the downregulation of Hippo signaling and increase in YAP/TAZ activity in this type of malignancy [17]. Recognizing the role of Merlin-Hippo axis in the control of tissue development and prevention of tumorigenesis, Merlin/Lats2 represses YAP/TAZ and allows the appropriate course of branching morphogenesis in murine kidney, avoiding renal hypodysplasia [18]. However, in a different context, unrestrained YAP/TAZ can induce abnormal renal cell growth, promote intratubular neoplasia and further cause clear cell renal cell carcinoma [16]. These discoveries highlight the relationship between Merlin and Hippo in maintaining tissue homeostasis and cancer.

### **WNT/ $\beta$ -catenin signaling pathway**

The WNT/ $\beta$ -catenin signaling pathway is crucial for embryonic developmental processes, especially in the regulation of PCP. In addition, WNT/ $\beta$ -catenin renews the pluripotent embryonic stem cell pool and maintains proper proliferation and differentiation in adult tissues [19, 20], such as in the plasticity of the mammary gland in

development and during pregnancy and lactation. The canonical WNT/ $\beta$ -catenin activation is blocked by a destruction complex (Axin, adenomatous polyposis coli (APC), CK1 $\alpha$  and GSK3 $\beta$ ) that eliminates  $\beta$ -catenin by proteasomal degradation. This inhibitory status is reversed when secreted WNT ligands bind to and activate Frizzled (FZD) transmembrane receptor and LRP co-receptor. The ensuing signaling events result in nuclear translocation of  $\beta$ -catenin and together with TCF/LEF transcription factors, culminate in activation of target gene expression [21].

Unrestrained WNT activity can cause malignant transformation and lead to development of cancers, such as colorectal, prostate, and breast tumors [22]. For instance, overexpression of WNT7A ligand and the FZD7 receptor promotes stem cell phenotype in the mammary tissue and can foster basal-like breast cancer. Furthermore, overexpression of FZD6 and FZD8 receptors exacerbates motility, invasion and metastatic potential in triple negative breast cancer cells [23]. The fact that these type of tumors also show some levels of Merlin loss or inactivation [2, 24] suggests a connection between Merlin and the WNT/ $\beta$ -catenin pathway. Moreover, Neurofibromatosis type 2 patients with schwannoma, a clinical manifestation of the disorder, accumulate high levels of  $\beta$ -catenin, further indicating that elevated WNT/  $\beta$ -catenin signaling activity is associated with deficient Merlin expression [21].

Indeed, it has been reported that Merlin's N-terminal FERM domain binds to LRP6, inhibits its phosphorylation, and maintains a functional  $\beta$ -catenin destruction complex thereby curbing cytoplasmic  $\beta$ -catenin accumulation [21]. Considering that phosphorylation of LRP is a hallmark of WNT pathway activation since it disassembles  $\beta$ -catenin destruction complex, Merlin presents as a key antagonist of WNT/  $\beta$ -catenin

signaling. Moreover, Merlin can also directly diminish the availability of free cytoplasmic  $\beta$ -catenin by physically interacting with it and localizing it to the cell membrane, where  $\beta$ -catenin establishes adherens junction together with E-cadherin and  $\alpha$ -catenin [25]. Furthermore, phosphorylation of  $\beta$ -catenin at Ser19 and Ser605 by Rac1-activated JNK2 kinase facilitates its nuclear transport. Merlin downregulates Rac1 and weakens JNK2 activation thereby restricting  $\beta$ -catenin's nuclear transport. Indeed, inhibition of Rac1 decreases WNT activity [26]. Thus, Merlin may control cell proliferation and ensure tissue organization by directly or indirectly controlling  $\beta$ -catenin's cytoplasmic availability and translocation into the nucleus, consequently blunting WNT/ $\beta$ -catenin signaling (Fig. 1B).

### **TGF- $\beta$ signaling pathway**

The TGF- $\beta$  signaling pathway is involved in the regulation of branching morphogenesis and extracellular matrix deposition such as in the development of the salivary gland [27]. Dysregulated TGF- $\beta$  signaling is known for causing developmental abnormalities, such as Marfan and Loeys-Dietz syndromes [28]. In cancer biology, TGF- $\beta$  signaling operates in a context-dependent manner, where it suppresses tumor growth in early stage cancer and promotes disease progression by inducing EMT and metastasis in late stages [29]. Canonical TGF- $\beta$  signaling leads to the phosphorylation and activation of SMAD2/3 transcription factors by TGF- $\beta$  receptors that, together with co-stimulator SMAD4, associate with transcriptional co-activators or co-repressors to induce or inhibit gene expression, respectively. The TGF- $\beta$  signaling pathway is blocked by its endogenous inhibitor SMAD7 [29]. Interestingly, SMAD7 levels were decreased concomitantly with loss of Merlin in breast tumor patient samples and cell line, resulting

in increased SMAD2/3 phosphorylation and SMAD-driven luciferase activity. The enhancement of TGF- $\beta$  signaling was involved in increased reliance of NF2-deficient breast cancer cells on aerobic glycolysis, a metabolic advantage that sustains cell malignancy [30].

Furthermore, non-canonical TGF- $\beta$  signaling has been found to be associated with Merlin activity as well. SMAD-independent TGF- $\beta$  signaling activates PAK2 through the binding of Cdc42 and Rac1. In mesenchymal cells, PAK2 phosphorylates Merlin and inhibits its contact growth inhibition role; this may be one mechanism by which TGF- $\beta$  signaling promotes growth and contributes to malignancy in late stage cancers. However, in epithelial cells, the binding of Merlin to epithelial-enriched protein Erbin limits the amount of free Merlin to be phosphorylated and inhibited by PAK2. In such context, Merlin's role in repressing cell overproliferation is maintained. It is likely that Merlin/Erbin disrupts the association between Cdc42/Rac1 and PAK, hinders the latter kinase activation, and imposes a restriction on TGF- $\beta$ -dependent proliferative activity [31]. Moreover, Cho et al. (2018) have reported that NF2/Merlin activates non-canonical TGF- $\beta$  type II receptor (TGFIIR) signaling. TGFIIR can inhibit TGF- $\beta$  type I receptor (TGFIR) and block its non-canonical oncogenic activity. In conditions of NF2/Merlin loss, TGFIIR expression is downregulated, resulting in the activation of TGFIR. As a kinase, TGFIR phosphorylates and inhibits the Raf kinase inhibitor protein (RKIP). Therefore, activated Raf, a downstream effector of Ras signaling, induces ERK activation and causes tumorigenesis through p53 and E-cadherin downregulation and cell cycle upregulation [32]. Overall, Merlin has different approaches to stall TGF- $\beta$  signaling (Fig. 1C). The paradoxically contrasting effects of TGF- $\beta$  signaling in cancer may be due

to the loss of tumor suppressors, such as Merlin, that normally interfere with TGF- $\beta$  activation. It is possible that the same scenario occurs in developing tissue, where Merlin deficiency may unbalance TGF- $\beta$  signaling causing aberrant developmental defects.

### **Receptor tyrosine kinase signaling**

Receptor tyrosine kinases (RTKs) are transmembrane receptors. In a context-dependent manner, ligands bind to extracellular domain of RTKs leading to dimerization of receptor monomers, phosphorylation of tyrosine residues on the intracellular domain, and activation of downstream pathways that play a role in a variety of cell behaviors, such as cell proliferation, survival, and migration. Unrestrained activation of RTK impairs development and can also cause cancer [33]. The cell membrane availability of the RTKs platelet-derived growth factor receptor (PDGFR) and epidermal growth factor receptor (EGFR), and consequently their downstream signaling, are regulated by Merlin, representing another mechanism by which Merlin keeps check on cell proliferation.

PDGFR/PDGF signaling is involved in various developmental functions, such as proliferation, migration, survival, deposition of extracellular matrix, and tissue remodeling factors [34]. Schwannoma primary human tissue and cell lines lack Merlin expression and were concomitantly found to express high levels of PDGFR and increase activation of its readouts, PI3K/AKT and MAPK/Erk1/2. Conversely, overexpression of NF2 in HEI 193 schwannoma cell line inhibited PDGFR/PDGF activity. Furthermore, the activation of PI3K/AKT and MAPK/Erk1/2 was also downregulated in cells overexpressing NF2 [35]. A mechanistic approach of how Merlin negatively modulates PDGFR may be explained by interactions that both proteins have on the inner face of the cell membrane. For instance, the autophosphorylation and consequent activation of

PDGFR $\beta$  signaling is elevated by its association with the Na<sup>+</sup>/H<sup>+</sup> exchange regulatory cofactor (NHERF). Interestingly, NHERF (also known as ERM binding protein 50 (EBP50)) binds the N-terminal domain of Merlin. As a PDZ domain-containing protein, NHERF/EBP50 plays a role in membrane receptor trafficking to endosomal compartments for lysosomal degradation or recycling back to the membrane [35, 36]. Therefore, it is proposed that Merlin interacts with PDGFR $\beta$  via NHERF/EBP50, causing receptor internalization, degradation, and overall downstream signal attenuation.

The ErbB protein family comprises 4 members, ErbB1–4, and is also referred to as human epidermal growth factor receptor (Her). ErbB RTKs are involved in several steps of mammalian development, such as the onset of tissue embryogenesis, cell fate determination, and tissue specialization. Moreover, ErbB is involved in adult tissue maintenance by regulating cell survival and apoptosis [37]. Increased membrane levels, phosphorylation and activity of ErbB2 and ErbB3 are observed in peripheral nerves of Nf2-deficient mice and patients with schwannomas, contributing to tumor growth. Cell proliferation was decreased by halting ErbB2 phosphorylation with the EGFR kinase inhibitor Lapatinib [38, 39]. Furthermore, generation of a transgenic, renal tubule-specific Nf2 knockout mouse resulted in renal invasive carcinoma with elevated EGFR signaling. In vitro proliferation of these renal tumor cells was EGF-dependent and treatment with Erlotinib arrested cell expansion. In addition, re-introduction of Nf2 also reversed cell proliferation supporting the role of Merlin in controlling EGF/EGFR signaling in the renal system [40]. In Nf2-deficient schwannomas, the Hippo transcription factor YAP induces the transcription of prostaglandin and amphiregulin, which activate EGFR [41]. Similar to its regulation of PDGFR availability, Merlin also blocks the internalization and

signaling of ErbB RTKs [42]. Merlin is recruited to nascent cell-cell adherens junctions and stabilizes the interaction between cadherin cell adhesion-associated catenins and the cytoskeleton structure. This interaction inhibits the activity of EGFR as the cell senses intercellular forces to stall cell growth [43]. Collectively, the availability of transmembrane PDGFR and EGFR for signaling reveals Merlin's modulation of cell surface properties in the cell cortex (Fig. 1D).

### **Notch signaling pathway**

Notch signaling is crucial for cell differentiation, stem cell maintenance, proliferation, migration, and apoptosis. Induction of these cell mechanisms is instrumental for the regulation of developmental processes, such as lateral inhibition, lineage decision, and inductive signaling [4]. In a context dependent manner, Notch ligands in the signal-emitting cells bind to Notch receptors in the signal-receiving cells. The receptors undergo proteolytic cleavage resulting in the release of their receptor intracellular domain (ICD) into the cytoplasm. The ICD translocates to the nucleus and form a transcriptional complex with other DNA-binding proteins to activate target genes, such as HES1 and SOX9 [44].

Deficiency of Notch function in development can manifest as Alagille syndrome, caused mainly by loss-of-function mutation or deletion of Jag1 ligand [45] or CADASIL, resulting from mutation in the Notch 3 receptor, among other disorders [46]. Notch-induced defects can also result from overexpression of either ligands or receptors of the Notch pathway leading to aberrant signaling. This is illustrated by the development of intrahepatic bile ducts where overexpression of Notch 2 receptor, caused by loss of NF2 and compromised Hippo activity, induced cholangiocyte overproliferation and excessive



bile duct development [44]. While gain-of-function mutations in Notch are recurrent in most hematological malignancies, they are not so frequent in breast and adenoid cystic carcinomas [47].

Recognizing Merlin's modulation of RTKs in the cell membrane, it is likely that Merlin also regulates membrane localization of Notch receptors. This represents a key node of regulation since the membrane availability of Notch receptors determines the rate of Notch signaling. Merlin's restraint on Notch activity was first proposed in the regulation of imaginal epithelial proliferation and differentiation in *Drosophila*. The physical interaction between Merlin and Expanded, another component of the FERM family of proteins, resulted in the removal of Notch receptors from the cell membrane. Merlin and Expanded might confine Notch transmembrane receptors at locations in the cell membrane marked for endocytosis and degradation by lysosomes. Therefore, loss of Merlin compromises the formation of the complex with Expanded, allowing Notch receptor abundance in the cell membrane and signaling [48] (Fig. (Fig.1E).1E). Although not elucidated yet, it may be possible that Merlin also clears Notch ligands from the cell membrane in the signal-emitting cells, further limiting Notch activity.

### **Hedgehog signaling pathway**

The Hedgehog (Hh) signaling pathway is implicated in the patterning of limbs, internal organs, and body heights in humans [49]. In the absence of secreted Hh ligands, Desert (Dhh), Indian (Ihh), and Sonic (Shh), Patched (PTCH) transmembrane protein represses the G-protein coupled receptor Smoothed (SMO). As a result, SMO-dependent signal transduction to GLI transcription factors is compromised. The binding of Hh ligands to PTCH induces GLI to translocate to the nucleus where it activates gene

expression [50]. Shh ligand activates Hh signaling and promotes proliferation of granule neuron precursor cells in the developing cerebellum. However, dysregulated stimulation by Shh leads to uncontrolled cell division resulting in medulloblastoma, the most common type of brain tumor in children [51]. Details about a possible regulation of Hh signaling by Merlin are yet to emerge. However, in NF2/Merlin-deficient breast cancer cells, reactive oxygen species (ROS) accumulation resulting from decreased levels of anti-oxidant, GSH, lead to elevated Hh signaling [52]. ROS are known to induce conformational changes in proteins, especially by oxidizing thiol groups on cysteine residues, and affect their enzymatic activity, post-translational modifications, or protein-protein interaction [53]. Therefore, it is possible that ROS oxidize and inhibit PTCH, enabling the release of SMO from PTCH repression. Alternatively, ROS may also modify GLI's ability to enable ligand-independent activation. It is also possible that ROS may upregulate expression of Hh ligands or enable nuclear translocation of GLI proteins. Overall, Merlin likely restricts GLI activity by modulating the oxidative intracellular milieu (Fig. (Fig.1F).1F). Given this pathway's important role in development patterning, it is likely that redox-imbalance-driven Hh activation may also be prevalent in tumors with loss of NF2 function.

### **Conclusion**

Merlin loss in early stages of development is lethal. Loss of Merlin's function in differentiated tissue results in aberrant cell proliferation causing benign and malignant tumor formation and progression (Fig. 2). These outcomes are explained by the fact that several of the signaling pathways with which Merlin intersects are instrumental in keeping optimally active development programs and adult tissue maintenance. Therefore,

Merlin represents an indispensable key regulator of signals in different phases of an organism's development, ranging from an embryo to a fully differentiated, functional system. Shedding light on how Merlin acts in different contexts is undoubtedly necessary for a comprehensive understanding of its loss in impacting disease onset and development. There is still no strategy to directly overcome Merlin deficiency in Neurofibromatosis type 2 and cancers; therefore, targeting the collateral effect of loss of Merlin function seems like a promising approach. Targeting aberrantly activated developmental signaling in Merlin-deficient malignancies offers a new therapeutic direction with several inhibitors having already received FDA approval for targeting these pathways (e.g. Hippo, WNT/ $\beta$ -catenin, TGF- $\beta$ , RTK, Notch, and Hedgehog). In addition, investigation of developmental syndromes from the perspective of Merlin may evolve the understanding of disorders and consequently therapeutic strategy as well.

### **Author's contributions**

MM and LAS designed the format of the review. MM wrote the manuscript under LAS supervision. The authors read and approved the final manuscript.

### **Acknowledgments**

We would like to acknowledge Dr. Rajeev Samant and Sarah Bailey for editorial suggestions, and the UAB O'Neal Comprehensive Cancer Center (P30CA013148).

### **Funding**

This work was funded by the Department of Defense (W81XWH-18-1-0036), NCI R01CA138850, UAB AMC21 funds, and The Breast Cancer Research Foundation of Alabama (BCRFA) to L.A.S.

### **Availability of data and materials**

Not applicable.

### **Ethics approval and consent to participate**

Not applicable.

### **Consent for publication**

Not applicable.

### **Competing interests**

The authors declare that they have no competing interests.

### **Footnotes**

Publisher's Note: Springer Nature remains neutral with regard to jurisdictional claims in published maps and institutional affiliations.

## Contributor Information

Mateus Mota, Email: mmota88@uab.edu.

Lalita A. Shevde, Email: lalitasamant@uabmc.edu.

## Abbreviations

APC: Adenomatous polyposis coli

CADASIL: Cerebral autosomal dominant arteriopathy with subcortical infarcts and leukoencephalopathy

CK1 $\alpha$ : Casein kinase 1 $\alpha$

DCAF: DDB1-and-Cullin 4-associated Factor 1

Dhh: Desert hedgehog

DLL: Delta-like

EBP50: ERM binding protein 50

EGFR: Epidermal growth factor receptor

ERM: Ezrin/Radixin/Moesin

FERM: 4.1, ERM

FZD: Frizzled

GSH: Glutathione

Hh: Hedgehog

ICD: Intracellular domain

Ihh: India hedgehog

JNK2: c-Jun N-terminal kinase 2

LATS: Large tumor suppressor kinase

LRP: Lipoprotein receptor-related protein

MST: Mammalian Sterile20-like kinase

MYPT1: Myosin phosphatase target subunit 1

NF2: Neurofibromin 2

NHERF: Na<sup>+</sup> – H<sup>+</sup> exchange regulatory cofactor

PAK: p21-activated kinase

PDGFR: Platelet-derived growth factor receptor

PKA: Protein kinase A

PTCH: Patched

RBPJ: Recombining binding protein suppressor of hairless

ROS: Reactive oxygen species

RTK: Receptor tyrosine kinase

SH2: Src Homology 2

Shh: Sonic hedgehog

SMO: Smoothened

TCF/LEF: T-cell factor/ lymphoid enhancing factor

TGFR: TGF- $\beta$  receptor

YAP: Yes-associated protein

## References

1. Cooper J, Giancotti FG. Molecular insights into NF2/Merlin tumor suppressor function. *FEBS Lett.* 2014;588(16):2743–2752.
2. Petrilli AM, Fernandez-Valle C. Role of Merlin/NF2 inactivation in tumor biology. *Oncogene.* 2016;35(5):537–548.
3. Li W, Cooper J, Karajannis MA, Giancotti FG. Merlin: a tumour suppressor with functions at the cell cortex and in the nucleus. *EMBO Rep.* 2012;13(3):204–215.
4. Perrimon N, Pitsouli C, Shilo BZ. Signaling mechanisms controlling cell fate and embryonic patterning. *Cold Spring Harb Perspect Biol.* 2012;4(8):a005975.
5. Freeman M, Gurdon JB. Regulatory principles of developmental signaling. *Annu Rev Cell Dev Biol.* 2002;18:515–539.
6. McClatchey AI, Saotome I, Ramesh V, Gusella JF, Jacks T. The Nf2 tumor suppressor gene product is essential for extraembryonic development immediately prior to gastrulation. *Genes Dev.* 1997;11(10):1253–1265.
7. McLaughlin ME, Kruger GM, Slocum KL, Crowley D, Michaud NA, Huang J, et al. The Nf2 tumor suppressor regulates cell-cell adhesion during tissue fusion. *Proc Natl Acad Sci U S A.* 2007;104(9):3261–3266.
8. McClatchey AI, Saotome I, Mercer K, Crowley D, Gusella JF, Bronson RT, et al. Mice heterozygous for a mutation at the Nf2 tumor suppressor locus develop a range of highly metastatic tumors. *Genes Dev.* 1998;12(8):1121–1133.
9. Ochoa-Espinosa A, Affolter M. Branching morphogenesis: from cells to organs and back. *Cold Spring Harb Perspect Biol.* 2012;4(10):a008243.
10. Devenport D. The cell biology of planar cell polarity. *J Cell Biol.* 2014;207(2):171–179. doi: 10.1083/jcb.201408039.
11. Butler MT, Wallingford JB. Planar cell polarity in development and disease. *Nat Rev Mol Cell Biol.* 2017;18(6):375–388.
12. Pugacheva EN, Roegiers F, Golemis EA. Interdependence of cell attachment and cell cycle signaling. *Curr Opin Cell Biol.* 2006;18(5):507–515.
13. Lopez EW, Vue Z, Broaddus RR, Behringer RR, Gladden AB. The ERM family member Merlin is required for endometrial gland morphogenesis. *Dev Biol.* 2018;442(2):301–314.

14. Pan D. The hippo signaling pathway in development and cancer. *Dev Cell*. 2010;19(4):491–505.
15. Poon CL, Mitchell KA, Kondo S, Cheng LY, Harvey KF. The hippo pathway regulates neuroblasts and brain size in *Drosophila melanogaster*. *Curr Biol*. 2016;26(8):1034–1042.
16. Han Y. Analysis of the role of the hippo pathway in cancer. *J Transl Med*. 2019;17(1):116.
17. Morrow KA, Das S, Metge BJ, Ye K, Mulekar MS, Tucker JA, et al. Loss of tumor suppressor Merlin in advanced breast cancer is due to post-translational regulation. *J Biol Chem*. 2011;286(46):40376–40385.
18. Reginensi A, Enderle L, Gregorieff A, Johnson RL, Wrana JL, McNeill H. A critical role for NF2 and the hippo pathway in branching morphogenesis. *Nat Commun*. 2016;7:12309.
19. Yang Y. Wnt signaling in development and disease. *Cell Biosci*. 2012;2(1):14.
20. Steinhart Z, Angers S. Wnt signaling in development and tissue homeostasis. *Development*. 2018;145(11):dev14658.
21. Kim M, Kim S, Lee SH, Kim W, Sohn MJ, Kim HS, et al. Merlin inhibits Wnt/beta-catenin signaling by blocking LRP6 phosphorylation. *Cell Death Differ*. 2016;23(10):1638–1647.
22. Zhan T, Rindtorff N, Boutros M. Wnt signaling in cancer. *Oncogene*. 2017;36(11):1461–1473.
23. Ghosh N, Hossain U, Mandal A, Sil PC. The Wnt signaling pathway: a potential therapeutic target against cancer. *Ann N Y Acad Sci*. 2019;1443(1):54–74.
24. Cacev T, Aralica G, Loncar B, Kapitanovic S. Loss of NF2/Merlin expression in advanced sporadic colorectal cancer. *Cell Oncol (Dordr)* 2014;37(1):69–77.
25. Morrow KA, Das S, Meng E, Menezes ME, Bailey SK, Metge BJ, et al. Loss of tumor suppressor Merlin results in aberrant activation of Wnt/ $\beta$ -catenin signaling in cancer. *Oncotarget*. 2016;7(14):17991–18005.
26. Bosco EE, Nakai Y, Hennigan RF, Ratner N, Zheng Y. NF2-deficient cells depend on the Rac1-canonical Wnt signaling pathway to promote the loss of contact inhibition of proliferation. *Oncogene*. 2010;29(17):2540–2549.



27. Hall BE, Zheng C, Swaim WD, Cho A, Nagineni CN, Eckhaus MA, et al. Conditional overexpression of TGF-beta1 disrupts mouse salivary gland development and function. *Lab Invest*. 2010;90(4):543–555.
28. Morissette R, Merke DP, McDonnell NB. Transforming growth factor- $\beta$  (TGF- $\beta$ ) pathway abnormalities in tenascin-X deficiency associated with CAH-X syndrome. *Eur J Med Genet*. 2014;57(2–3):95–102.
29. Derynck R, Zhang YE. Smad-dependent and Smad-independent pathways in TGF-beta family signalling. *Nature*. 2003;425(6958):577–584.
30. Mota MSV, Jackson WP, Bailey SK, Vayalil P, Landar A, Rostas JW, 3rd, et al. Deficiency of tumor suppressor Merlin facilitates metabolic adaptation by co-operative engagement of SMAD-hippo signaling in breast cancer. *Carcinogenesis*. 2018;39(9):1165–1175.
31. Wilkes MC, Repellin CE, Hong M, Bracamonte M, Penheiter SG, Borg JP, et al. Erbin and the NF2 tumor suppressor Merlin cooperatively regulate cell-type-specific activation of PAK2 by TGF-beta. *Dev Cell*. 2009;16(3):433–444.
32. Cho JH, Oh AY, Park S, Kang SM, Yoon MH, Woo TG, et al. Loss of NF2 induces TGFbeta receptor 1-mediated noncanonical and oncogenic TGFbeta signaling: implication of the therapeutic effect of TGFbeta receptor 1 inhibitor on NF2 syndrome. *Mol Cancer Ther*. 2018;17(11):2271–2284.
33. Basson MA. Signaling in cell differentiation and morphogenesis. *Cold Spring Harb Perspect Biol*. 2012;4(6):a008151.
34. Hoch RV, Soriano P. Roles of PDGF in animal development. *Development*. 2003;130(20):4769.
35. Fraenzer JT, Pan H, Minimo L, Jr, Smith GM, Knauer D, Hung G. Overexpression of the NF2 gene inhibits schwannoma cell proliferation through promoting PDGFR degradation. *Int J Oncol*. 2003;23(6):1493–1500.
36. Ammoun S, Hanemann CO. Emerging therapeutic targets in schwannomas and other merlin-deficient tumors. *Nat Rev Neurol*. 2011;7:392.
37. Wieduwilt MJ, Moasser MM. The epidermal growth factor receptor family: biology driving targeted therapeutics. *Cellular Molecular Life Sci*. 2008;65(10):1566–1584.
38. Lallemand D, Manent J, Couvelard A, Watilliaux A, Siena M, Chareyre F, et al. Merlin regulates transmembrane receptor accumulation and signaling at the plasma membrane in primary mouse Schwann cells and in human schwannomas. *Oncogene*. 2009;28(6):854–865.

39. Ammoun S, Cunliffe CH, Allen JC, Chiriboga L, Giancotti FG, Zagzag D, et al. ErbB/HER receptor activation and preclinical efficacy of lapatinib in vestibular schwannoma. *Neuro-Oncology*. 2010;12(8):834–843.
40. Morris ZS, McClatchey AI. Aberrant epithelial morphology and persistent epidermal growth factor receptor signaling in a mouse model of renal carcinoma. *Proc Natl Acad Sci U S A*. 2009;106(24):9767–9772.
41. Guerrant W, Kota S, Troutman S, Mandati V, Fallahi M, Stemmer-Rachamimov A, et al. YAP mediates tumorigenesis in Neurofibromatosis type 2 by promoting cell survival and proliferation through a COX-2-EGFR signaling Axis. *Cancer Res*. 2016;76(12):3507–3519.
42. Curto M, Cole BK, Lallemand D, Liu CH, McClatchey AI. Contact-dependent inhibition of EGFR signaling by Nf2/Merlin. *J Cell Biol*. 2007;177(5):893–903.
43. Chiasson-MacKenzie C, Morris ZS, Baca Q, Morris B, Coker JK, Mirchev R, et al. NF2/Merlin mediates contact-dependent inhibition of EGFR mobility and internalization via cortical actomyosin. *J Cell Biol*. 2015;211(2):391.
44. Wu N, Nguyen Q, Wan Y, Zhou T, Venter J, Frampton GA, et al. The hippo signaling functions through the notch signaling to regulate intrahepatic bile duct development in mammals. *Lab Investig*. 2017;97(7):843–853.
45. Turnpenny PD, Ellard S. Alagille syndrome: pathogenesis, diagnosis and management. *Eur J Hum Genet*. 2012;20(3):251–257.
46. Masek J, Andersson ER. The developmental biology of genetic notch disorders. *Development*. 2017;144(10):1743–1763.
47. Aster JC, Pear WS, Blacklow SC. The varied roles of notch in cancer. *Annu Rev Pathol*. 2017;12:245–275.
48. Maitra S, Kulikauskas RM, Gavilan H, Fehon RG. The tumor suppressors Merlin and Expanded function cooperatively to modulate receptor endocytosis and signaling. *Curr Biol*. 2006;16(7):702–709.
49. Jiang J, Hui CC. Hedgehog signaling in development and cancer. *Dev Cell*. 2008;15(6):801–812.
50. Varjosalo M, Taipale J. Hedgehog: functions and mechanisms. *Genes Dev*. 2008;22(18):2454–2472.
51. Lee EY, Ji H, Ouyang Z, Zhou B, Ma W, Vokes SA, et al. Hedgehog pathway-regulated gene networks in cerebellum development and tumorigenesis. *Proc Natl Acad Sci U S A*. 2010;107(21):9736–9741.

52. Das S, Jackson WP, Prasain JK, Hanna A, Bailey SK, Tucker JA, et al. Loss of Merlin induces metabolomic adaptation that engages dependence on hedgehog signaling. *Sci Rep.* 2017;7:40773.
53. Wang K, Jiang J, Lei Y, Zhou S, Wei Y, Huang C. Targeting metabolic-redox circuits for cancer therapy. *Trends Biochem Sci.* 2019;44(5):401–414.

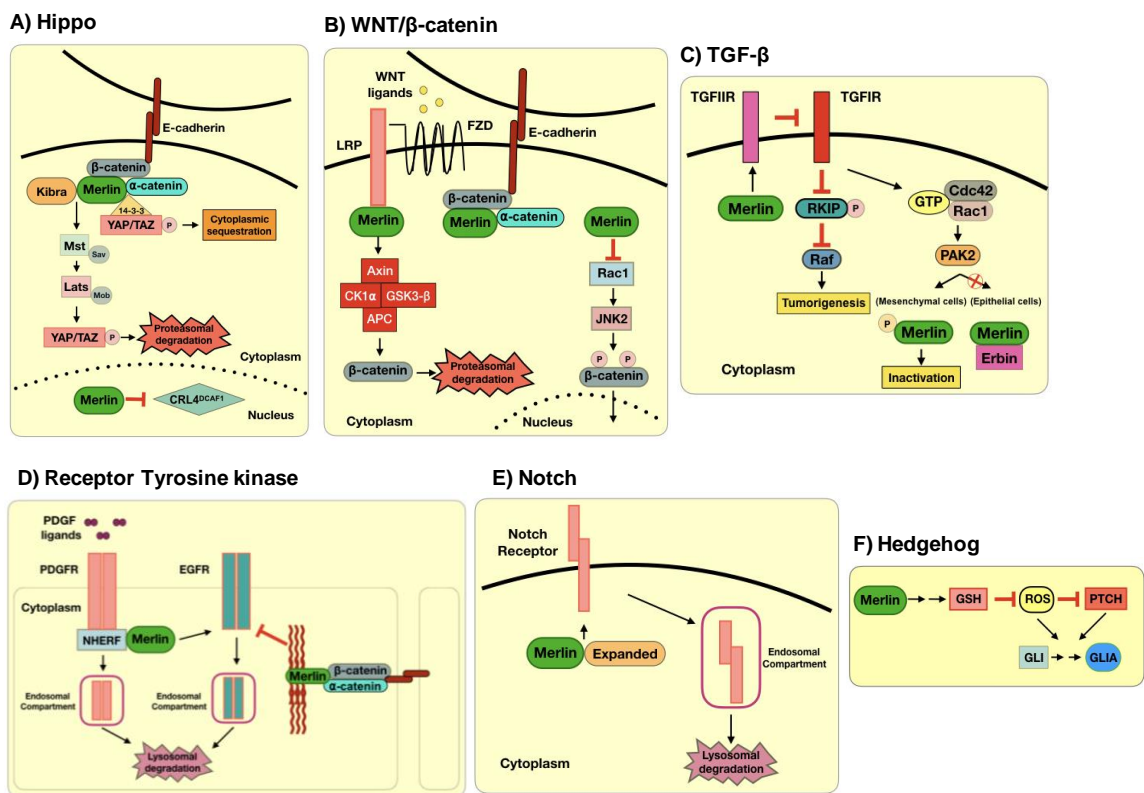


**Figure 1: Merlin regulates different developmental signaling pathways.** Merlin (A) enables Hippo-dependent YAP/TAZ destruction, (B) restrains  $\beta$ -catenin nuclear activity in the WNT pathway, (C) regulates TGF- $\beta$  signaling activation, (D) restricts activation of PGFR and EGFR, (E) controls Notch receptor levels availability, and (F) disturbs the oxidative milieu resulting in the activation of Hh signaling pathway

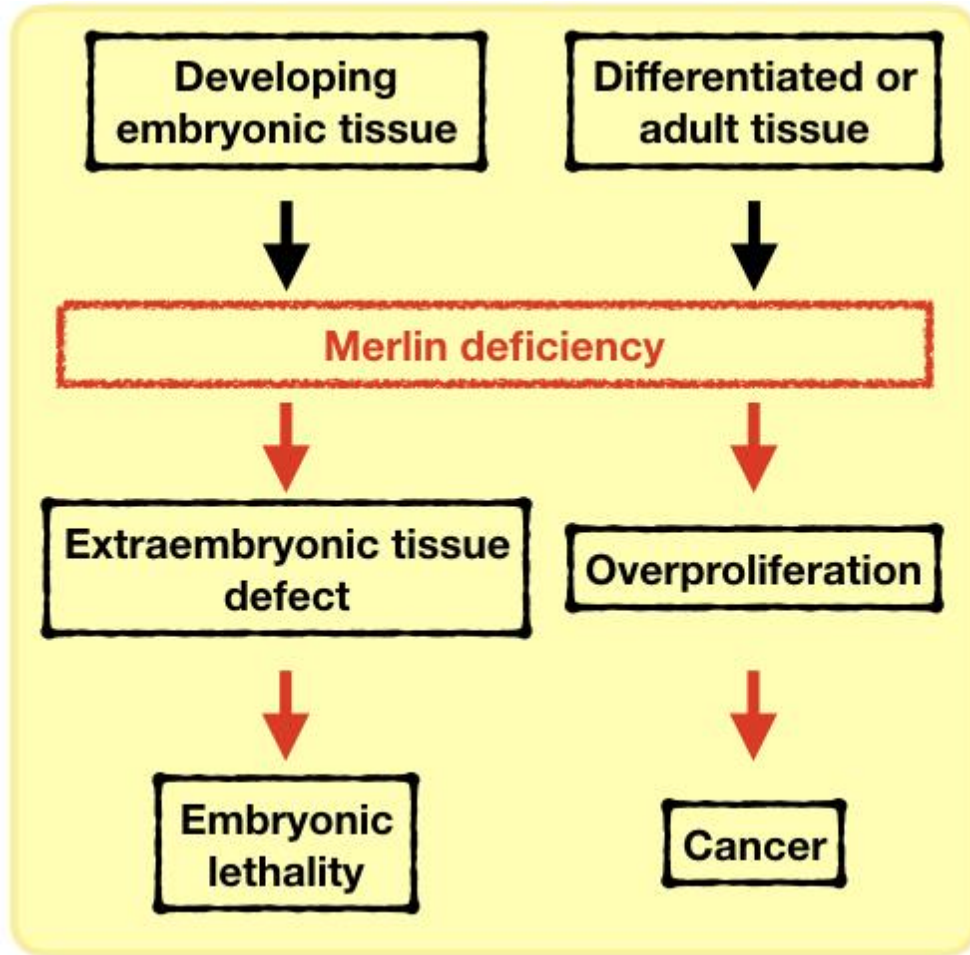


**Figure 2: Merlin depletion negatively impacts embryonic development and tissue maintenance.** Merlin is indispensable for normal extraembryonic structure formation and its loss is embryonic lethal. In differentiated and normal tissues, Merlin loss results in cell overproliferation due to defective contact-growth inhibition and promotes cancer

DEFICIENCY OF TUMOR SUPPRESSOR MERLIN FACILITATES METABOLIC  
ADAPTATION BY CO-OPERATIVE ENGAGEMENT OF SMAD-HIPPO  
SIGNALING IN BREAST CANCER

by

MATEUS S V MOTA, WILLIAM P JACKSON, SARAH K BAILEY, PRAVEEN  
VAYALIL, AIMEE LANDAR, JACK W ROSTAS, III, MADHURI S MULEKAR,  
RAJEEV S SAMANT, LALITA A SHEVDE

*Carcinogenesis: Integrative Cancer Research*

Copyright

2018

by

Oxford University Press

Used by permission

Format adapted for dissertation

## Abstract

The NF2 gene encodes the tumor and metastasis suppressor protein Merlin. Merlin exerts its tumor suppressive role by inhibiting proliferation and inducing contact-growth inhibition and apoptosis. In the current investigation, we determined that loss of Merlin in breast cancer tissues is concordant with the loss of the inhibitory SMAD, SMAD7, of the TGF- $\beta$  pathway. This was reflected as dysregulated activation of TGF- $\beta$  signaling that cooperatively engaged with effectors of the Hippo pathway (YAP/TAZ/TEAD). As a consequence, the loss of Merlin in breast cancer resulted in a significant metabolic and bioenergetic adaptation of cells characterized by increased aerobic glycolysis and decreased oxygen consumption. Mechanistically, we determined that the co-operative activity of the Hippo and TGF- $\beta$  transcription effectors caused upregulation of the long non-coding RNA Urothelial Cancer-Associated 1 (UCA1) that disengaged Merlin's check on STAT3 activity. The consequent upregulation of Hexokinase 2 (HK2) enabled a metabolic shift towards aerobic glycolysis. In fact, Merlin deficiency engendered cellular dependence on this metabolic adaptation, endorsing a critical role for Merlin in regulating cellular metabolism. This is the first report of Merlin functioning as a molecular restraint on cellular metabolism. Thus, breast cancer patients whose tumors demonstrate concordant loss of Merlin and SMAD7 may benefit from an approach of incorporating STAT3 inhibitors.

## Introduction

As the end-product of glucose catabolism, pyruvate is mainly converted to acetyl-CoA in cells under normoxia. Acetyl-CoA initiates the tricarboxylic acid cycle (TCA) that generates coenzymes for ATP production through oxidative phosphorylation (OXPHOS), among other components. Under hypoxia, pyruvate is primarily converted into lactate via anaerobic glycolysis. In cancer cells, even under proper oxygen-supplied environment, pyruvate is preferentially processed into lactate via aerobic glycolysis. Although aerobic glycolysis releases less ATP, it is still advantageous since it is a fast-rate process that increases glucose uptake and produces abundant intermediate precursors to the generation of NADPH, ribose-6-phosphate, amino acid and lipids necessary to fuel the high biomass state of malignant cells (1). Furthermore, release of a high amount of lactate acidifies the tumor milieu and contributes to a favorable tumor microenvironment (2). Genetic aberrations in TCA cycle enzymes, such as mutations in fumarase and downregulation of  $\alpha$ -ketoglutarate dehydrogenase by promoter hypermethylation, have been reported in breast cancer (3). These alterations likely contribute to the metabolic shift in breast cancer. However, the TCA-OXPHOS path is not fully inoperative in cancer cells. Despite its lower activity, it still cooperates with aerobic glycolysis to better fulfill the energy requirements of cancer cells.

Merlin is a tumor suppressor encoded by the neurofibromin 2 (NF2) gene. Merlin is a member of the 4.1 protein, ezrin, radixin, moesin (FERM) domain family of proteins and exerts its tumor suppressive role by inducing contact-growth inhibition and apoptosis (4). Merlin also was demonstrated to inhibit proliferation by downregulating cyclin D1 (5). Merlin is primarily known for its loss in benign tumors of the nervous system, such



as schwannomas, meningiomas and ependymomas, characterizing the Neurofibromatosis 2 disorder (4). The loss of Merlin has also been reported in malignancies such as mesothelioma, melanoma and breast cancers (6–8). While there are no significant mutations detected in NF2 transcript levels, the protein levels of Merlin are reduced in advanced and metastatic breast cancer. This downregulation of Merlin was identified to be the outcome of osteopontin-induced activation of protein kinase B (AKT) signaling that marks Merlin for ubiquitination and proteasomal degradation (8). Moreover, in both, breast and pancreatic cancers, Merlin targeted the Wnt pathway transcription co-factor,  $\beta$ -catenin, for degradation, consequently reducing the abundance of nuclear  $\beta$ -catenin (9). In addition, Merlin loss led to accumulation of reactive oxygen species in breast cancer cells which consequently caused dysregulated activation of Hedgehog signaling (10).

Homozygous knockout of NF2 is embryonically lethal in mice by day 7 of gestation, displaying poorly structured extraembryonic ectoderm (11). Heterozygous knockout mice survive but typically develop multiple cancers with increased metastatic events (12). Specific conditional NF2 knockout mouse models targeting Schwann cells, keratinocytes, hepatocytes and biliary epithelial cells have been generated for the study of schwannomas, epidermal and liver development, respectively (13–15). In addition, an approach for inducible knockout of NF2 has been applied to investigate the role of NF2 in the hematopoietic compartment and kidney tumorigenesis (16,17).

Merlin is an upstream activator of the Hippo signaling pathway that is well recognized for its role in organ size control by repressing cell proliferation and promoting apoptosis. Activation of Hippo signaling leads to phosphorylation of Yes-associated protein (YAP)/transcriptional coactivator with PDZ-binding motif (TAZ) co-

transcriptional factors that are retained in the cytoplasm or degraded. Upon loss of Merlin, the Hippo pathway is inactivated, YAP/TAZ are free to translocate to the nucleus, associate with TEA domain transcription factor (TEAD) transcriptional activators and activate target genes (18). Active YAP/TAZ plays an important role in the activation of transforming growth factor  $\beta$  (TGF- $\beta$ ) signaling in the maintenance of human embryonic stem cells. YAP/TAZ bind to active TGF- $\beta$  effectors, SMAD2/3–4 in the nucleus, enabling the accumulation and accommodation of a complex that triggers TGF- $\beta$ -target genes. A cross-talk between nuclear YAP/TAZ and TGF- $\beta$  signaling revealed convergent roles for signals that coordinate a specific pro-tumorigenic transcriptional program (19). In the current study, we investigated the relationship between loss of Merlin with decreased expression of SMAD7 in patient-derived breast tumors corresponding to advanced breast cancer. Our investigations have revealed cooperative transcriptional activities of YAP/TAZ/SMAD that facilitate glycolytic metabolic adaptation of Merlin-deficient breast cancer cells.

## **Materials and methods**

### **Cell culture**

The ER+PR+Her2- MCF7 breast cancer cell line resembles luminal A breast cancer (obtained from ATCC, Manassas, VA). MCF10AT is an immortalized, triple negative breast epithelial cell line transformed by transfection with T24 c-Ha-ras oncogene (obtained from Karmanos Cancer Center). The triple negative SUM159 cell line was obtained from Asterand Biosciences (Detroit MI). Cells, including stable

transfectants for knockdown or re-expression of Merlin, were cultured as previously described (8–10).

Cells were treated with 4  $\mu$ M TGF- $\beta$  type I receptor inhibitor A8301 (Stemgent, Lexington, MA), 1  $\mu$ M phospho-AKT inhibitor MK2206, (Selleckchem, Houston, TX) or 2 $\mu$ M phospho-STAT3 inhibitor STATTIC (Selleckchem) using DMSO vehicle (Fisher Bioreagents, Fair Lawn, NJ).

### **Cell line authentication**

All cell lines were validated for authentication using STR based assays of genomic DNA from the cell lines. The results of the assays were compared/validated using ATCC-STR database. Cell lines were authenticated when acquired and before cells were frozen in early passages, while the culture was actively growing. Cells were replaced from frozen stocks after a maximum of 12 passages or 3 months continuous culture. Cell lines were periodically confirmed negative for mycoplasma contamination using PCR assays.

### **Transwell invasion assay**

Cells were pre-treated with STATTIC or DMSO and seeded in serum-free growth medium containing the respective treatments in BioCoat™ Matrigel® Invasion Chambers (Corning, Bedford, MA). Serum-free growth medium with fibronectin was added to each well containing the chamber insert. Cell-containing inserts were incubated in 5% CO<sub>2</sub> incubator at 37°C for 16h then fixed with 4% paraformaldehyde, stained with crystal violet for 10 min and rinsed with deionized water. Photographs of inserts were taken using Nikon Eclipse Ti-U microscope (Nikon, Tokyo, Japan) using 10 $\times$  objective. Each

experimental condition was performed in duplicate and four random fields of each insert were recorded. Area of invaded cells was measured by ImageJ.

### **3D culture**

Cells were pre-treated with STATTC or DMSO and seeded in growth media supplemented with 2% 3D Culture Matrix Reduced Growth Factor Basement Membrane Extract (Trevigen, Gaithersburg, MD) in a chamber cover glass slide (Millipore, Billerica, MA) pre-coated with 3D Culture Matrix Reduced Growth Factor Basement Membrane Extract. The chamber slide was incubated in 5% CO<sub>2</sub> at 37°C with media replacement at every 4 days. Morphology was registered using Nikon Eclipse Ti-U microscope (Nikon, Tokyo, Japan) 20× objective.

### **UCA1 silencing**

Cells were transfected with 50 nM control-siRNA or UCA1-siRNA (Dharmacon, Lafayette, CO) overnight following the protocol of Lipofectamine® 2000 Transfection Reagent (Invitrogen, Carlsbad, CA). Cells were lysed 48 h post-transfection with NP40 lysis buffer (150 mM NaCl, 50 mM TRIS, 1% NP40) and total protein solution quantified using Precision Red Advanced Protein Assay (Cytoskeleton, Denver, CO).

### **Quantitative RT-PCR**

RNA was harvested using the RNeasy MiniKit (Qiagen, Hilden, Germany), and complementary DNA was synthesized according to the High Capacity complementary DNA Reverse Transcription kit (Applied Biosystems, Vilnius, Lithuania). Quantitative PCR (qPCR) was conducted with the TaqMan Fast Advanced Master Mix (Applied Biosystem, Austin, TX) and data analyzed with the  $2^{-\Delta\Delta C_t}$  method. Primers for the

genes of interest (GLUT, MCT, LDH, CTGF, CYR61 and UCA1) and control (ACTB) were purchased from Applied Biosystems.

### **Western blotting analysis**

Protein lysate was collected using NP40 lysis buffer and immunoblotted using the following antibodies: phospho-SMAD2 [Ser465/467]/SMAD3 [Ser423/425], SMAD2/3, SMAD4, SMAD6, phospho-YAP, TAZ, GAPDH, phospho-AKT [Ser473], pan-AKT, phospho-STAT3 [Tyr705], STAT3, Hexokinase 2 and HSP90 (all from Cell Signaling Technology, Beverly, MA); SMAD7 (R&D Systems, Minneapolis, MN), phospho-TAZ [Ser89] (Santa Cruz Biotechnology, Dallas, Texas) and  $\beta$ -Actin (Sigma-Aldrich).

### **Glucose consumption and lactate production assays**

Glucose and lactate levels in conditioned culture media were measured using the Amplex Red Glucose/Glucose Oxidase Assay Kit (Invitrogen) and Lactate Colorimetric/Fluorometric Assay Kit (BioVision, Milpitas, CA), respectively.

### **Bioenergetics assessments**

For extracellular flux assays (XF assays), cells were seeded at a density of  $4 \times 10^4$  cells/well 24 h prior to the assay. XF assays were performed in the same aforementioned basal media without bicarbonate supplementation and with 0.5% fetal bovine serum, pH 7.4. The buffer capacity of each media was determined prior to the assay. Cells were equilibrated in a non-CO<sub>2</sub> incubator for one hour before measurement of oxygen consumption rates (OCRs) and extracellular acidification rates (ECARs).

### **Targeted metabolomics**

Cells ( $3 \times 10^6$  cells/10 cm petri dish or  $1.5 \times 10^6$  cells/10 cm petri dish) were treated with 2  $\mu$ M of STATTIC inhibitor for 48 h or silenced for UCA1 (siRNA-UCA1), respectively. DMSO and non-targeting siRNA were used as respective controls. Cells were briefly washed with ice-cold phosphate-buffered saline, scraped in ice-cold methanol and incubated on ice for 30 min. One volume of ice cold methanol was added and cell lysate was centrifuged at  $12,000 \times g$  at  $-10^\circ\text{C}$  for 10 min. The supernatant was collected and taken for analysis. A separate culture of each condition was also maintained for protein lysate collection and concentration measure for further normalization. Krebs's Cycle components were analyzed by liquid-chromatography mass spectrometry (LC-MS) as previously described (20). Peak areas of metabolites in the sample extracts were compared in MultiQuant software (Sciex, Redwood City, CA) to those of known standards to calculate metabolite concentrations. Calculations for concentrations of structural isomers, G6P and F6P, which share mass transitions and co-elute were determined by a previously published method (21). Metabolite concentration was normalized by protein concentration.

### **Anchorage independence growth assay**

A 6-well plate was coated with DMEM/F12 medium supplemented with 10% fetal bovine serum and 0.1% insulin mixed with 1.5% BD BACTO™ Agar (Beckton Dickson, Franklin Lakes, NJ) (1:1 ratio). Cells were seeded at a density of 3000 cells/well in DMEM/F12 supplemented with 10% fetal bovine serum and 10  $\mu$ g/ml insulin mixed with 0.7% bacteriological agar (1:1 ratio). After 24 h, medium containing STATTIC was added to designated wells. Colonies were enumerated after 10–14 days.

## **Reporter assays**

Cells were plated in 96-well plates and transfected with 50 ng of 8xGT10C or SBE4 or STAT3 luciferase reporters (Addgene, Cambridge, MA) using FuGENE 6 Transfection Reagent (Promega, Madison, WI). The media was changed to regular growth media 24 h post-transfection. The assay was terminated 32 h post-transfection and read using the Luciferase Assay System (Promega).

## **Immunohistochemistry**

Breast tumor tissue microarrays from the NCI Cooperative Breast Tumor Tissue Resource were immunohistochemically stained for Merlin and SMAD7 (Supplementary Table 1, available at Carcinogenesis Online). The University of South Alabama Institutional Review Board granted this study an exemption from ethics approval. Specifically, immunohistochemical staining was performed using the streptavidin biotin complex method with 3,3'-diaminobenzidine chromogen LSAB+ System-HRP reagents (K4065) (DAB) (which included a 3% hydrogen peroxide peroxidase block) in a Dako Autostainer Plus automated immunostainer (Glostrup, Denmark). Heat induced antigen retrieval was performed with EDTA buffer, pH 8.0 (Thermo Fisher Scientific PT Module Buffer 2) for Merlin and with sodium citrate buffer, pH 6.0 (Thermo Fisher Scientific PT Module Buffer 1) for SMAD7. Blocking was performed with an avidin/biotin blocking kit (SP-2001; Vector Laboratories, Burlingame, CA). The following antibodies were used: Merlin: NF2 (A-19), and SMAD7 (H-79) (Santa Cruz Biotechnology, Inc.). The intensity of cytoplasmic staining was quantitated with computer-assisted image analysis in a Dako ACIS III Image Analysis System (Glostrup, Denmark). Images were captured

at 20× magnifications by the DS-L4 Microscope Camera Control unit using a NIKON Eclipse E200 microscope.

### **Statistical methods**

Statistical analysis was conducted using JMP Pro 13.0 (product of SAS Institute Inc., Cary, NC). Significance level of 0.05 was used to determine significance of results. Parallel dotplots and boxplots were used to compare distribution of Merlin and SMAD7 values by different clinical parameters (grade, stage, metastatic status and nodal involvement) to compare graphically and analysis of variance (ANOVA) was used to compare means of by groups. Dunnett's comparison with control method was used to compare means of different levels with that for normal breast tissue. Pearson's correlation coefficient was used to establish linear association and least squares regression technique was used to estimate linear relation.

## **Results**

### **Loss of Merlin in advanced breast cancer tissues is concordant with loss of SMAD7**

We evaluated the expression of Merlin and SMAD7 by immunohistochemical staining of breast tumor tissue microarrays. As represented in Figure 1, the staining intensities for Merlin and SMAD7 were significantly decreased in breast tumors when analyzed by the grade (I, II or III) (Figure 1A and B), nodal involvement (N0, N1 or N2) (Figure 1C and D), metastatic status (M0 or M1) (Figure 1E and F) or disease stage (Figure 1G and H). While normal breast tissue stained intensely for Merlin (Figure 1I; a, c) and SMAD7 (Figure 1I; b, d), tumor tissues showed characteristically reduced staining for both proteins (Figure 1I; e–h). The staining for Merlin was largely cytoplasmic with a



medium level of nuclear staining. In contrast, SMAD7 was predominantly nuclear. This is consistent with its role as a transcription co-repressor (22). When the mean immunohistochemistry (IHC) scores for Merlin and SMAD7 were computed with respect to tumor stage, it was evident that there is a very strong positive linear relation between them ( $R^2 = 0.97$ , ANOVA  $p = 0.0003$ ). The resulting least squares regression line represents  $\text{mean (Merlin)} = -83.15 + 20.17 * \text{Mean (SMAD7)}$ , with a Pearson's correlation coefficient  $r = 0.985$  (Figure 1J and Supplementary Table 1, available at Carcinogenesis Online). Collectively, the data demonstrate that the loss of Merlin and SMAD7 are concordant events.

### **Loss of Merlin contributes to unrestrained YAP/TAZ activity and TGF- $\beta$ signaling**

In order to mimic the loss of Merlin seen in breast cancer progression, MCF7 and MCF10AT breast cancer cell lines were stably knocked down for NF2. With the loss of Merlin associating closely with the loss of SMAD7, we evaluated the transcriptional activity of TGF- $\beta$  in cells engineered to be stably deficient for Merlin. The activity of the SMAD-dependent luciferase reporter was significantly upregulated in Merlin-deficient cells (Figure 2A). Merlin is known to activate Hippo signaling that involves phosphorylation and subsequent inhibition of YAP/TAZ co-transcriptional factors by cytoplasmic retention or degradation (18). Indeed, luciferase reporter activity assays showed that upon NF2 silencing, transcriptional activity of the Hippo pathway TEAD proteins is increased (Figure 2B). This is in agreement with decreased inhibitory phosphorylation of YAP and TAZ at Ser127 and Ser89, respectively, in Merlin-deficient cells (Figure 2C) simultaneous with an increase in regulatory and co-regulatory effectors of the TGF- $\beta$  pathway. Cells knocked down for Merlin demonstrated an increase in

phosphorylated SMAD2/3 and SMAD4. The inhibitory effector SMAD7 was downregulated (Figure 2C). Conversely, restoration of Merlin in SUM159, a breast cancer cell line with low Merlin expression, attenuated the activity of SMAD (Figure 2A) and TEAD (Figure 2B) luciferase reporters. This was in agreement with inhibition of TGF- $\beta$  pathway-related proteins and increased inhibitory phosphorylation of the YAP and TAZ proteins (Figure 2C). These results collectively indicate that loss of Merlin contributes to unrestrained YAP/TAZ activity and TGF- $\beta$  signaling.

The association of TGF- $\beta$ -regulated SMADs with active YAP/TAZ in a transcriptional complex is reported to shift TGF- $\beta$  signaling pathway's role from functioning in a tumor suppressive role to a pro-tumorigenic role. The YAP/TAZ/SMAD transcriptional complex targets a set of genes distinct from the ones they modulate independently (19). In accordance with this, we observed that expression of three characteristic YAP/TAZ/SMAD target genes were enhanced upon loss of Merlin (Figure 2D; Supplementary Figure 1A, available at *Carcinogenesis* Online). Cells restored for Merlin showed the most decrease in the levels of target gene urothelial cancer associated 1 (UCA1) (Figure 2D). Treatment of cells with A8301, a TGF- $\beta$  type I receptor inhibitor, caused a decrease in UCA1 expression (Supplementary Figure 1B, available at *Carcinogenesis* Online) confirming that UCA1 is in fact, a target of SMAD activity. Cumulatively, the results corroborate with the co-operative activity of YAP/TAZ/SMAD leading to upregulation of UCA1 upon Merlin loss. UCA1 encodes for a recently discovered long non-coding RNA that plays a role in various malignancies, including breast cancer, by modulating several genes involved in tumorigenesis, cell proliferation, migration, invasion and metabolism, particularly glycolysis (23–25). Therefore, we

evaluated the potential role of UCA1 as a novel mechanistic effector in the glycolytic shift of NF2-silenced breast cancer cells.

### **Loss of Merlin alters cancer cell metabolism and bioenergetics**

UCA1 directs activation of AKT and STAT3 with consequential effects on promoting proliferation and blocking apoptosis (26,27). Accordingly, Merlin deficient cells show upregulated phospho-AKT (Ser473) and phospho-STAT3 (Tyr705) (Figure 3A) with a simultaneous increase in hexokinase 2 (HK2) expression. This is in agreement with increased transcriptional activity of STAT3 reporter (Supplementary Figure 1C, available at *Carcinogenesis* Online). Conversely, Merlin restoration in SUM159 cells reduced phospho-AKT and phospho-STAT3 levels concomitantly with decreased HK2 expression (Figure 3A). HK2 is a crucial enzyme that mediates the rate limiting-step of glycolysis. HK2 mediates conversion of glucose into glucose-6-phosphate, and this phosphorylation impedes glucose's ability to leave the cell, committing it to undergo glycolysis. Thus, upregulation of HK2 is an important attribute of glycolysis.

Given the increased levels of HK2 in Merlin-silenced cells, we evaluated the impact of Merlin deficiency on breast tumor cell metabolism. Loss of Merlin increased glucose uptake and lactate export in both MCF7 and MCF10AT cell lines (Figure 3B and C). Conversely, SUM159 cells re-expressing Merlin showed reduced glucose consumption and lactate production. Merlin-deficient cells also presented greater ECAR consistent with increased glycolysis (Figure 3D). Oxygen consumption rate was decreased in Merlin-deficient cells compared to control cells (Figure 3E). This phenotype was reversed in cells restored for Merlin expression characterized by a decrease in ECAR and an increase in OCR (Figure 3D and E).

We analyzed the levels of metabolites of the TCA pathway using a targeted metabolomics approach. SUM159 cells re-expressing Merlin showed a collective increase in cellular abundance of TCA metabolites (Figure 4A). In contrast, knocking down Merlin in MCF10AT cells caused a decrease in cellular levels of TCA metabolites. Concomitant with these metabolic changes, loss of Merlin in MCF10AT and in MCF7 cells caused an increase in transcript levels of glucose transporters 3 and 4 (GLUT3 and GLUT4) (Figure 4B). This is consistent with increased glucose consumption (Figure 3B) and increased levels of glucose-6-phosphate (Supplementary Figure 2A, available at *Carcinogenesis* Online). The levels of monocarboxylate transporters (MCT 1, 2, 3), that transport lactate to the extracellular media, were also elevated in cells deficient for Merlin when compared with their controls (Figure 4C). Merlin deficiency resulted in increased levels of lactate dehydrogenase (LDHA and LDHB), enzymes that channel the final step in glycolysis by converting pyruvate into lactate (Figure 4D). Conversely, in SUM159 cells restored for Merlin the levels of glucose and lactate transporters were decreased with simultaneous decreases in LDHA and LDHB (Figure 4B and D). Collectively these data indicate that Merlin keeps a check on components of glucose consumption and glycolysis mediators, and the loss of Merlin induces metabolic and bioenergetics adaptations in breast cancer cells.

### **UCA1 directs cell metabolism towards aerobic glycolysis through AKT and STAT3 activation in Merlin-deficient cells**

We hypothesized that upregulation of UCA1 was vital to the metabolic adaptations observed in Merlin-deficient cells. In order to address this, we silenced UCA1 in Merlin-deficient MCF7 cells. UCA1 silencing resulted in decreased phosphorylation of both, AKT and STAT3 (Figure 5A; Supplementary Figure 2B, available at *Carcinogenesis* Online).

Importantly, HK2 expression was also reduced (Figure 5A). These findings suggest that loss of Merlin modulates cell metabolism towards aerobic glycolysis by invoking the participation of UCA1, AKT and STAT3.

With HK2 playing an important role in the glycolytic process, we queried the effects of UCA1 and STAT3 in regulating HK2 when Merlin expression is deficient. Merlin-deficient MCF7 cells silenced for *UCA1* showed a decrease in glucose consumption and lactate production relative to non-targeting control-transfected cells (Figure 5B and C). Further, Merlin-deficient cells silenced for UCA1 demonstrated a recovery in the cellular levels of TCA metabolites (Figure 5D), indicating a shift in cellular metabolism. In order to position a role for AKT and STAT3 activation leading to HK2 upregulation, we treated Merlin-deficient MCF7 cells with MK2206 and STAT3IC, small molecule inhibitors of AKT and STAT3 phosphorylation, respectively. Both, MK2206 and STAT3IC reduced HK2 expression relative to respective vehicle control (Figure 5E; Supplementary Figure 2C, available at *Carcinogenesis* Online), supporting AKT and STAT3 as upstream effectors of HK2 upregulation. Importantly, STAT3IC attenuated glucose consumption and lactate production in Merlin-deficient MCF7 cells (Figure 5F and G) and recovered the cellular levels of TCA metabolites (Figure 5H). These outcomes support that the loss of Merlin induces aerobic glycolysis in breast cancer cells through the combined activities of Hippo-TGF- $\beta$  signaling that impinge on the shift in cellular metabolism.

### **STAT3 inhibition preferentially impacts Merlin-deficient cells**

Given the profound effects of STAT3 inhibition on re-aligning the metabolism of Merlin-deficient cells, we hypothesized that STAT3 signaling is essential for sustenance

and/or malignant attributes of Merlin-deficient cells. We addressed this by evaluating the effect of the STAT3 inhibitor, STATTIC, on 3D cell growth. Merlin-deficient cells form characteristically invasive structures compared to Merlin-expressing MCF7 cells that give rise to well-defined spherical structures. STATTIC not only restored the circularity of the MCF7 kd structures but also seemed to limit their growth, suggesting a greater sensitivity of the Merlin-deficient cells to STAT3 inhibition (Figure 6A). When assayed for transwell invasion the MCF7 kd cells are significantly more invasive than their respective controls. While STATTIC caused a notable decrease in invasiveness of both cells, the effect on Merlin-deficient cells was strikingly greater (Figure 6B). Furthermore, a colony formation assay revealed increased sensitivity of the Merlin-deficient cells to STAT3 inhibition. The level of cell killing was notably greater in the cells knocked down for Merlin (kd) relative to the control cells, indicating that STAT3 signaling is vital for cells with Merlin deficiency (Figure 6C). Collectively, the data suggest that the loss of Merlin directs cancer cell metabolism towards aerobic glycolysis that is critically impacted by STAT3.

## **Discussion**

Merlin has thus far been demonstrated to be at the nexus of critical developmental signaling events. This is evident in the fact that Merlin-knockout mice are embryonically lethal (11). Inactivation of the Hippo signaling pathway is one of the well-characterized consequences of Merlin loss. The Hippo signaling pathway is activated by Merlin through either modulating adherens junctions at the cell membrane or by inactivating the activity of CRL4DCAF1 ubiquitin ligase complex in the nucleus (28). Loss of Merlin abolishes the activity of Hippo, leading to dysregulated activation of transcription co-

effectors YAP/TAZ, and consequently deregulated proliferation and organ size control (4,29).

In this study, we demonstrate a direct correlation between the loss of Merlin and concordant loss of SMAD7 in advanced breast cancer tissues. SMAD7 is an inhibitory SMAD of the TGF- $\beta$  signaling pathway. SMAD7 exerts its negative effect by either competing with r-SMADs for binding to the type I receptor, by recruiting the SMAD specific E3 ubiquitin protein ligase (SMURF) to mark TGF- $\beta$  receptor for degradation, or by binding to SMAD-binding elements in the DNA, compromising the r-SMADS/co-SMADs complex transcriptional activity (30,31). While Merlin and SMAD7 were robustly expressed in normal breast tissue, the two molecules appeared to have distinct cellular presence. While Merlin had an overall cellular presence, SMAD7 expression was predominantly nuclear, consistent with its role in inhibiting cell proliferation (22). The loss of Merlin in tumor tissues is in agreement with our previous study that reported the first role for Merlin in breast cancer (8). In the present study, we did not register a change in the transcript levels of SMAD7 (data not shown). Thus, the loss of SMAD7 is likely due to its post-transcriptional or post-translational regulation. The stability of SMAD7 is closely regulated by SMURF proteins, in particular SMURF1 and 2 that function as E3 ubiquitin ligases (32,33). Post-transcriptionally, mir-182, upregulated by TGF- $\beta$  signaling, targets SMAD7 for translational inhibition and disengages the negative feedback chain of TGF- $\beta$  during metastasis (31). The regulation of SMAD7 by the mir-106b-25 microRNA cluster induces a Six1-dependent epithelial-to-mesenchymal transition and a tumor initiating cell phenotype in breast cancer cells (34). It is likely that Merlin regulates SMAD7 through one or multiple of these mechanisms. Interestingly,

TGF- $\beta$  signaling has a tumor suppressor function in early cancer stage. However, as disease progresses, TGF- $\beta$  activity is coopted to support tumor progression and metastasis (35). Therefore, TGF- $\beta$  signaling inhibition has been a common therapeutic target in cancer. Although not in clinical trial, A8301 is a potent small molecule inhibitor of TGF- $\beta$  type I receptor ALK5 kinase, type I activin/nodal receptor ALK4 and type I nodal receptor ALK7. A8301 has been shown to inhibit epithelial to mesenchymal transition (EMT), a crucial step of metastasis (36).

The loss of SMAD7 in Merlin-deficient breast cancer cells enabled co-operative action of Hippo transcription co-factors and TGF- $\beta$  transcription factors, YAP/TAZ/SMAD2/3, which was evident by the upregulation of signature transcriptional targets of this co-operative activity. One of the prominently upregulated targets was UCA1, an oncogenic long non-coding RNA first discovered in human bladder cancer tissue and considered a biomarker (37). Functionally, UCA1 activates PI3K-AKT signaling and potentiates bladder cancer progression (38). Unrestrained activation of AKT signaling pathway results in tumorigenesis, metastasis, and chemo-radiation resistance. A promising strategy to target AKT signaling is by the administration of the MK-2206 allosteric inhibitor that prevents phosphorylation of the T308 and S473 sites required for full AKT activation. MK-2206 has advanced to phase I and phase II clinical trials as a monotherapy or in combination with other commonly used chemotherapeutics showing tolerable side effects (39). The oncogenic role of UCA1 has been further described in many other malignancies including breast, colorectal and hepatocellular carcinoma (23). While the mechanistic association between UCA1 and cancer



metabolism is still poorly characterized, UCA1 has been demonstrated to induce aerobic glycolysis (38).

Hexokinase 2 (HK2) is an enzyme bound to the outer mitochondrial membrane by the voltage-dependent anion channel (VDAC). VDAC enables transport of ATP generated in mitochondria to associate with HK2 inducing phosphorylation of glucose to glucose-6-phosphate (40). HK2 stimulates glucose flux into cancer cells resulting in a glucose gradient (41). Increased HK2 activity in cancer cells is accompanied by upregulation of glucose transporters (GLUTs), conversion of pyruvate to lactate mediated by lactate dehydrogenase enzymes (LDH) and transport of excessive intracellular lactate to the extracellular microenvironment through monocarboxylate transporters (MCT). Thus, upregulation of UCA1 leading to increased HK2 levels represents an important mechanism that enables Merlin deficient tumor cells to maintain their metabolic requirements. Merlin-deficient cells registered activated phospho-STAT3 as an outcome of upregulated UCA1. Several target genes of STAT3 include proteins that are involved in cell survival and proliferation. Although its pleiotropic nature was reported across multiple studies, STAT3 is generally considered a growth-promoting anti-apoptotic factor. STAT3 activation in both, tumors and immune cells, contributes to several malignant phenotypes of human cancers and to compromised anticancer immunity, cumulatively leading to poor clinical outcomes (42,43). STAT3 overexpression is significantly linked to poor prognosis in breast cancer, NSCLC (adenocarcinoma) and gastric cancers (44). STAT3 has prominent impacts on glycolytic functions, partly mediated by c-myc, that upregulate glycolysis genes such as GLUT-1, HK2, ENO-1 and PFKM (45,46). STAT3 directly activates transcription of HK2 and enhances glycolysis in

breast cancer cells (47). Our data corroborates with this finding and further demonstrates a critical role for STAT3 in impacting glycolysis in breast cancer cells that have decreased Merlin expression. We also have observed that STAT3 inhibition in Merlin-deficient cells alters cellular metabolism to reduce glycolysis and pivots cells towards enhanced utilization of the TCA pathway with a concomitant decrease in their invasive attributes. Merlin deficiency engenders cellular dependence on STAT3 signaling, endorsing a critical role for STAT3-mediated metabolic adaptation in sustaining these cells (Figure 6D). The STAT3 signaling pathway has different sites that may be intervened in order to inhibit its activity, such as the SH2, DNA binding and N-terminal domains (48). Disruption of STAT3 signaling increases apoptosis. As such, application of STAT3 inhibitors represents a promising cancer therapeutic strategy. While STAT3 inhibitors show high selectivity for STAT3-addicted tumor cells compared to healthy cells, unexpected toxicity is observed in clinical trials (49). As such, patient stratification would ideally obviate some of the unnecessary side-effects in those who may not benefit from this treatment. Our findings can help identify a patient population of Merlin and SMAD7-deficient breast tumors that may benefit from treatment with STAT3 inhibitors.

The reset of cancer cells' metabolism is one of the prominent hallmarks of malignancy once the neoplastic cells identify the need to acquire extra energy to sustain their proliferative and maintenance processes (50). This is characterized by an increase in glucose consumption and aerobic glycolysis and by profound bioenergetics adaptations in the cancer cells. Our data provides evidence that loss of Merlin engages the cell to employ co-operative signaling activities of the Hippo and TGF- $\beta$  pathways that enable alterations in cellular metabolism and bioenergetics.

## **Acknowledgements**

We also would like to acknowledge the UAB Targeted Metabolomics and Proteomics Laboratory for their expertise in metabolomics analyses.

*Authors' contributions:* WPJ, MM, RSS and LAS designed the study and the approaches.

WPJ, MM, JWR, PV, AL and SKB acquired the data. WPJ, MM, MSM, RSS, PV, AL and LAS analyzed and interpreted the results. MM, PV and LAS wrote the manuscript.

*Consent for publication:* All authors have read and agreed with the final paper. The information in this manuscript has been agreed for submission by all authors and we confirm that this work has not been published or submitted for publication elsewhere.

*Competing interests/conflict of interest:* We declare no conflict of interest.

*Ethics approval:* The immunohistochemistry study was granted an exemption from requiring ethics approval from the institutional review board at the University of South Alabama.

*Conflict of Interest Statement:* None declared.

## **Funding**

National Cancer Institute (R01CA138850, R01CA169202 to L.A.S.); Department of Defense (W81XWH-14-1-0516 and W81XWH-18-1-0036 to L.A.S.); The George and Ameilia G Tapper Foundation; Breast Cancer Research Foundation of Alabama (to L.A.S.); NCI R01CA194048 and BX003374 to R.S.S.

## Abbreviations

ANOVA: analysis of variance

AKT: protein kinase B

CRL4<sup>DCAF1</sup>: Cullin-ring ligase 4. DNA damage-binding protein 1 and cul4-associated factor 1

ECAR: extracellular acidification rate

FERM: four-point-one, ezrin, radixin, moesin

HK2: hexokinase 2

IHC: immunohistochemistry

MCT: monocarboxylate transporter

Mir: microRNA

NF2: neurofibromin 2

OCR: oxygen consumption rate

RT-PCR: reverse transcriptase polymerase chain reaction

SMURF: SMAD specific E3 ubiquitin protein ligase

STAT3: signal transducer and activator of transcription 3

TAZ: transcriptional coactivator with PDZ-binding motif

TCA: tricarboxylic acid

TEAD: TEA domain transcription factor

TGF- $\beta$ : transforming growth factor  $\beta$

UCA1: urothelial cancer associated 1

YAP: Yes-associated protein

## References

1. Kalyanaraman, B. (2017) Teaching the basics of cancer metabolism: developing antitumor strategies by exploiting the differences between normal and cancer cell metabolism. *Redox Biol.*, 12, 833–842.
2. Mishra, P. et al. (2015) Metabolic signatures of human breast cancer. *Mol. Cell. Oncol.*, 2, e992217-1–e992217-10.
3. Anderson, N.M. et al. (2018) The emerging role and targetability of the TCA cycle in cancer metabolism. *Protein Cell*, 9, 216–237.
4. Petrilli, A.M. et al. (2016) Role of Merlin/NF2 inactivation in tumor biology. *Oncogene*, 35, 537–548.
5. Xiao, G.H. et al. (2005) The NF2 tumor suppressor gene product, merlin, inhibits cell proliferation and cell cycle progression by repressing cyclin D1 expression. *Mol. Cell. Biol.*, 25, 2384–2394.
6. Thurneysen, C. et al. (2009) Functional inactivation of NF2/merlin in human mesothelioma. *Lung Cancer*, 64, 140–147.
7. Murray, L.B. et al. (2012) Merlin is a negative regulator of human melanoma growth. *PLoS One*, 7, e43295.
8. Morrow, K.A. et al. (2011) Loss of tumor suppressor Merlin in advanced breast cancer is due to post-translational regulation. *J. Biol. Chem.*, 286, 40376–40385.
9. Morrow, K.A. et al. (2016) Loss of tumor suppressor Merlin results in aberrant activation of Wnt/ $\beta$ -catenin signaling in cancer. *Oncotarget*, 7, 17991–18005.
10. Das, S. et al. (2017) Loss of Merlin induces metabolomic adaptation that engages dependence on Hedgehog signaling. *Sci. Rep.*, 7, 40773.
11. McClatchey, A.I. et al. (1997) The Nf2 tumor suppressor gene product is essential for extraembryonic development immediately prior to gastrulation. *Genes Dev.*, 11, 1253–1265.
12. McClatchey, A.I. et al. (1998) Mice heterozygous for a mutation at the Nf2 tumor suppressor locus develop a range of highly metastatic tumors. *Genes Dev.*, 12, 1121–1133.
13. Giovannini, M. et al. (2000) Conditional biallelic Nf2 mutation in the mouse promotes manifestations of human neurofibromatosis type 2. *Genes Dev.*, 14, 1617–1630.

14. Gladden, A.B. et al. (2010) The NF2 tumor suppressor, Merlin, regulates epidermal development through the establishment of a junctional polarity complex. *Dev. Cell*, 19, 727–739.
15. Zhang, N. et al. (2010) The Merlin/NF2 tumor suppressor functions through the YAP oncoprotein to regulate tissue homeostasis in mammals. *Dev. Cell*, 19, 27–38.
16. Larsson, J. et al. (2008) Nf2/merlin regulates hematopoietic stem cell behavior by altering microenvironmental architecture. *Cell Stem Cell*, 3, 221–227.
17. Morris, Z.S. et al. (2009) Aberrant epithelial morphology and persistent epidermal growth factor receptor signaling in a mouse model of renal carcinoma. *Proc. Natl. Acad. Sci. USA.*, 106, 9767–9772.
18. Piccolo, S. et al. (2014) The biology of YAP/TAZ: hippo signaling and beyond. *Physiol. Rev.*, 94, 1287–1312.
19. Hiemer, S.E. et al. (2014) The transcriptional regulators TAZ and YAP direct transforming growth factor  $\beta$ -induced tumorigenic phenotypes in breast cancer cells. *J. Biol. Chem.*, 289, 13461–13474.
20. Redmann, M. et al. (2018) Methods for assessing mitochondrial quality control mechanisms and cellular consequences in cell culture. *Redox Biol.*, 17, 59–69.
21. Ross, K.L. et al. (2009) Liquid chromatography/tandem mass spectrometry of glycolytic intermediates: deconvolution of coeluting structural isomers based on unique product ion ratios. *Anal. Chem.*, 81, 4021–4026.
22. Emori, T. et al. (2012) Nuclear Smad7 overexpressed in mesenchymal cells acts as a transcriptional corepressor by interacting with HDAC-1 and E2F to regulate cell cycle. *Biol. Open*, 1, 247–260.
23. Xue, M. et al. (2016) Urothelial cancer associated 1: a long noncoding RNA with a crucial role in cancer. *J. Cancer Res. Clin. Oncol.*, 142, 1407–1419.
24. Li, H.J. et al. (2015) Long non-coding RNA UCA1 promotes glutamine metabolism by targeting miR-16 in human bladder cancer. *Jpn. J. Clin. Oncol.*, 45, 1055–1063.
25. Zuo, Z.K. et al. (2017) TGF $\beta$ 1-Induced LncRNA UCA1 upregulation promotes gastric cancer invasion and migration. *DNA Cell Biol.*, 36, 159–167.
26. Yang, C. et al. (2012) Long non-coding RNA UCA1 regulated cell cycle distribution via CREB through PI3-K dependent pathway in bladder carcinoma cells. *Gene*, 496, 8–16.

27. Wu, W. et al. (2013) Ets-2 regulates cell apoptosis via the Akt pathway, through the regulation of urothelial cancer associated 1, a long noncoding RNA, in bladder cancer cells. *PLoS One*, 8, e73920.
28. Li, W. et al. (2012) Merlin: a tumour suppressor with functions at the cell cortex and in the nucleus. *EMBO Rep.*, 13, 204–215.
29. Serrano, I. et al. (2013) Inactivation of the Hippo tumour suppressor pathway by integrin-linked kinase. *Nat. Commun.*, 4, 2976.
30. Stolfi, C. et al. (2013) The dual role of Smad7 in the control of cancer growth and metastasis. *Int. J. Mol. Sci.*, 14, 23774–23790.
31. Yu, J. et al. (2016) MicroRNA-182 targets SMAD7 to potentiate TGF $\beta$  induced epithelial-mesenchymal transition and metastasis of cancer cells. *Nat. Commun.*, 7, 13884.
32. Grönroos, E. et al. (2002) Control of Smad7 stability by competition between acetylation and ubiquitination. *Mol. Cell*, 10, 483–493.
33. Fukasawa, H. et al. (2004) Down-regulation of Smad7 expression by ubiquitin-dependent degradation contributes to renal fibrosis in obstructive nephropathy in mice. *Proc. Natl. Acad. Sci. USA.*, 101, 8687–8692.
34. Smith, A.L. et al. (2012) The miR-106b-25 cluster targets Smad7, activates TGF- $\beta$  signaling, and induces EMT and tumor initiating cell characteristics downstream of Six1 in human breast cancer. *Oncogene*, 31, 5162–5171.
35. Massagué, J. (2008) TGF $\beta$  in Cancer. *Cell*, 134, 215–230.
36. Tojo, M. et al. (2005) The ALK-5 inhibitor A-83-01 inhibits Smad signaling and epithelial-to-mesenchymal transition by transforming growth factor-beta. *Cancer Sci.*, 96, 791–800.
37. Wang, X.S. et al. (2006) Rapid identification of UCA1 as a very sensitive and specific unique marker for human bladder carcinoma. *Clin. Cancer Res.*, 12, 4851–4858.
38. Li, Z. et al. (2014) Long non-coding RNA UCA1 promotes glycolysis by upregulating hexokinase 2 through the mTOR-STAT3/microRNA143 pathway. *Cancer Sci.*, 105, 951–955.
39. Nitulescu, G.M. et al. (2016) Akt inhibitors in cancer treatment: the long journey from drug discovery to clinical use (Review). *Int. J. Oncol.*, 48, 869–885.
40. Mathupala, S.P. et al. (2006) Hexokinase II: cancer's double-edged sword acting as both facilitator and gatekeeper of malignancy when bound to mitochondria. *Oncogene*, 25, 4777–4786.

41. Patra, K.C. et al. (2013) Hexokinase 2 is required for tumor initiation and maintenance and its systemic deletion is therapeutic in mouse models of cancer. *Cancer Cell*, 24, 213–228.
42. Carpenter, R.L. et al. (2014) STAT3 target genes relevant to human cancers. *Cancers (Basel)*, 6, 897–925.
43. Aleskandarany, M.A. et al. (2016) The prognostic significance of STAT3 in invasive breast cancer: analysis of protein and mRNA expressions in large cohorts. *Breast Cancer Res. Treat.*, 156, 9–20.
44. Chiba, T. (2016) STAT3 inhibitors for cancer therapy-the rationale and remained problems. *EC cancer*, 1, S1.
45. Poli, V. et al. (2015) STAT3-mediated metabolic reprogramming in cellular transformation and implications for drug resistance. *Front. Oncol.*, 5, 121.
46. San-Millán, I. et al. (2017) Reexamining cancer metabolism: lactate production for carcinogenesis could be the purpose and explanation of the Warburg Effect. *Carcinogenesis*, 38, 119–133.
47. Jiang, S. et al. (2012) A novel miR-155/miR-143 cascade controls glycolysis by regulating hexokinase 2 in breast cancer cells. *EMBO J.*, 31, 1985–1998.
48. Yue, P. et al. (2009) Targeting STAT3 in cancer: how successful are we? *Expert Opin. Investig. Drugs*, 18, 45–56.
49. Wong, A.L.A. et al. (2017) Do STAT3 inhibitors have potential in the future for cancer therapy? *Expert Opin. Investig. Drugs*, 26, 883–887.
50. Hanahan, D. et al. (2011) Hallmarks of cancer: the next generation. *Cell*, 144, 646–674



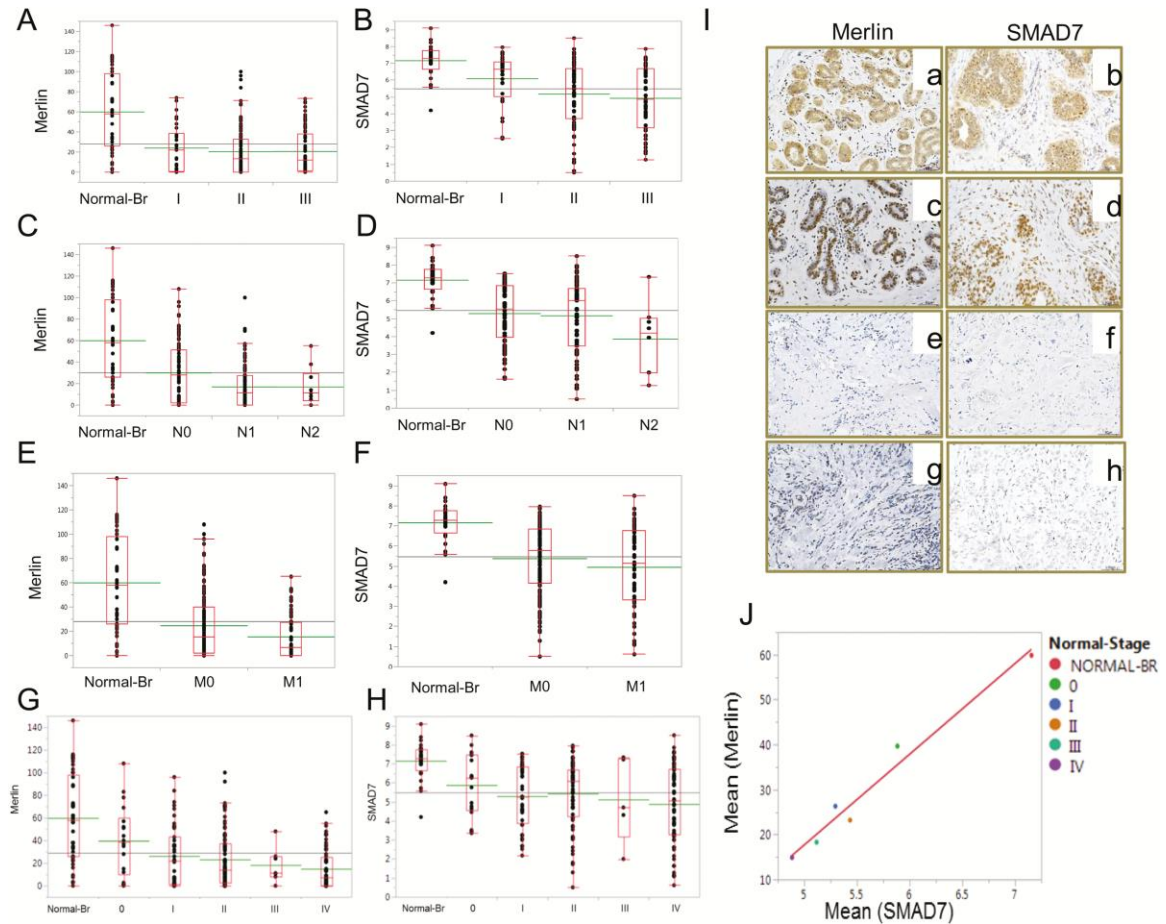


**Figure 1: Loss of Merlin is concordant with the loss of SMAD7 in breast cancer.** Breast tumor tissue microarrays were stained by immunohistochemistry for the expression of Merlin and SMAD7. The staining intensity is depicted as an IHC score. (A, B) represent the scores of Merlin and SMAD7 with respect to the grade of the tumor when compared to normal breast tissue; (C, D) represent IHC scores for Merlin and SMAD7 with respect to nodal involvement; (E, F) represent staining for Merlin and SMAD7 in relation to the occurrence of metastasis; (G, H) represent staining for Merlin and SMAD7 in relation to the disease stage. Mean Merlin and mean SMAD7 IHC scores were computed with respect to tumor grade. The mean Merlin score for normal breast tissue is significantly higher than that in tumor tissues of all grades (Dunnett's test,  $P < 0.0001$  for each). SMAD7 staining intensity decreases with advanced grade of the tumor tissue (normal tissue versus grades II and III: Dunnett's test,  $P < 0.0001$  for each). The difference in SMAD7 intensity with respect to grade I is not significant (Dunnett's test,  $P = 0.0553$ ). The staining intensity for Merlin and SMAD 7 are concordantly significantly decreased with nodal involvement (Dunnett's test,  $P < 0.0001$  for each). Merlin and SMAD7 levels are significantly decreased overall in breast tumor tissues (Dunnett's test,  $P < 0.0001$  for each) regardless of metastasis. (I) Representative immunohistochemistry images are shown for Merlin and SMAD7 staining. Panels a and c represent normal breast tissues stained for Merlin; panels b and d

represent normal breast tissues stained for SMAD7; panels e and g are representative of Merlin staining seen in node negative and metastatic breast cancer tissues; panels f and h depict SMAD7 for the corresponding tissues. **(J)** Denotes the correlation between Merlin expression and SMAD7. A scatterplot of mean IHC scores of Merlin versus SMAD7 shows a very strong positive linear relation between them ( $R^2 = 0.97$ , ANOVA  $P = 0.0003$ ). The resulting least squares regression line (or line of best fit) is  $\text{Mean (Merlin)} = -83.15 + 20.17 * \text{Mean (SMAD7)}$ . It shows that one unit increase in Mean (SMAD7) corresponds on the average to 20.17 units increase in Mean (NF2) levels. Pearson's correlation coefficient between mean Merlin and mean SMAD7 when analyzed with respect to tumor grade is  $r = 0.985$ .

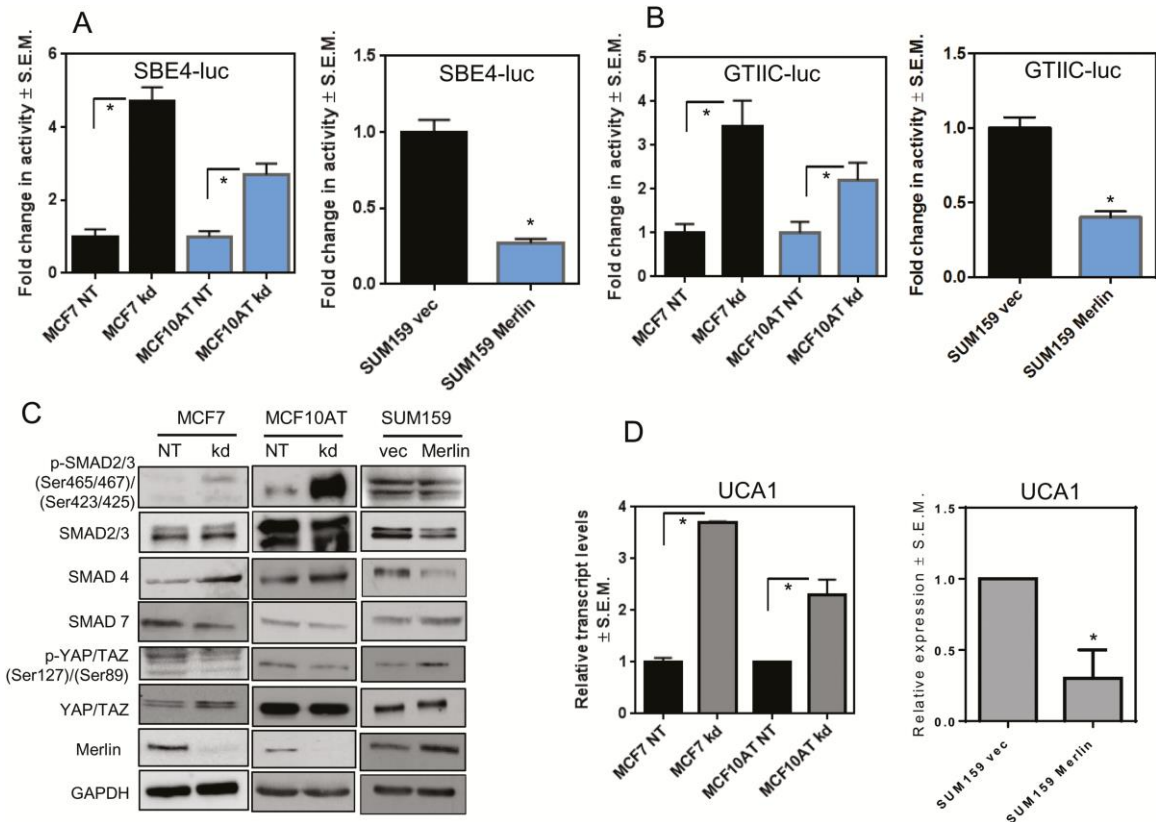


**Figure 2: Merlin deficiency leads to the co-operative activation of YAP/TAZ/SMAD signaling.** MCF7 and MCF10AT cells knocked down for NF2 (MCF7 kd and MCF10AT kd), control (MCF7 NT and MCF10AT NT), and SUM159 cells restored for Merlin expression were analyzed for **(A)** SMAD binding site activity by SBE4 luciferase reporter assay and **(B)** YAP/TAZ activity with an 8XGTIIC luciferase reporter assay. Merlin deficient cells demonstrate upregulated TGF- $\beta$  signaling evidenced by increased activity of the Smad-binding element with concomitant inactive Hippo signaling as evident by increased activity of the TEAD-binding element. Merlin restoration reduced SMAD and YAP/TAZ activities. **(C)** Control and Merlin-deficient MCF7 and MCF10AT cells and SUM159 cells (vector control and Merlin expressing) were immunoblotted for the effectors of TGF- $\beta$  signaling pathway: total SMAD2/3, phosphorylated SMAD2/3 (Ser465/467 and Ser423/425, respectively), SMAD4 and SMAD7, and for members of the Hippo pathway (total YAP/TAZ, inhibitory phosphorylated YAP and TAZ (Ser127 and Ser89, respectively)). GAPDH was used as a loading control. **(D)** Merlin deficient MCF7 and MCF10AT cells (kd) demonstrate significantly increased levels of UCA1. In contrast, SUM159 cells re-expressing Merlin show significantly decreased levels of UCA1. UCA1 levels were analyzed by quantitative RT-PCR.  $\beta$ -actin was used as control gene. Relative expression was measured by  $2^{-\Delta\Delta Ct}$  method.

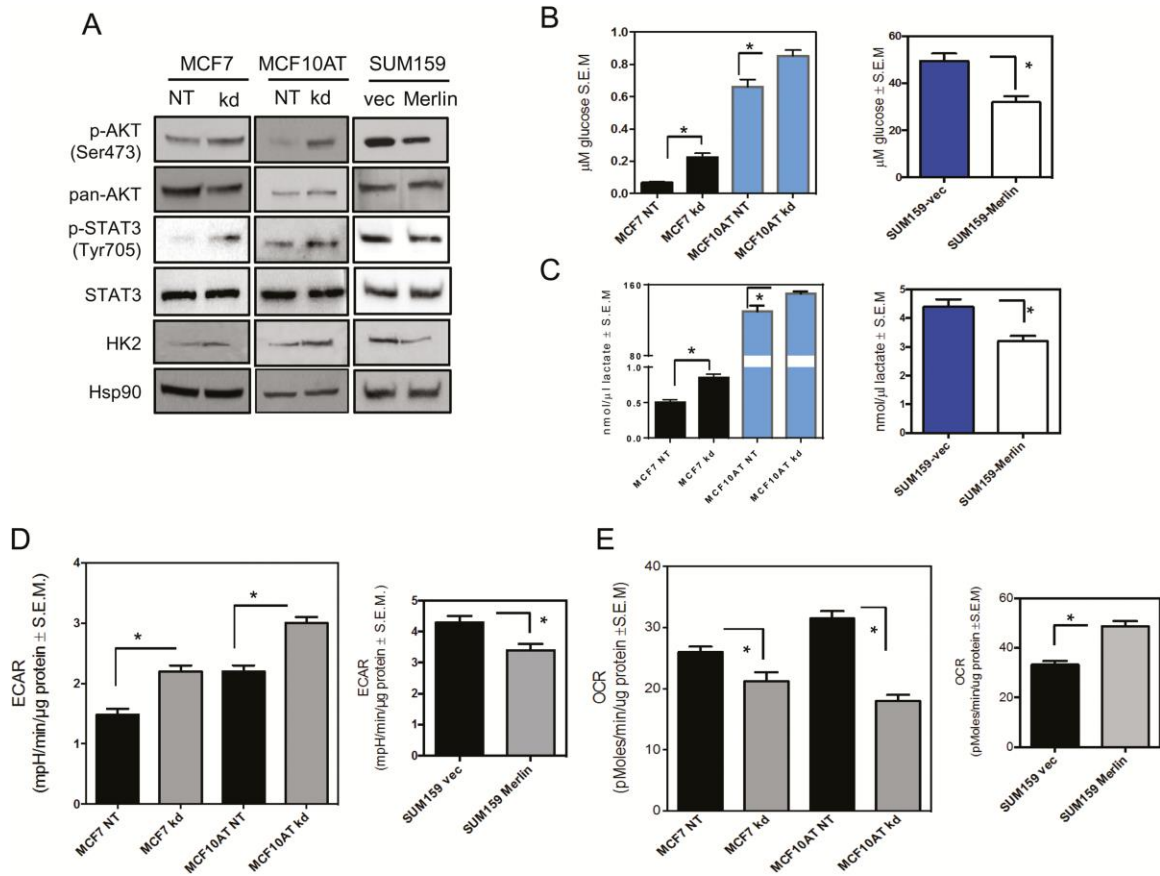


**Figure 3: Loss of Merlin induces bioenergetics alterations in breast cancer cells. (A)** Protein lysates of MCF7 and MCF10AT cells silenced for Merlin (kd) and control (NT) and SUM159 Merlin restored and vector control cells were immunoblotted for STAT3, phosphorylated STAT3 (Tyr705), total AKT (pan-AKT), phosphorylated AKT (Ser473) and HK2. Cell-free culture media of MCF7 and MCF10AT cells knocked down for NF2 (MCF7 kd and MCF10AT kd, respectively), their control (MCF7 NT and MCF10AT NT, respectively) and SUM159 cells (vector control and Merlin-reexpressing) was assayed for **(B)** glucose consumption **(C)** and lactate production. Values were normalized to total protein. **(D)** Cells depleted for Merlin displayed an increased ECAR indicating increased glycolysis in the cells. SUM159 cells restored for Merlin expression demonstrated decreased ECAR. **(E)** Merlin deficient cells demonstrated decreased OCR and increased glycolysis, in contrast to SUM159 cells restored for Merlin expression.

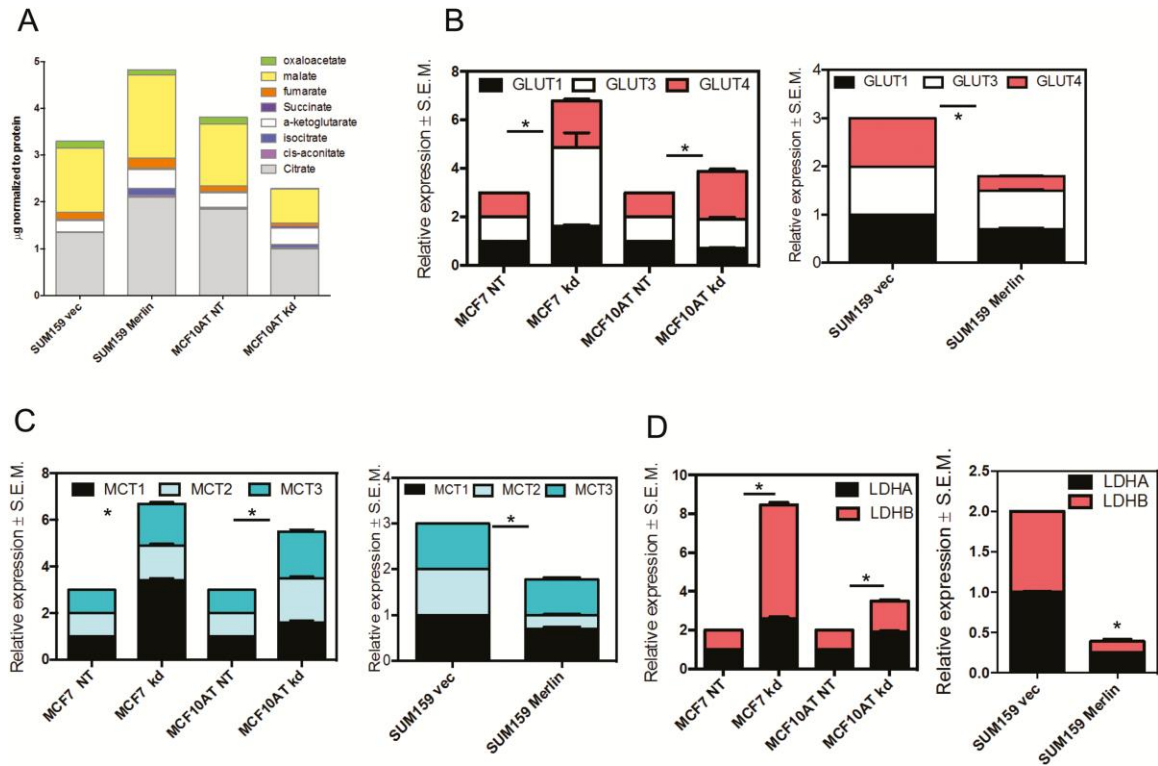


**Figure 4: Merlin keeps a check on cellular metabolism and glycolysis mediators. (A)** The lysates of MCF10AT cells knocked down for Merlin (kd) and the respective control (NT) and SUM159 cells (vector only and restored for Merlin) were analyzed by a targeted metabolomics assessment for the levels of the indicated metabolites of the TCA cycle. Restoration of Merlin increases the total cellular levels of TCA intermediates while Merlin deficiency has the opposite effect. The steady-state transcript levels of glucose transporters (GLUT) (**B**), monocarboxylate transporters transporters (MCT) (**C**) and lactate dehydrogenase (LDHA and LDHB) (**D**) were analyzed by quantitative RT-PCR from MCF10AT and MCF7 cells (NT and kd) and SUM159 cells restored for Merlin (SUM159 Merlin) and their respective vector control (SUM159 vec).  $\beta$ -actin was used as control gene. \* $P < 0.05$  relative to their indicated respective controls.

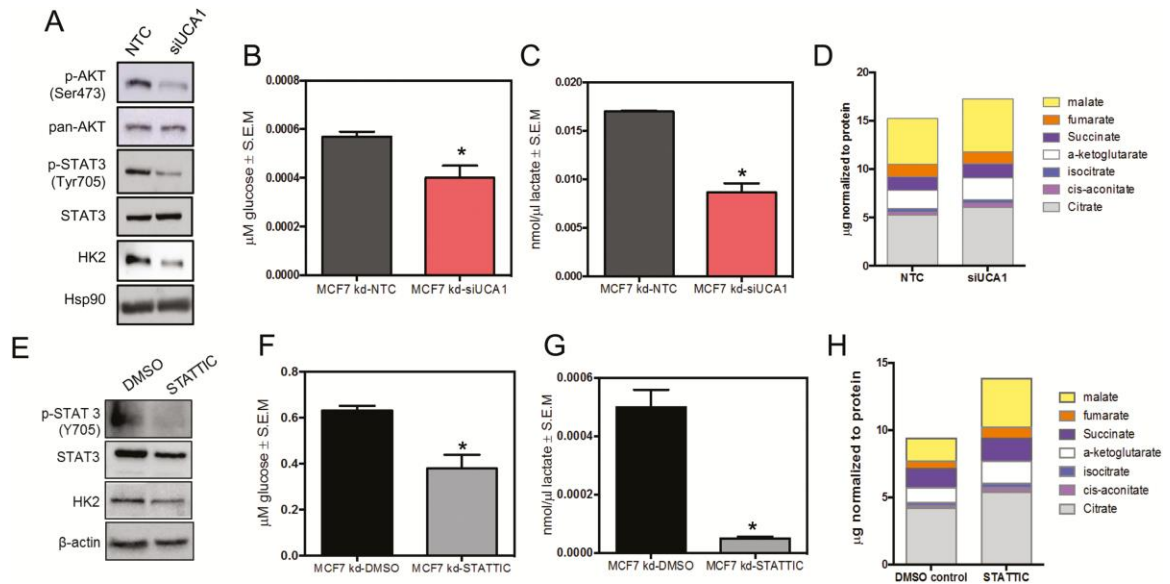


**Figure 5: UCA1 directs cell metabolism towards aerobic glycolysis through AKT and STAT3 activation in Merlin-deficient cells.** (A) Immunoblotting of protein lysates of Merlin-deficient MCF7 cells silenced for UCA1 (siUCA1) and non-target control (NTC) showed reduced level of phosphorylated AKT (Ser473), phosphorylated STAT3 (Tyr705) and HK2 upon UCA1 silencing. HSP90 was used a loading control. The levels of glucose uptake (B) and lactate export (C) were decreased and the overall amounts of metabolites of the TCA cycle were increased (D) as a result of blunted UCA1 expression. (E) Protein lysates of NF2-deficient MCF7 cells treated with 2  $\mu$ M of STATTIC inhibitor or DMSO (vehicle control) for 48h were collected. The expression of phosphorylated STAT3 (Tyr705) and HK2 were attenuated upon STAT3 activity inhibition;  $\beta$ -actin was used as a loading control. The levels of glucose consumption (F) and lactate production (G) were also reduced following STATTIC treatment. (H) There was an overall increase in the amounts of metabolites of the TCA cycle in STATTIC treated MCF7 cells deficient for Merlin. \*P < 0.05.

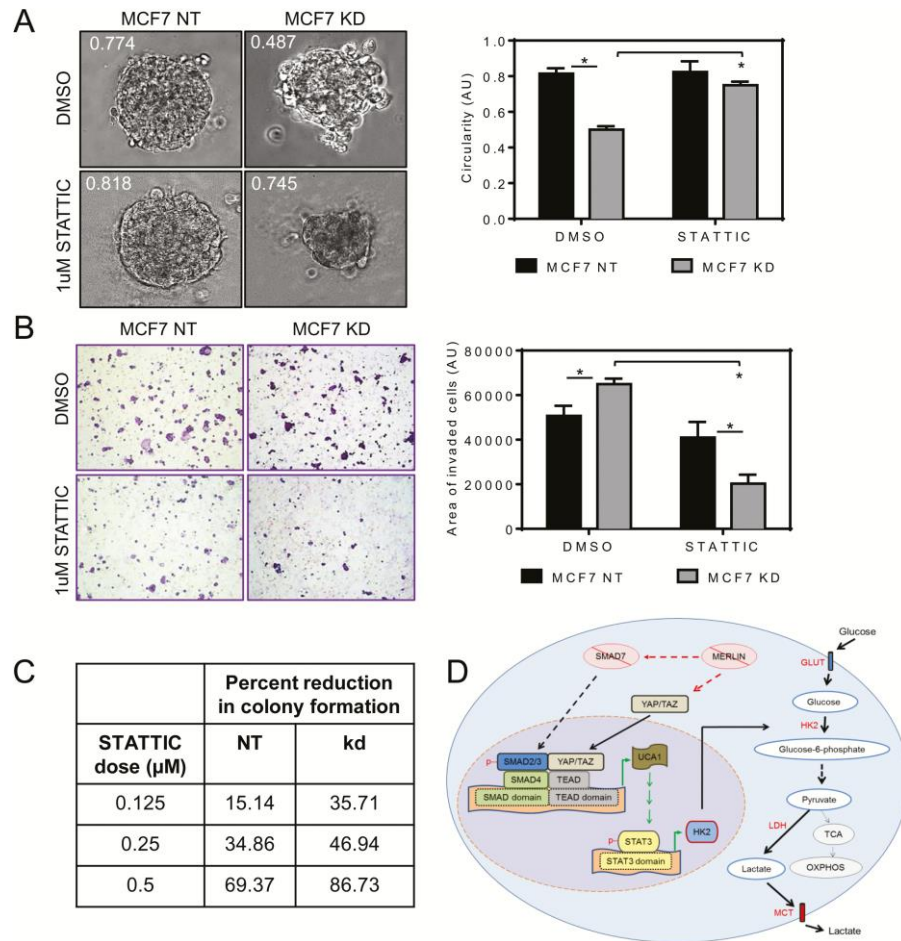


**Figure 6: STAT3 inhibition preferentially impacts Merlin-deficient cells. (A)** Merlin-deficient cells develop an invasive 3D morphology. The STAT3 inhibitor, STATTIC, appears to not only restore circularity to this structure but also limits its growth. **(B)** STATTIC inhibits invasive potential of Merlin-deficient MCF7 cells through the modified Boyden chamber. **(C)** The ability of anchorage-independent growth was assessed by soft agar colony assay and, in a dose-dependent effect, STAT3 inhibition diminished colony formation, being more effective in NF2-silenced cells (kd). \* $P < 0.05$ . **(D)** Deficiency in Merlin expression results in the degradation of SMAD7, which uncouples its inhibitory modulation on the TGF- $\beta$  signaling pathway. The resulting collaborative activity of TGF- $\beta$  and Hippo effectors upregulates HK2 expression that dictates a metabolic preference towards aerobic glycolysis.

MERLIN DEFICIENCY ALTERS THE REDOX MANAGEMENT PROGRAM IN  
BREAST CANCER

by

MATEUS MOTA, BRANDON J. METGE, DOMINIQUE C. HINSHAW, HEBA A.  
ALSHEIKH, DONGQUAN CHEN, RAJEEV S. SAMANT, AND LALITA A. SHEVDE

Submitted for *Molecular Oncology*

Format adapted for dissertation



## Abstract

The expression of Merlin tumor suppressor protein encoded by *NF2* gene is remarkably decreased in metastatic breast cancer tissues. In order to ascribe clinical relevance, we recapitulated the loss of Merlin in breast cancer cells and generated a unique, mammary-specific *Nf2*<sup>-/-</sup> mouse mammary tumor model to overcome embryonic lethality of a total *Nf2*-knockout (*Nf2*<sup>-/-</sup>). Merlin-deficient breast tumor cells and *Nf2*<sup>-/-</sup> mouse embryonic fibroblasts (MEFs) displayed a robustly invasive phenotype. Detailed transcriptomic assessment of *Nf2*<sup>-/-</sup> MEFs revealed notable alterations in redox management networks, implicating a role for Merlin in redox homeostasis. This programmatic alteration resonated with pathways that emerged from breast tumor cells engineered for Merlin deficiency. Further investigations revealed that cells engineered for Merlin deficiency supported reduced activity of the Nrf2 antioxidant transcription factor, concomitant with elevated expression of NADPH oxidase enzymes. Importantly, mammary specific *Nf2*<sup>-/-</sup> in an MMTV Neu+ murine breast cancer model accelerated tumorigenesis. Tumor-derived primary organoids and cell lines were characteristically invasive with evidence of a dysregulated cellular redox management system. As such, Merlin deficiency programmatically influences redox imbalance that orchestrates malignant attributes of mammary/breast cancer.

Keywords: Merlin; ROS; NRF2, NOX, DUOX, breast

## Introduction

The cytoskeleton-associated Merlin tumor suppressor, encoded by the Neurofibromin 2 (*NF2*) gene, is critically involved in sensing cell-cell contact and bringing about contact-dependent inhibition of growth. Merlin functions as a scaffold-like protein that localizes beneath the cell membrane enabling Merlin to integrate extracellular information to ultimately modulate cellular behavior. *NF2*-inactivating mutations are a hallmark of Neurofibromatosis type 2 and some non-nervous system cancers [1-3].

We and others have shown that breast cancer is not associated with any significant mutations and transcript level alterations in the *NF2* gene [4-6]. Despite this, we found that Merlin protein levels are significantly reduced in metastatic breast cancer tissues irrespective of the breast cancer subtype. Mechanistically, we demonstrated that Merlin is post-translationally modified, marking it for ubiquitin-mediated proteasomal degradation [6]. This frames Merlin as a potentially important regulator of malignant attributes. In order to ascribe clinical relevance, we re-capitulated Merlin deficiency in breast cancer cells. To overcome the challenge of embryonic lethality of a total *Nf2*-knockout [7], we have generated a unique mammary-specific *Nf2*-knockout mouse mammary tumor model. Using an unbiased global transcriptomics approach, we identified that Merlin-deficiency programmatically alters a redox management signature, characterized by elevated levels of cellular reactive oxygen species (ROS).

Low-to-intermediate levels of ROS can act as second messengers altering protein functions and regulating signaling pathways [8-12]. In cancer, ROS can reversibly inactivate tumor suppressor proteins, such as phosphatase and tensin homolog (PTEN) [8,

13, 14]; on the other hand, oxidation by ROS can also activate Src family, Ras, and receptor tyrosine kinase (RTK) [11, 12]. Therefore, ROS have become a subject of extensive investigations for supporting tumorigenesis and tumor progression. There is a well-coordinated antioxidant system to ensure ROS maintenance under a tolerable threshold. Nuclear factor erythroid 2-related factor 2 (Nrf2) has a key role in the activation of detoxification- and antioxidant-related genes, including those involved in the synthesis and regeneration of reduced glutathione (GSH), the most abundant antioxidant cofactor [15-17].

In the current study, we have identified that Merlin-deficiency disables the redox management system marked by a redox production system in hyperdrive, and an under-functioning Nrf2 antioxidant system, leading to elevated cellular ROS accumulation. This presents a potentially novel mechanism whereby Merlin keeps ROS levels in check, suppressing tumor formation and progression. This highlights a heretofore unknown mechanism by which Merlin restrains malignant attributes of breast cancer.

## **Materials and methods**

### **Human cell lines**

MCF7 (ATCC, Manassas, VA) and MCF10AT (Karmanos Cancer Center) cell lines were stably knocked down for *NF2*, generating MCF7 KD and MCF10AT KD, respectively. SUM159 cell line (Asterand Biosciences, Detroit, MI) was stably restored for *NF2*, generating SUM159 Merlin. These cell lines were cultured as previously described [6, 18]. The cell lines T47D and BT474 knocked out for *NF2* were acquired from Synthego,

Redwood City, CA and named T47D KD and BT474 KD, respectively. The T47D pair was cultured in RPMI 1640 medium (ThermoFisher, Grand Island, NY) + 10% heat inactivated FBS (ThermoFisher) + 10  $\mu$ g/ml insulin (Sigma-Aldrich, St. Louis, MO). The BT474 pair was cultured in RPMI 1640 + 20% heat inactivated FBS + 10  $\mu$ g/ml human insulin.

### **Mouse embryonic cell line generation**

*Nf2<sup>fl/fl</sup>* mice (BALB/c) were procured from Riken BioResource Research Center (Japan). The strain background was back-crossed onto pure FVB background in the Animal Facility of the University of Alabama at Birmingham (UAB) in accordance with the guidelines of the IACUC. This was confirmed by genome scanning service by Jackson Laboratory (Bar Harbor, ME). Mouse embryonic fibroblasts (MEFs) were harvested from pregnant *Nf2<sup>fl/fl</sup>* mouse on day 13 (d.13), dissociated into a single cell suspension, immortalized with SV40 large T antigen Purified Lentifect Lentiviral Particles (GeneCopoeia, Rockville, MD), and transduced with vector-control CMV-GFP lentivirus or CMV-Cre GFP lentivirus (puro) (Cellomics Technology, Halethorpe, MD), generating MEF *Nf2<sup>fl/fl</sup>* or MEF *Nf2<sup>-/-</sup>*, respectively.

### **Mouse models**

*Nf2<sup>fl/fl</sup>* and MMTV Neu (FVB/N-Tg(MMTVneu)202Mul/J, stock no: 002376) mice (Jackson Laboratory) were maintained and crossed to generate *Nf2<sup>fl/fl</sup>* MMTV Neu mice in the Animal Facility of UAB in accordance with the guidelines of the IACUC. This was confirmed by amplification of genomic DNA from tail clips by PCR.

*Nf2<sup>fl/fl</sup>* MMTV Neu mice went through one pregnancy and litter were weaned 7 days after birth. Following 7 days post-weaning, mice were anesthetized in a container with oxygen/isoflurane flow and placed on an illuminated stereoscope with the snout positioned

into constant oxygen/isoflurane flow tube. Intraductal injection was performed based on Krause et al. 2013 method [19].  $3.6 \times 10^7$  TU vector-control CMV-GFP lentivirus or CMV-Cre GFP lentivirus (puro) (Cellomics Technology) were intraductally injected into the inguinal mammary glands to generate control *Nf2<sup>fl/fl</sup>* MMTV Neu+ or mammary specific *Nf2<sup>-/-</sup>* MMTV Neu+, respectively. The efficiency of the intraductal injection technique was examined by intraductally injecting PBS with 0.2% Evans blue dye, enabling visualization of the mammary ductal tree. Mice were monitored for tumor latency every other day. When tumors reached approximately 12x12mm, mice were euthanized in a CO<sub>2</sub> chamber and tumor harvested.

### **RNA sequencing analysis**

Total RNA was extracted using the RNeasy Mini Kit (Qiagen, Hilden, Germany) per manufacturer's protocol. Preparation of complementary DNA (cDNA) libraries, sequencing using Next Generation Sequencing (NGS) platform, and analysis and interpretation of resultant data were performed by GENEWIZ, South Plainfield, NJ. The datasets used and/or analyzed have been deposited at the Gene Expression Omnibus (GEO) under the accession number GSE157677. Heatmaps for RNA-sequencing data were generated using Morpheus (<https://software.broadinstitute.org/morpheus>). Data was adjusted using one plus log 2, and then a Marker-2 selection (t-test) was performed to generate the top and bottom 100 most significantly altered genes. These genes were then run separately through the GSEA Molecular Signature Database (MSigDB) to generate significantly altered upregulated and downregulated pathways [20, 21]. Specifically, GO Pathway signatures (Biological Processes, Molecular Function, and Cell Component), and oncogenic pathway signatures were selected for analysis. Relevant, significantly altered

pathways are reported in tables. To generate the network figures, respective RNA-sequencing datasets were narrowed down to reflect metabolism-related genes. This was based off of metabolism-related pathways in the KEGG and PANTHER databases. Metabolism-relevant genes were analyzed using NetworkAnalyst [22-24]. Relevant pathways are depicted as network figures with corresponding tables containing relevant gene lists and pathway p-values.

### **NQO1 luciferase reporter assay**

NQO1-ARE luciferase reporter plasmid was donated by Dr. Melissa Fishel from the Indiana University – School of Medicine.  $2 \times 10^4$  cells were seeded in 96-well plates and transfected with 5, 10 or 100ng of NQO1-ARE luciferase reporters using Lipofectamine 2000 Transfection Reagent (Invitrogen, Carlsbad, CA) or FuGENE 6 Transfection Reagent (Promega, Madison, WI) (conditions cell line-dependent). The assay was terminated 30h post-transfection and read according to the Luciferase Assay System (Promega) in a GloMax 20/20 luminometer.

### **Oxidative Stress RT<sup>2</sup> Profiler PCR Arrays**

A panel of oxidative stress-associated genes was analyzed by an RT<sup>2</sup> Profiler PCR Array for Human Oxidative Stress or Mouse Oxidative Stress and Antioxidant Defense (Qiagen). Total RNA was harvested as above, genomic DNA was eliminated, and cDNA synthesized according to the RT<sup>2</sup> First Strand Kit protocol (Qiagen). The array was run on an ABI StepOnePlus (ThermoFisher) thermocycler using RT<sup>2</sup> SYBR Green ROX qPCR Mastermix (Qiagen). Data was analyzed in the GeneGlobe Data Analysis Center (Qiagen; <https://geneglobe.qiagen.com/us/analyze/>). Prooxidant and antioxidant scores were

calculated by summing the fold change expression values of selected genes in *NF2*-silenced or restored cells compared to their controls.

### **Quantitative RT-PCR**

Total RNA was harvested as above and cDNA synthesized using the High Capacity complementary DNA Reverse Transcription kit (Applied Biosystems, Vilnius, Lithuania) per manufacturer's protocol. Human and mouse primer probes to query the gene expression of *NF2*, *NOX4*, *DUOX1*, *DUOX2*, *GCLC*, *GCLM*, and  $\beta$ -*ACTIN* were acquired from ThermoFisher, and quantitative RT-PCR was performed with the TaqMan Fast Advanced Master Mix reagent (Applied Biosystems) on an ABI StepOnePlus (ThermoFisher) thermocycler. Data was analyzed by the  $2^{-\Delta\Delta C_t}$  method.

### **Immunoblotting**

Whole cell protein lysates were obtained by lysing cells with RIPA lysis buffer (Millipore, Darmstadt, Germany) supplemented with Halt Protease and Phosphatase Inhibitor Cocktail (ThermoFisher). Protein lysates were immunoblotted overnight using the following primary antibodies from Cell Signaling Technology (Danvers, MA): Nrf2 (#12721), Keap1 (#8047), SOD1 (#4266), Merlin (#12888); Novus Biologicals: Nox4 (#NB110-58849) and Duox2 (#NB110-61576); GeneTex: Duox1 (#GTX119160). Rabbit IgG HRP-linked whole antibody (from donkey) and mouse IgG HRP-linked whole antibody (GE Healthcare) were used as secondary antibodies and  $\beta$ -actin (Sigma-Aldrich #A3854) as loading control. Signal was detected by ECL Prime or Select Western Blotting Detection Reagents on an Amersham Imager 600 (GE Healthcare). Immunoblot bands were quantified by Alpha Ease software.

### **ROS assay**

ROS levels were assessed by following the instructions of the DCFDA/H2DCFDA - Cellular ROS Assay Kit (Abcam) or Cellular ROS assay kit (Deep Red) (Abcam). When applicable, cells were treated with 10mM L-Glutathione Reduced (Tocris, Bristol, UK) for 18h before ROS measurement. Ultra pure water was used vehicle control. Fluorescence was measured by the BD Accuri™ C6 Plus flow cytometer (BD Biosciences, San Jose, CA) using the FITC or APC channels.

### **Transwell invasion assay**

Cells were pretreated with 10mM L-Glutathione Reduced (Tocris) or ultra pure water as vehicle control for 18h, followed by seeding in serum-free growth medium in BioCoat Matrigel Invasion Chambers (Corning, Bedford, MA). Serum-free growth medium containing 10ug/ml of fibronectin was added to the bottom of each well where the invasion chambers were inserted. After incubation in 5% CO<sub>2</sub> incubator at 37°C for 16h, cell-seeded invasion chambers were fixed with 4% paraformaldehyde for 10 minutes at RT, stained with 0.1% crystal violet/10% ethanol for 10 min at RT, and rinsed with deionized water. Images of four random fields on each of two chambers for each condition were visualized by Nikon Eclipse E200 and photographs of inserts captured using the 10x objective of the DS-L4 microscope system (Nikon, Tokyo, Japan). Area of invaded cells was measured by ImageJ.

### **3D culture assay**

A suspension of  $5 \times 10^3$  cells in growth media supplemented with 2% 3D Culture Matrix Reduced Growth Factor Basement Membrane Extract (R&D Systems, Minneapolis, MN) was seeded in pre-coated chamber cover glass slide (Millipore, Ireland)



with undiluted 3D Culture Matrix Reduced Growth Factor Basement Membrane Extract (R&D Systems).. The seeded cells were incubated in 5% CO<sub>2</sub> at 37°C with media replaced every other day; when treated with L-Glutathione Reduced, media were replaced every day. When acini-like structures were formed, cells were washed with PBS, fixed with 2% paraformaldehyde + 0.1% glutaraldehyde in PBS for 30 minutes, permeabilized with 0.1% Triton-X-100 for 15 minutes, and blocked with 5% BSA 0.1% Triton-X-100 in PBS for 1h at room temperature (RT). Cells were labeled with anti-laminin-5 ( $\gamma$ 2 chain) antibody, clone D4B5 (Millipore #MAB19562) overnight followed by secondary antibody incubation with goat anti-mouse IgG1 cross-adsorbed secondary antibody, Alexa Fluor 594 (Invitrogen, Eugene, OR) for 1h at RT. Nuclei were stained with VECTASHIELD Antifade Mounting Medium with DAPI (Vector Laboratories, Burlingame, CA). Acinar morphology was captured using the 20x objective of Nikon Eclipse Ti-U microscope (Nikon, Tokyo, Japan).

### **Vinculin/F-actin Immunofluorescence**

Cells were seeded on a poly-L-lysine-coated cover slip (Corning). After 48h under 5% CO<sub>2</sub> at 37°C incubation, the cells were fixed with 4% paraformaldehyde for 30 minutes and permeabilize with 2% Triton-X-100 for 15 minutes at RT. Blocking with 5% BSA + 2% Triton-X-100 for 1h at RT was followed by co-incubation with Alexa Fluor 594 Phalloidin (ThermoFisher) and monoclonal anti-vinculin antibodies (Sigma-Aldrich, St. Louis, MO) for 1h at RT. Then, cells were washed 3x with PBS and incubated with goat anti-mouse IgG (H+L) cross-adsorbed secondary antibody, Alexa Fluor 488 (Invitrogen, Eugene, OR) for 1h at RT. After 3x washes with PBS, the cover slip was mounted on a

slide with VECTASHIELD antifade mounting medium with DAPI. Images were acquired on Nikon Eclipse Ti-U using the 40x objective.

### **Immunohistochemistry**

Sections from paraffin-embedded tissue were deparaffinized and rehydrated through passages in xylene and graded ethanol. Heat-induced antigen retrieval was performed in boiling sodium citrate buffer for 5 minutes, followed by incubation with Dual Endogenous Enzyme Block (Dako, Carpinteria, CA) for 15 minutes. Following 10-minute wash with Tris-buffered NaCl solution supplemented with 0.01% Triton-X-100, tissues were blocked with 3% goat serum for 40 minutes and incubated with NF2/Merlin Antibody (Novus Biologicals # NBP1-33531) or HNE-Michael Adducts (Millipore #393207) overnight in 4°C. After washing, EnVision+ System- HRP Labelled Polymer Anti-Rabbit (Dako) was applied for 40 minutes at room temperature. For antibody visualization, tissues were incubated with Liquid DAB+ Substrate Chromogen System (Dako) for 7 minutes and counterstained with Harris Hematoxylin (Surgipath; diluted 1:2 in tap water). After tissue dehydration, slides were mounted in Cytoseal (ThermoScientific) with coverslips. Images were visualized by Nikon Eclipse E200 and captured using the 40x objective of the DS-L4 microscope system (Nikon). The immunostaining score was based on the method described on Frolova et al. 2009 [25].

### **Clinical database**

For survival analysis, patient's microarray data for 683 breast cancer primary tumors [26] was accessed from public data portal (<https://xenabrowser.net>) June 2020. Normalized microarray data was used as NF2 gene expression values, and the median was used to classify samples into high and low expression groups for distant metastasis free

survival analysis. A Kaplan-Meier curve was generated and log-rank test applied. Patient's protein data, measured by reverse-phase protein array (RPPA) for 887 breast cancer primary tumors (cohort: Invasive Carcinoma TCGA, Firehouse Legacy) was accessed from public data portal (<https://www.cbioportal.org>) in August 2020. Data were extracted for analysis and NF2 protein expression were examined in correlation of Neoplasm Disease Lymph Node Stage American Joint Committee on Cancer Code. Another cohort of 747 breast cancer primary tumors from TCGA Breast Cancer - BRCA was accessed from public data portal (<https://xenabrowser.net>) in August 2020. Data were extracted for analysis and NF2 protein expression was examined in correlation of axillary lymph node stage (Pathological\_N). One-way Anova method was used for statistical analysis, using GraphPad Prism version 8 (GraphPad Software, La Jolla, CA). Comparisons were considered statistically significant for p-value < 0.05.

### **Statistical analysis**

An unpaired Student's *t* test was applied for statistical analysis, unless otherwise mentioned, using GraphPad Prism version 8. Comparisons were considered statistically significant for p-value < 0.05. Error bars represent +/- S.E.M.

## **Results**

### **Merlin deficiency modulates a redox signaling signature.**

In order to evaluate a role for Merlin in the context of normal biology, we harvested embryonic fibroblasts from *Nf2<sup>fl/fl</sup>* female mice and immortalized these mouse embryonic fibroblasts (MEFs) with SV40 large T antigen lentiviral particles. We stably transduced these MEFs with either Cre-expressing lentivirus to knockout *Nf2* (MEF *Nf2<sup>-/-</sup>*

) or control empty vector (MEF *Nf2<sup>fl/fl</sup>*) (Fig. 1A). In order to characterize alterations in gene expression as a result of *Nf2* loss, we sequenced the transcriptome of these MEFs (Fig. S1A). This revealed prominent alterations in metabolism-related pathways. Further data inquiry through the Network Analyst platform revealed significant downregulation of signatures related to glutathione transferase and antioxidant activities (Fig. 1B). We also performed RNAseq analysis of MCF10AT breast tumor cells stably silenced for *NF2* (MCF10AT KD). Similar to *Nf2<sup>-/-</sup>* MEFs, MCF10AT cells deficient for Merlin showed downregulation of redox-associated pathways compared to their control MCF10AT NT cells (Fig. S1B). These data suggest that the association between Merlin and redox mechanisms is not breast cancer system-specific; rather it is a direct consequence of Merlin deficiency.

Redox imbalance is reflective of either decreased clearance or increased production of ROS. Thus, in order to examine the effect of Merlin deficiency in modulating the cellular redox profile, we assessed a panel of human oxidative stress-associated genes by a quantitative PCR array comparing *NF2*-silenced breast cancer cells MCF7 (MCF7 KD), T47D (T47D KD), and MEF *Nf2<sup>-/-</sup>* to their respective non-target control transfectants MCF7 (MCF7 NT) (Fig. S1C), T47D (T47D NT) (Fig. S1D), and MEF *Nf2<sup>fl/fl</sup>* (Fig. S1E). Cells stably silenced for Merlin show significant alterations in antioxidant and prooxidant genes [MEFs (Fig. 1C) and MCF7 (Fig. 1D)]. Moreover, silencing of *NF2* manifests as a lower magnitude of change in antioxidant genes relative to prooxidant genes (Fig. 1F). Conversely, the redox profile of *NF2*-restored SUM159 (SUM159 Merlin) and its vector control SUM159 (SUM159 VEC) (Fig. 1E; Fig. S1F) showed higher magnitude of cumulative change of antioxidant genes than prooxidant

genes (Fig. 1F). Collectively, the data supports a role for Merlin in regulating redox homeostasis in breast cancer cells.

### **ROS clearance attenuates migratory and invasive phenotypes in *NF2*-deficient cells.**

Based on leads presented thus far, we surmised that loss of Merlin would alter cellular levels of ROS. In fact, Merlin-deficient MCF7 and T47D cells show significantly greater levels of total ROS (Fig. 2A and 2B). In order to test if higher ROS accumulation could be a consequence of defective quenching mechanisms, we cultured cells in medium supplemented with GSH (+ GSH). Exogenous administration of cell-permeable GSH reduced ROS levels in both, MCF7 KD (Fig. 2A) and T47D KD (Fig. 2B) breast cancer cells, suggestive of a dysfunctional ROS clearance system in context of Merlin deficiency.

As a tumor suppressor recognized for its role in regulating proliferation, we queried the relationship between deficiency of Merlin protein and clinical attributes of breast cancer using publicly available data. Tumor tissues deficient in Merlin protein expression show greater lymph node involvement as coded by nodal status assessment from different studies (Fig. S2A and S2B). The ability of tumor cells to spread and invade is a key behavior associated with tumor progression and aggressiveness. Interestingly, MEF *Nf2*<sup>-/-</sup> cells showed an upregulated molecular signature associated with cytoskeletal rearrangement and cell motility compared to MEF *Nf2*<sup>fl/fl</sup> cells (Fig. S2C). We assessed focal adhesion, an important attribute of cell migration, by staining for vinculin/F-actin assembly. Vinculin is essential at focal adhesions, providing the mechanical force for traction and strengthening of integrin-F-actin linkages. While MCF7 NT (Fig. 2C) and MEF *Nf2*<sup>fl/fl</sup> (Fig. 2D) presented with shorter and less protruded

lamellipodia, MCF7 KD (Fig. 2C) and MEF *Nf2<sup>-/-</sup>* (Fig. 2D) displayed longer and more extended lamellipodia, suggesting enhanced migratory capability. In addition, actin filaments are less organized in the MCF7 KD (Fig. 2C-inset) and MEF *Nf2<sup>-/-</sup>* (Fig. 2D-inset) cells compared to their controls, reaffirming the role of Merlin in arranging the cytoskeleton. Exogenous GSH reversed these cytoskeletal changes suggesting that elevated ROS levels impinge upon focal adhesions in the context of Merlin-deficiency (Fig. 2C and 2D). Concordant with this, MCF7 KD and T47D KD cells are remarkably more invasive than MCF7 NT (Fig. 2E) and T47D NT cells (Fig. 2F), respectively, and GSH mitigates this invasiveness in KD cells. In order to evaluate the invasive properties in 3D, we cultured cells as spheroids in a 3D matrix. MCF7 NT spheroids displayed an intact basement membrane stained with laminin V and formed a circumscribed acinar structure in 3D cell culture (Fig. 2G). On the other hand, MCF7 KD spheroids presented a breached basement membrane, with distinct projections indicating an invasive phenotype (Fig. 2G). Treatment of MCF7 KD cells with exogenous GSH attenuated this invasive behavior, indicating that elevated ROS levels contribute to notably enhanced malignant phenotypes in *NF2*/Merlin-deficient cells. Thus, in the context of Merlin deficiency, elevated ROS configures an invasive phenotype.

### **Merlin-deficient breast cancer cells display a dysfunctional anti-oxidant system.**

GSH is synthesized *de novo* in a two-step reaction where the rate-limiting step is mediated by glutamate-cysteine ligase (GCL). GCL is comprised of the GCL catalytic (*GCLC*) and GCL modifier (*GCLM*) subunits [27, 28]. Expression of these two subunits was negatively impacted by Merlin deficiency (Fig. 1C and D) while restoring Merlin induced the expression of both genes (Fig 1E). Further, validation of *GCLC* and *GCLM*

transcript levels showed that their steady-state expression was downregulated in MCF7 KD (Fig. 3A and B, respectively), T47D KD (Fig. 3C and D, respectively), and MCF10AT KD (Fig. S3A and S3B, respectively) compared to their NT controls. Conversely, gene expression of both, *GCLC* and *GCLM*, was upregulated in SUM159 Merlin expressors (Fig. 3E and 3F) compared to SUM159 VEC, suggesting that Merlin impacts key determinants of the rate of GSH *de novo* synthesis.

Both, *GCLC* and *GCLM* are *bonafide* transcriptional targets of the Nrf2 transcription factor. Nrf2 is a master regulator in cellular stress response and plays a key role in the activation of antioxidant and detoxification genes. We used an NQO1-driven Nrf2 luciferase assay as a readout of Nrf2 activity [29]. Nrf2 activity was significantly reduced in MCF7 KD (Fig. 3G), T47D KD (Fig. 3H), and MCF10AT KD (Fig. S3C) cells compared to their respective controls; while SUM159 Merlin expressor cells supported upregulated Nrf2 activity (Fig. 3I). The protein levels of Nrf2 were aligned with the levels of Merlin (Fig. 3J; Fig. S3D). Nrf2 is a substrate of Keap1 adaptor protein which assists in Nrf2 degradation via Cul3-dependent ubiquitin ligase complex. *NF2*-silenced cells showed elevated Keap1 expression compared to their controls (Fig. 3J) suggesting that attenuation of Nrf2 activity in conditions of Merlin deficiency may be caused by increased Keap1-dependent Nrf2 degradation.

We see that the levels of SOD1, also an Nrf2 transcriptional target [30], are decreased in breast tumor cells deficient for Merlin in comparison to their respective controls; while SUM159 Merlin expressors support increased SOD1 levels (Fig. 3K). SOD1 mediates the conversion of superoxide ( $O_2^{\cdot-}$ ) into hydrogen peroxide ( $H_2O_2$ ) so it can be broken down into  $H_2O$  in a GSH-dependent enzymatic reaction. Decreased SOD1

levels also foster conditions that are permissive for accumulation of superoxide ( $O_2^{\cdot-}$ ) in cells [31]. As such, reduced Nrf2 activity, decreased levels of *GCLC*, *GCLM*, and *SOD1* cumulatively reflect a remarkable decrease in the antioxidant system, corresponding with an overall increase in cellular ROS in Merlin-deficient cells.

### **Merlin deficiency upregulates proteins from the pro-oxidative NOX family.**

In addition to a compromised anti-oxidant system, increased ROS accumulation could result from increased ROS generation. Among the prooxidant-associated genes detected in the gene expression array of Merlin-deficient cells (Fig. 1C and 1D), NADPH oxidase 4 (NOX4), Dual oxidase 1 (DUOX1) and DUOX2 were of great interest because they belong to the NADPH oxidase (NOX) family which is recognized for its role in generating ROS. Thus, in order to confirm the impact of Merlin deficiency on the expression of NADPH oxidase enzymes, we evaluated the steady state transcript levels of NOX4, DUOX1, and DUOX2. Expression of all – NOX4, DUOX1, DUOX2 – were upregulated in MCF7 KD (Fig. 4A, 4B, 4C) and T47D KD (Fig. 4D, 4E, 4F) cells compared to their control counterparts. Additionally, expression of NOX4 and DUOX2 was also increased in MCF10AT KD compared to NT cells (Fig. S4). Not just limited to tumor cells, we see that MEF *Nf2<sup>-/-</sup>* cells support elevated levels of NOX4 and DUOX2 (Fig. 4G, H, I) compared to MEF *Nf2<sup>fl/fl</sup>*. In contrast, SUM159 cells restored for Merlin showed a significant decrease in NOX4, DUOX1, and DUOX2 transcripts (Fig. 4J, 4K, 4L). The expression of NOX4, DUOX1, and DUOX2 proteins are largely consistent with the observed transcript levels (Fig. 4M). Overall, we see that expression of NADPH oxidase enzymes is increased in Merlin-deficient conditions and re-expression of Merlin reverses this trend.



## Genetically-engineered oncogene-driven Merlin deficient mammary tumors harbor elevated oxidative stress.

In order to investigate the functional and mechanistic role of Merlin on mammary tumor development *in vivo*, we generated a *Nf2<sup>fl/fl</sup>* MMTV Neu mouse model and intraductally injected female mice with Cre-expressing lentivirus to generate a mammary-specific *Nf2* knockout mouse (*Nf2<sup>-/-</sup>* MMTV Neu+) (Fig. 5A). We confirmed *Nf2* deletion in the mammary gland by immunohistochemistry (IHC) that showed significantly reduced Merlin levels in *Nf2<sup>-/-</sup>* MMTV Neu+ mammary glands compared to *Nf2<sup>fl/fl</sup>* MMTV Neu+ mammary glands (Fig. 5B). The minimum residual amounts of Merlin in the *Nf2*-deleted tissue is likely a consequence of mosaicism of Cre activity. 4-hydroxynonenal (4-HNE) serves as a surrogate indicator of oxidative stress in tissues [32, 33]. We stained these mammary glands for 4-HNE. *Nf2<sup>-/-</sup>* MMTV Neu+ mammary glands demonstrated remarkably increased staining for 4-HNE residues compared to glands from *Nf2<sup>fl/fl</sup>* MMTV Neu+ mice (Fig. 5B), recapitulating the *in vitro* impact of Merlin deficiency in the accumulation of ROS.

In the *Nf2*-deleted mammary glands, tumor latency was shorter - at day 56, 50% of the mice in the *Nf2<sup>-/-</sup>* MMTV Neu+ group were tumor-free, while that mark was hit at day 74 for the control group (Fig. S5A). In addition, the level of Merlin in *Nf2<sup>-/-</sup>* MMTV Neu+-derived tumor tissue was significantly lower than in the tumors derived from *Nf2<sup>fl/fl</sup>* MMTV Neu+ mice (Fig. 5C), suggesting that faster tumor onset was attributable to *Nf2* deletion. In order to score the level of oxidative stress in the tumor tissues, we evaluated 4-HNE staining. The intensity of 4-HNE detection was significantly greater in *Nf2<sup>-/-</sup>* MMTV Neu+-derived tumor tissue (Fig. 5C), indicative of an increased oxidative stress in these tumors that developed with shorter latency.

In order to evaluate the phenotype that these tumor cells would display in 3D, we evaluated the morphology of tumor-derived organoids in 3D culture. *Nf2<sup>fl/fl</sup>* MMTV Neu+-derived primary tumor cells formed spheroids with a defined, intact morphology and few projections. This was in stark contrast with *Nf2<sup>-/-</sup>* MMTV Neu+ organoids that presented a breached, disorganized structure (Fig. 5D). We also established primary cell lines from *Nf2<sup>fl/fl</sup>* MMTV Neu+- (283) and *Nf2<sup>-/-</sup>* MMTV Neu+- (285) derived primary tumors. Interestingly, 285 showed notably higher levels of NOX4, DUOX1, and DUOX2 than 283 (Fig. 5E), further supporting that the expression of these pro-oxidative proteins is regulated by Merlin.

## Discussion

The role of ROS in cancer biology has been contentious. Basal levels of ROS are critical to relay signal transduction and maintain proper tissue function [34, 35]. However, distorted redox homeostasis during tumorigenesis as well as metastasis can be lethal. In order to avoid oxidative stress, tumor cells increase their antioxidant ability to prevent toxic accumulation of ROS [28].

Breast cancer patients with high-Merlin expressing tumors manifested higher rates of distant metastasis free survival compared to patients with tumors having lower levels of Merlin (Fig. S5B). Our investigations have revealed that Merlin-deficiency dysregulates the cellular redox management program, eliciting a markedly invasive phenotype in MEFs and breast cancer cells. This is also recapitulated in our mammary-specific *Nf2*-knockout mice, which presented with significantly accelerated development of invasive tumors.

Participating as a cofactor in antioxidant enzymatic reactions, GSH enables breakdown of H<sub>2</sub>O<sub>2</sub> into non-toxic components [27, 36]. In Merlin-deficient model systems, dysregulated ROS accumulation impacted an invasive cytoskeletal reconfiguration. Exogenous GSH mitigated the effects of Merlin-deficiency, evident as decreased invasive potential of *NF2*/Merlin-defective cells. These data established a role for elevated ROS in regulating malignant behavior in the context of Merlin-deficiency and put the spotlight on the Nrf2 transcription factor.

Nrf2 homeostatic levels are regulated by ubiquitination and degradation mediated by KEAP1, an E3 ubiquitin ligase substrate adaptor. Under oxidative stress, KEAP1 is oxidized and undergoes a conformational change, releasing its repression on Nrf2 [16, 17, 37]. Breast tumor cells engineered for Merlin-deficiency supported significantly diminished Nrf2 activity, marked by decreased levels of anti-oxidant regulators and effectors. Additionally, when Merlin levels are compromised, NOX4, DUOX1, and DUOX2 proteins were significantly elevated. These NOX enzymes actively generate ROS [34, 38, 39] and are upregulated in several types of malignancies including breast cancer [6, 40-47]. Notably, oxidative stress resultant of NOX-derived ROS is the main promoter of tumorigenesis, invasion and metastasis [9]. Our investigations have revealed that Merlin-deficiency disables the redox management system. The redox production system is aberrantly activated simultaneous with an under-functioning of the Nrf2 antioxidant system, leading to intensified oxidative stress. Oxidative stress aids in the formation of invadopodia during tumor cell invasion and migration by enabling cytoskeletal rearrangements, and by stimulating proteolytic degradation of ECM components [48, 49]. In a breast cancer model, tumor cells that survived hypoxia showed

a ROS-resistant phenotype that provided invasive and metastatic advantage [50]. We see that Merlin deficient cells are unable to effectively limit ROS accumulation and also are resistant to and survive the resultant oxidative stress, with a remarkable invasive phenotype.

White and colleagues demonstrated that in cells harboring mutant Merlin, activation of YAP/TAZ programs a metabolic circuitry that enables growth and proliferation. In the absence of exogenous growth factors, *NF2*-mutant tumor cells rely on YAP/TAZ-signaling to maintain growth-promoting signaling through engaging the activities of AKT and RTKs. Interestingly, they reported that YAP/TAZ function to limit mitochondrial respiration, prevent ROS buildup, and reduce oxidative stress cell death under nutrient stress such as glutamine deprivation [51]. We previously demonstrated that Merlin-deficient breast cancer cells metabolically adapt towards aerobic glycolysis by cooperatively engaging SMAD-Hippo signaling [52]. Our current findings indicate that Merlin deficiency enables ROS accumulation – a contrast to the previous study that can be explained by several factors – our studies are centered on breast cancer cells that do not harbor mutations in *NF2* and are not conducted in nutrient-limiting conditions. Additionally, NOX enzymes are well-known producers of intracellular ROS. This suggests that the main source of generation of ROS in our system is not sustained by mitochondrial-related activities. It also is likely that co-operative activity of Hippo and SMAD signaling orchestrates a metabolism in nutrient-replete conditions that is distinct from that in nutrient-limiting conditions.

In the cell cortex, Merlin integrates extracellular cues and intracellular responses [1-3]. As such, its loss or deficiency enables the activation of several signaling pathways

that converge upon unrestricted cell growth [53]. Many of these mechanisms can lead to elevated cellular ROS, which in turn, can aberrantly activate several signaling nodes [9, 54, 55]. Thus, it is unsurprising that a total Merlin knockout has an embryonic lethal phenotype. Our new mammary model of Merlin deficiency surmounts this limitation and uncovers a potential mechanism whereby Merlin keeps levels of ROS in check, suppressing mammary tumor formation and invasive behavior. The findings endorse a novel function for Merlin in restraining tumorigenesis and tumor progression that is beyond its well-known function in hindering over-proliferation.

### **Conclusion**

In conclusion, we find that lack of normal Merlin function induces mismanagement of the cellular redox system, converging upon unrestricted cell growth and intensification of malignant attributes. Mechanisms of ROS management, represented by Nrf2-related clearance functions and ROS generation associated with NADPH oxidase enzyme family, were altered in Merlin-deficient breast cancer cells. This is also reflected in elevated levels of oxidative stress marked by 4-HNE staining. The use of MEFs, a non-cancerous cell system, evidences that the impact of Merlin deficiency reaches beyond breast cancer biology. The findings uncover a novel mechanism by which Merlin intersects with redox homeostasis in restricting malignant characteristics.

### **Data accessibility**

The datasets for the RNA sequencing of the MEF cell lines have been deposited at the Gene Expression Omnibus (GEO) under the accession number GSE157677.

### **Author contribution**

MM, BM, RS, and LS designed the study and experiments. MM conducted the *in vitro* experiments. MM and BM conducted the *in vivo* experiments. DH acquired the molecular signature database. HA acquired the clinical database. DC extracted and edited the RNA sequencing dataset. MM, BM, DH, HA, DC, RS, and LS analyzed and interpreted the results. MM and LS wrote the manuscript.

### **Acknowledgements**

We thank Dr. Melissa Fishel from the Indiana University – School of Medicine for the NQO1-luciferase construct and Sarah Kammerud from the University of Alabama at Birmingham – Department of Pathology for critical reviewing and editing of the manuscript. This work was supported by CA169202 (NCI/NIH) to L.A.S., the United States Department of Defense [W81XWH-18-1-0036 and W81XWH-19-1-0755 to L.A.S.], the University of Alabama at Birmingham AMC21 [to L.A.S.], the Breast Cancer Research Foundation of Alabama [to L.A.S.], Merit Review Award number I01 BX003374 (from the U.S. Department of Veterans Affairs BLRD service BX003374) and CA194048 (NCI/NIH) to R.S.S.

### **Conflict of interest**

The authors declare no potential conflicts of interest.

## Abbreviations

DUOX = Dual oxidase

GCLC = Glutamate-cysteine ligase catalytic subunit

GCLM = Glutamate-cysteine ligase modifier subunit

GPX = Glutathione peroxidase

GSH = reduced glutathione

GSSG = Glutathione disulfide

GR = Glutathione reductase

MEF = Mouse embryonic fibroblast

MMTV = Mouse mammary tumor virus

NADPH = Reduced nicotinamide adenine dinucleotide phosphate

NEU = erb-b2 receptor tyrosine kinase 2

NF2 = Neurofibromin 2

NOX = NADPH oxidase

Nrf2 = Nuclear factor, erythroid 2 like 2

ROS = Reactive oxygen species

SOD = Superoxide dismutase

## References

1. Li, W., et al., *Merlin: a tumour suppressor with functions at the cell cortex and in the nucleus*. EMBO reports, 2012. **13**(3): p. 204-215.
2. Cooper, J. and F.G. Giancotti, *Molecular insights into NF2/Merlin tumor suppressor function*. FEBS Lett, 2014. **588**(16): p. 2743-52.
3. Petrilli, A.M. and C. Fernández-Valle, *Role of Merlin/NF2 inactivation in tumor biology*. Oncogene, 2016. **35**(5): p. 537-48.
4. Arakawa, H., et al., *Alternative splicing of the NF2 gene and its mutation analysis of breast and colorectal cancers*. Hum Mol Genet, 1994. **3**(4): p. 565-8.
5. Yaegashi, S., et al., *Low incidence of a nucleotide sequence alteration of the neurofibromatosis 2 gene in human breast cancers*. Jpn J Cancer Res, 1995. **86**(10): p. 929-33.
6. Morrow, K.A., et al., *Loss of tumor suppressor Merlin in advanced breast cancer is due to post-translational regulation*. J Biol Chem, 2011. **286**(46): p. 40376-85.
7. McClatchey, A.I., et al., *The Nf2 tumor suppressor gene product is essential for extraembryonic development immediately prior to gastrulation*. Genes Dev, 1997. **11**(10): p. 1253-65.
8. Liou, G.-Y. and P. Storz, *Reactive oxygen species in cancer*. Free radical research, 2010. **44**(5): p. 479-496.
9. Hurd, T.R., M. DeGennaro, and R. Lehmann, *Redox regulation of cell migration and adhesion*. Trends Cell Biol, 2012. **22**(2): p. 107-15.
10. DeBerardinis, R.J. and N.S. Chandel, *Fundamentals of cancer metabolism*. Science advances, 2016. **2**(5): p. e1600200-e1600200.
11. Weng, M.-S., et al., *The interplay of reactive oxygen species and the epidermal growth factor receptor in tumor progression and drug resistance*. Journal of experimental & clinical cancer research : CR, 2018. **37**(1): p. 61-61.
12. Perillo, B., et al., *ROS in cancer therapy: the bright side of the moon*. Exp Mol Med, 2020. **52**(2): p. 192-203.
13. Hecht, F., et al., *The role of oxidative stress on breast cancer development and therapy*. Tumour Biol, 2016. **37**(4): p. 4281-91.
14. Chio, I.I.C. and D.A. Tuveson, *ROS in Cancer: The Burning Question*. Trends in molecular medicine, 2017. **23**(5): p. 411-429.



15. Gorrini, C., I.S. Harris, and T.W. Mak, *Modulation of oxidative stress as an anticancer strategy*. Nat Rev Drug Discov, 2013. **12**(12): p. 931-47.
16. Niture, S.K., R. Khatri, and A.K. Jaiswal, *Regulation of Nrf2-an update*. Free Radic Biol Med, 2014. **66**: p. 36-44.
17. Pandey, P., et al., *The see-saw of Keap1-Nrf2 pathway in cancer*. Crit Rev Oncol Hematol, 2017. **116**: p. 89-98.
18. Das, S., et al., *Loss of Merlin induces metabolomic adaptation that engages dependence on Hedgehog signaling*. Sci Rep, 2017. **7**: p. 40773.
19. Krause, S., A. Brock, and D.E. Ingber, *Intraductal injection for localized drug delivery to the mouse mammary gland*. J Vis Exp, 2013(80).
20. Liberzon, A., et al., *Molecular signatures database (MSigDB) 3.0*. Bioinformatics, 2011. **27**(12): p. 1739-40.
21. Subramanian, A., et al., *Gene set enrichment analysis: a knowledge-based approach for interpreting genome-wide expression profiles*. Proc Natl Acad Sci U S A, 2005. **102**(43): p. 15545-50.
22. Xia, J., et al., *INVEX--a web-based tool for integrative visualization of expression data*. Bioinformatics (Oxford, England), 2013. **29**(24): p. 3232-3234.
23. Xia, J., M.J. Benner, and R.E.W. Hancock, *NetworkAnalyst--integrative approaches for protein-protein interaction network analysis and visual exploration*. Nucleic acids research, 2014. **42**(Web Server issue): p. W167-W174.
24. Zhou, G., et al., *NetworkAnalyst 3.0: a visual analytics platform for comprehensive gene expression profiling and meta-analysis*. Nucleic acids research, 2019. **47**(W1): p. W234-W241.
25. Frolova, N., et al., *A shift from nuclear to cytoplasmic breast cancer metastasis suppressor 1 expression is associated with highly proliferative estrogen receptor-negative breast cancers*. Tumour biology : the journal of the International Society for Oncodevelopmental Biology and Medicine, 2009. **30**(3): p. 148-159.
26. Yau, C., et al., *A multigene predictor of metastatic outcome in early stage hormone receptor-negative and triple-negative breast cancer*. Breast Cancer Res, 2010. **12**(5): p. R85.
27. Forman, H.J., H. Zhang, and A. Rinna, *Glutathione: overview of its protective roles, measurement, and biosynthesis*. Molecular aspects of medicine, 2009. **30**(1-2): p. 1-12.

28. Harris, I.S., et al., *Glutathione and thioredoxin antioxidant pathways synergize to drive cancer initiation and progression*. *Cancer Cell*, 2015. **27**(2): p. 211-22.
29. Fishel, M.L., et al., *Apurinic/aprimidinic endonuclease/redox factor-1 (APE1/Ref-1) redox function negatively regulates NRF2*. *The Journal of biological chemistry*, 2015. **290**(5): p. 3057-3068.
30. Wasik, U., et al., *Protection against oxidative stress mediated by the Nrf2/Keap1 axis is impaired in Primary Biliary Cholangitis*. *Scientific reports*, 2017. **7**: p. 44769-44769.
31. Glasauer, A., et al., *Targeting SOD1 reduces experimental non-small-cell lung cancer*. *J Clin Invest*, 2014. **124**(1): p. 117-28.
32. Pizzimenti, S., et al., *The "two-faced" effects of reactive oxygen species and the lipid peroxidation product 4-hydroxynonenal in the hallmarks of cancer*. *Cancers (Basel)*, 2010. **2**(2): p. 338-63.
33. Zhong, H. and H. Yin, *Role of lipid peroxidation derived 4-hydroxynonenal (4-HNE) in cancer: focusing on mitochondria*. *Redox biology*, 2015. **4**: p. 193-199.
34. Panday, A., et al., *NADPH oxidases: an overview from structure to innate immunity-associated pathologies*. *Cell Mol Immunol*, 2015. **12**(1): p. 5-23.
35. Skonieczna, M., et al., *NADPH Oxidases: Insights into Selected Functions and Mechanisms of Action in Cancer and Stem Cells*. *Oxidative medicine and cellular longevity*, 2017. **2017**: p. 9420539-9420539.
36. Mullarky, E. and L.C. Cantley, *Diverting Glycolysis to Combat Oxidative Stress*, in *Innovative Medicine: Basic Research and Development*, K. Nakao, N. Minato, and S. Uemoto, Editors. 2015, Springer Copyright 2015, The Author(s). Tokyo. p. 3-23.
37. Wang, X.-J., et al., *Nrf2 enhances resistance of cancer cells to chemotherapeutic drugs, the dark side of Nrf2*. *Carcinogenesis*, 2008. **29**(6): p. 1235-1243.
38. Bedard, K. and K.H. Krause, *The NOX family of ROS-generating NADPH oxidases: physiology and pathophysiology*. *Physiol Rev*, 2007. **87**(1): p. 245-313.
39. Roy, K., et al., *NADPH oxidases and cancer*. *Clin Sci (Lond)*, 2015. **128**(12): p. 863-75.
40. Benhamouche, S., et al., *Nf2/Merlin controls progenitor homeostasis and tumorigenesis in the liver*. *Genes & development*, 2010. **24**(16): p. 1718-1730.

41. Eun, H.S., et al., *Gene expression of NOX family members and their clinical significance in hepatocellular carcinoma*. Sci Rep, 2017. **7**(1): p. 11060.
42. Horiguchi, A., et al., *Inactivation of the NF2 tumor suppressor protein merlin in DU145 prostate cancer cells*. Prostate, 2008. **68**(9): p. 975-84.
43. Pettigrew, C.A., J.S. Clerkin, and T.G. Cotter, *DUOX enzyme activity promotes AKT signalling in prostate cancer cells*. Anticancer Res, 2012. **32**(12): p. 5175-81.
44. Cačev, T., et al., *Loss of NF2/Merlin expression in advanced sporadic colorectal cancer*. Cell Oncol (Dordr), 2014. **37**(1): p. 69-77.
45. Laurent, E., et al., *Nox1 is over-expressed in human colon cancers and correlates with activating mutations in K-Ras*. International journal of cancer, 2008. **123**(1): p. 100-107.
46. Murray, L.B., Y.K. Lau, and Q. Yu, *Merlin is a negative regulator of human melanoma growth*. PLoS One, 2012. **7**(8): p. e43295.
47. Yamaura, M., et al., *NADPH oxidase 4 contributes to transformation phenotype of melanoma cells by regulating G2-M cell cycle progression*. Cancer Res, 2009. **69**(6): p. 2647-54.
48. Denisenko, T.V., A.S. Gorbunova, and B. Zhivotovsky, *Mitochondrial Involvement in Migration, Invasion and Metastasis*. Frontiers in cell and developmental biology, 2019. **7**: p. 355-355.
49. Cheung, E.C., et al., *Dynamic ROS Control by TIGAR Regulates the Initiation and Progression of Pancreatic Cancer*. Cancer Cell, 2020. **37**(2): p. 168-182.e4.
50. Godet, I., et al., *Fate-mapping post-hypoxic tumor cells reveals a ROS-resistant phenotype that promotes metastasis*. Nat Commun, 2019. **10**(1): p. 4862.
51. White, S.M., et al., *YAP/TAZ Inhibition Induces Metabolic and Signaling Rewiring Resulting in Targetable Vulnerabilities in NF2-Deficient Tumor Cells*. Dev Cell, 2019. **49**(3): p. 425-443.e9.
52. Mota, M.S.V., et al., *Deficiency of tumor suppressor Merlin facilitates metabolic adaptation by co-operative engagement of SMAD-Hippo signaling in breast cancer*. Carcinogenesis, 2018. **39**(9): p. 1165-1175.
53. Sato, T. and Y. Sekido, *NF2/Merlin Inactivation and Potential Therapeutic Targets in Mesothelioma*. International journal of molecular sciences, 2018. **19**(4): p. 988.

54. Krstić, J., et al., *Transforming Growth Factor-Beta and Oxidative Stress Interplay: Implications in Tumorigenesis and Cancer Progression*. *Oxidative medicine and cellular longevity*, 2015. **2015**: p. 654594-654594.
55. Sarmiento-Salinas, F.L., et al., *Breast Cancer Subtypes Present a Differential Production of Reactive Oxygen Species (ROS) and Susceptibility to Antioxidant Treatment*. *Frontiers in oncology*, 2019. **9**: p. 480-480.

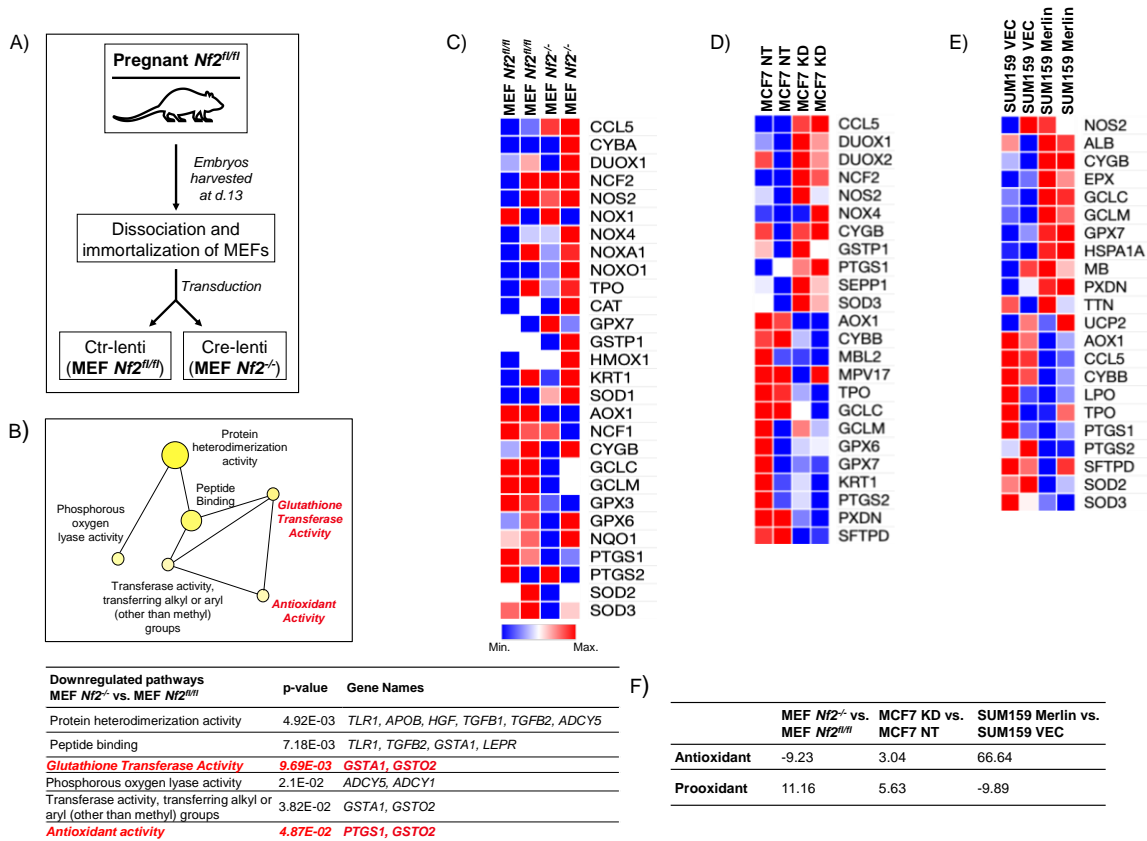


**Figure 1: Merlin deficiency modulates a redox signaling signature.** (A) Mouse embryonic fibroblasts (MEFs) were harvested from pregnant *Nf2<sup>fl/fl</sup>* mouse on day 13 (d.13), dissociated into single cell suspension, immortalized with SV40 large T antigen lentiviral particles, and transduced with vector-control lentivirus (Ctr-lenti) or Cre-lentivirus (Cre-lenti), generating MEF *Nf2<sup>fl/fl</sup>* or MEF *Nf2<sup>-/-</sup>*, respectively. (B) Glutathione transferase and antioxidant-associated genes were downregulated in MEF *Nf2<sup>-/-</sup>* compared to MEF *Nf2<sup>fl/fl</sup>* ( $n = 3$  for each group). Student's  $t$  test was applied for statistical analysis. A panel of redox-associated genes was assessed by gene expression array, and selected genes were plotted as heatmap ( $n = 2$  for each group) for (C) MEF *Nf2<sup>fl/fl</sup>* and MEF *Nf2<sup>-/-</sup>*, (D) control and *NF2*-silenced MCF7 (MCF7 NT and MCF7 KD, respectively), and (E) control and *NF2*-restored SUM159 (SUM159 VEC and SUM159 Merlin, respectively). (F) Antioxidant and prooxidant score of MEF *Nf2<sup>-/-</sup>* x MEF *Nf2<sup>fl/fl</sup>*, MCF7 KD x MCF7 NT, and SUM159 Merlin x SUM159 VEC.

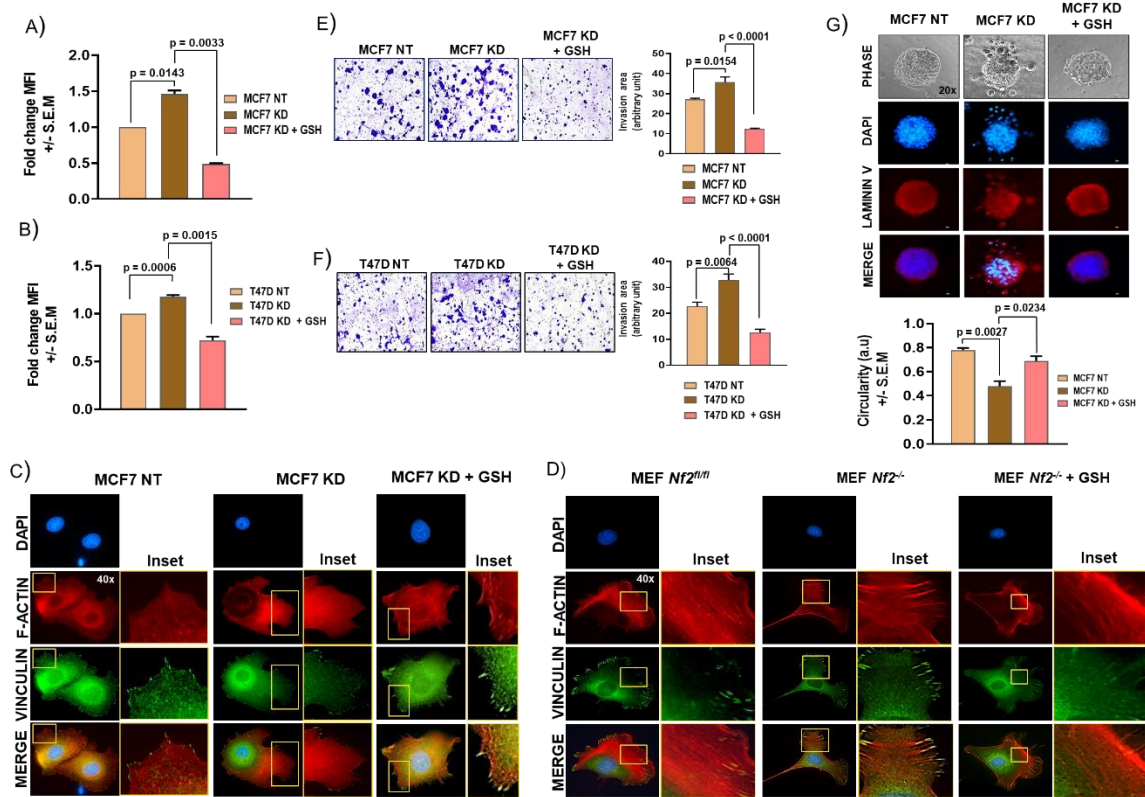


**Figure 2: ROS clearance attenuates migratory and invasion phenotypes in *NF2*-deficient cells.** (A) MCF7 KD and (B) T47D KD cells show significantly elevated ROS levels than MCF7 NT ( $p = 0.0143$ ) and T47D NT ( $p = 0.0006$ ), respectively, and exogenous GSH treatment (+ GSH) reduced intracellular ROS levels in both MCF7 KD ( $p = 0.0033$ ) and T47D KD ( $p = 0.0015$ ) cells ( $n = 2$  for each group). (C) MCF7 KD and (D) MEF *Nf2*<sup>-/-</sup> displayed longer and more extended lamellipodia with disorganized arrangement of actin filaments (inset) than MCF7 NT and MEF *Nf2*<sup>fl/fl</sup>, respectively; this phenotype was attenuated by + GSH. Scale bar = 50uM. Images representative of at least 3 different fields of each group. Transwell invasion assay showed enhanced invasion ability of (E) MCF7 KD and (F) T47D KD compared to MCF7 NT cells ( $p = 0.0154$ ) and T47D NT ( $p = 0.0064$ ), respectively, and + GSH reduced invasion of both MCF7 KD ( $p < 0.0001$ ) and T47D KD ( $p < 0.0001$ ) cells; quantification of invasion was calculated based on images of four different fields of each group ( $n = 2$ ) and represented as invasion area (arbitrary units). Scale bar = 100uM. (G) MCF7 KD cells presented a breached basement membrane in contrast to an intact, circumscribed one of MCF7 NT cells when analyzed by laminin V-stained 3D cell culture; + GSH attenuated the invasion behavior of MCF7 KD cells. Circularity of spheroids (arbitrary units) was measured based on three different 3D-culture organoids (MCF7 KD x MCF7 NT;  $p = 0.0027$ ) (MCF7 KD + GSH x MCF7 KD;  $p = 0.0234$ ). DAPI was used to label nuclear DNA. Scale bar = 50uM. Error bars represent  $\pm$  S.E.M. Student's *t* test was applied for statistical analysis.

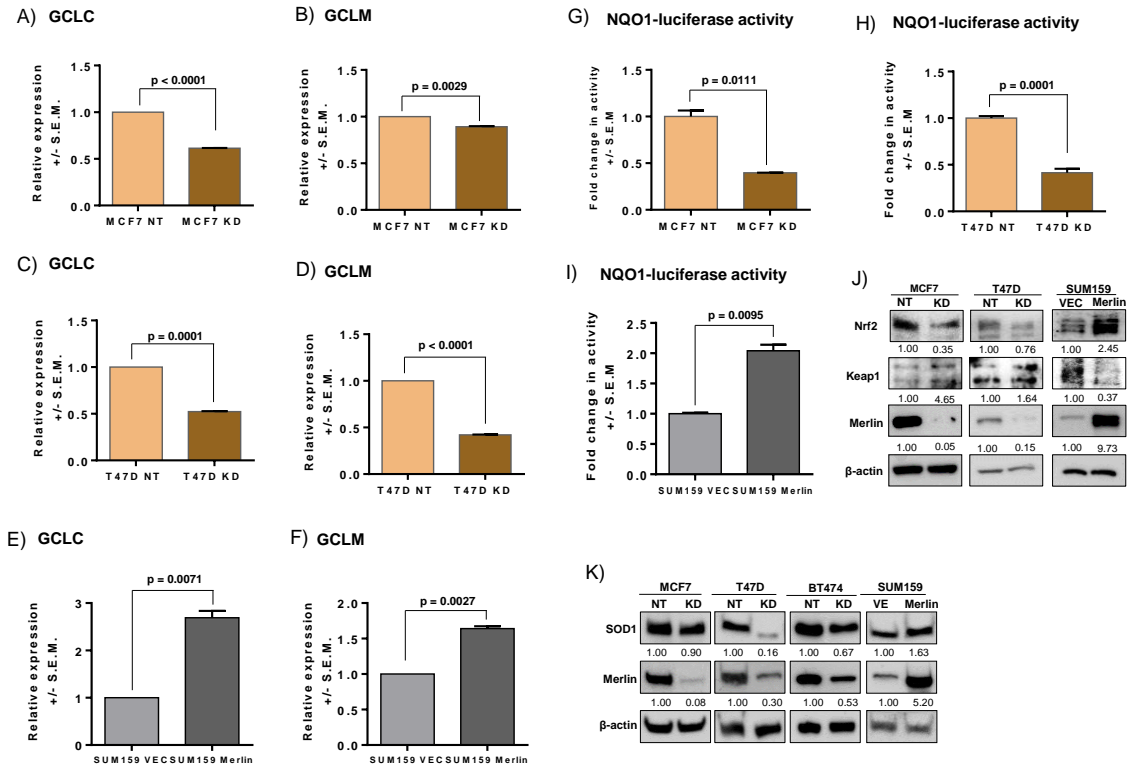


**Figure 3: Merlin-deficient breast cancer cells display a dysfunctional anti-oxidant system.** Expression levels of *GCLC* and *GCLM* were decreased in MCF7 KD (**A** and **B**, respectively) ( $p < 0.0001$  and  $p = 0.0029$ , respectively) and T47D KD (**C** and **D**, respectively) ( $p = 0.0001$  and  $p < 0.0001$ , respectively) compared to their NT controls. In contrast, expression levels of *GCLC* and *GCLM* were increased in SUM159 Merlin (**E** and **F**, respectively) ( $p = 0.0071$  and  $p = 0.0027$ , respectively) compared to SUM159 VEC. Nrf2 activity was measured by an NQO1-driven Nrf2 luciferase assay which showed decreased activity in MCF7 KD (**G**) ( $p = 0.0111$ ) and T47D KD (**H**) ( $p = 0.0001$ ) compared to their respective NT controls; Nrf2 activity was increased in (**I**) SUM159 Merlin ( $p = 0.0095$ ) compared to SUM159 VEC ( $n = 3$  for each group). (**J**) Protein levels of Nrf2 were decreased while Keap1 increased in Merlin-deficient cells compared to controls; the opposite was seen in the comparison between SUM159 Merlin and SUM159 VEC ( $n = 3$  for each group). (**K**) SOD1 protein expression is decreased in *NF2*-silenced breast cancer cells, MCF7 KD, T47D KD, and BT474 KD compared to their non-target (NT) controls. In contrast, SOD1 is upregulated in SUM159 Merlin compared to SUM159 VEC. Error bars represent +/- S.E.M. Student's *t* test was applied for statistical analysis. Band densitometry of immunoblotting is shown.  $\beta$ -actin was used as loading control.

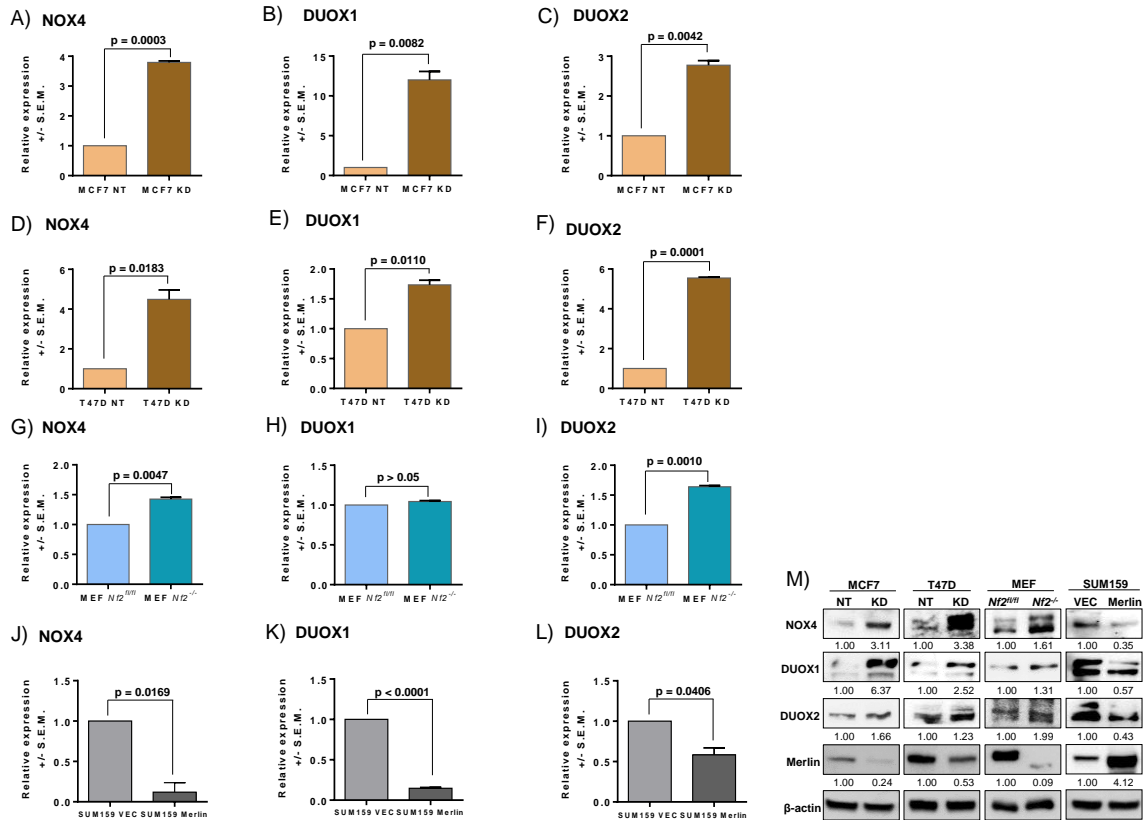


**Figure 4: Merlin deficiency upregulates proteins from the pro-oxidative NOX family.** Gene expression of NOX4, DUOX1, and DUOX2, was upregulated in MCF7 KD (A) ( $p = 0.0003$ ), (B) ( $p = 0.0082$ ), (C) ( $p = 0.0042$ ), respectively, and T47D KD (D) ( $p = 0.0183$ ), (E) ( $p = 0.0110$ ), (F) ( $p = 0.0001$ ), respectively, compared to their NT controls. Expression of (G) NOX4 ( $p = 0.0047$ ) was upregulated in MEF *Nf2<sup>-/-</sup>* compared to MEF *Nf2<sup>fl/fl</sup>*, however, no significant expression change was observed for DUOX1 (H) ( $p > 0.05$ ). In contrast, DUOX2 (I) ( $p = 0.0010$ ) was upregulated in MEF *Nf2<sup>-/-</sup>* compared to MEF *Nf2<sup>fl/fl</sup>*. Gene expression of NOX4 (J) ( $p = 0.0169$ ), DUOX1 (K) ( $p < 0.0001$ ), and DUOX2 (L) ( $p = 0.0406$ ) was downregulated in SUM159 Merlin compared to SUM159 VEC ( $n = 3$  for each group). (M) Validation of the levels of NOX4, DUOX1, and DUOX2 was assessed by immunoblotting. Error bars represent +/- S.E.M. Student's *t* test was applied for statistical analysis.  $\beta$ -actin was used as loading control. Representative immunoblot band densitometry is shown.



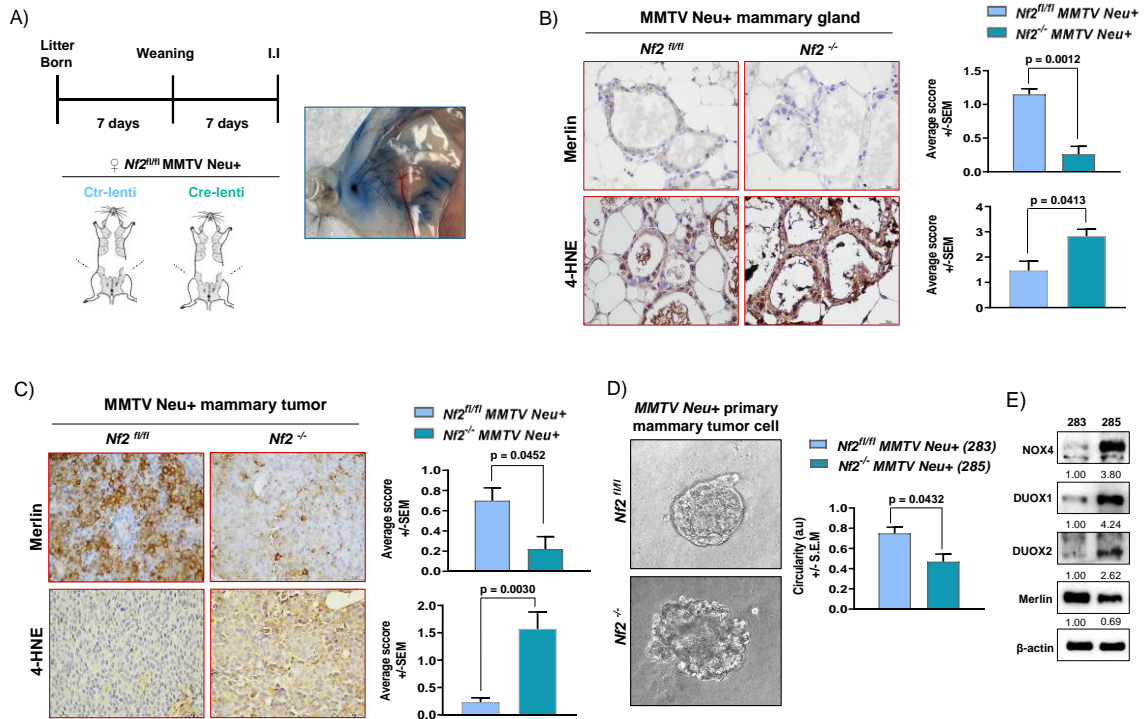


**Figure 5: Genetically-engineered oncogene-driven Merlin deficient mammary tumors harbor elevated oxidative stress.** (A) Pups of pregnant *Nf2<sup>fl/fl</sup>* MMTV Neu mice were weaned 7 days after birth, the mice were intraductally injected (I.I) with vector-control lentivirus (Ctr-lenti) or Cre-lentivirus (Cre-lenti) in both 4th mammary glands 7 days post-weaning to generate *Nf2<sup>fl/fl</sup>* MMTV Neu+ and *Nf2<sup>-/-</sup>* MMTV Neu+ mice, respectively. I.I efficiency test with PBS with 0.2% Evans blue dye enabling the visualization of the ductal tree is shown. (B) Loss of Merlin and increased 4-HNE staining are observed in mammary gland harvested from *Nf2<sup>-/-</sup>* MMTV Neu+ compared to *Nf2<sup>fl/fl</sup>* MMTV Neu+ by immunohistochemistry (IHC); IHC score for Merlin ( $p = 0.0012$ ) and 4-HNE ( $p = 0.0413$ ) is shown. Scale bar =  $30\mu\text{M}$ . Images representative of 4 different fields of each group ( $n = 2$ ) (C) Mammary tumor tissue harvested from *Nf2<sup>-/-</sup>* MMTV Neu+ showed lower levels of Merlin and increased 4-HNE staining than *Nf2<sup>fl/fl</sup>* MMTV Neu+; IHC score for Merlin ( $p = 0.0452$ ) and 4-HNE ( $p = 0.0030$ ) is shown. Scale bar =  $30\mu\text{M}$ . Images representative of 4 different fields of each group ( $n = 2$ ) (D) 3D cell culture of primary mammary tumor cells harvested from *Nf2<sup>-/-</sup>* MMTV Neu+ showed a very breached and disorganized structure compared to *Nf2<sup>fl/fl</sup>* MMTV Neu+. Circularity of the spheres is shown ( $p = 0.0432$ ). Scale bar =  $50\mu\text{M}$ . Images representative of 3 different 3D-culture organoids. (E) *Nf2<sup>fl/fl</sup>* MMTV Neu+ and *Nf2<sup>-/-</sup>* MMTV Neu+ derived primary tumor cells were immortalized and named 283 and 285, respectively; 285 cells had lower levels of Merlin and higher levels of NOX4, DUOX1, and DUOX2 than 283. Error bars represent +/- S.E.M. Student's *t* test was applied for statistical analysis.  $\beta$ -actin used as loading control. Immunoblot band densitometry is shown.

## DISCUSSION

Understanding cell metabolism has become crucial to elucidating the mechanisms behind cancer onset, progression, and metastasis. These investigations have enabled a comprehensive understanding of tumor biology and allowed novel therapeutic strategies. This specifically gives hope to the treatment of diseases with unknown drug treatment options, like in *Nf2*/Merlin-deficient conditions. For instance, there is no approach to directly overcome the lack of Merlin activity in Neurofibromatosis type 2; when tumors grow and put the life of patients at risk, the primary line of treatment is resection of the tumor, followed by radiation therapy (57). The same lack of chemotherapy or targeted therapy options is also encountered in *Nf2*/Merlin-deficient malignant tumors. Therefore, the discovery that Merlin deficiency disturbs metabolism and enhances malignant behavior represents a potential path for treatment exploitation.

The majority of studies focus on how Merlin can inhibit cell proliferation by regulating many signaling pathways. Although some of them are associated with metabolism, metabolic reprogramming has never been approached from the perspective of *NF2*/Merlin loss. In my first work, I showed that Merlin-deficient breast cancer cells have lower OXPHOS, evidenced by decreased oxygen consumption rate (OCR), and higher use of aerobic glycolysis, shown by increased extracellular acidification rate (ECAR). Indeed, glucose consumption and lactate production were elevated upon *NF2* deficiency.

Decreased levels of phosphorylated YAP/TAZ in Merlin-deficient breast cancer cells indicated defective Hippo signaling. Concomitantly, we observed decreased expression of inhibitory SMAD7, and increased levels of phosphorylation of receptor-regulated SMAD2/3. Additionally, protein expression of common SMAD, SMAD4, was also upregulated and enhanced TGF- $\beta$  signaling was confirmed by a SMAD-dependent luciferase reporter assay. YAP/TAZ and SMAD2/3/4 are reported to form a transcriptional complex that elevated the expression of the long noncoding RNA, UCA1. UCA1 has been reported to induce STAT3 activation (58), which was also found in our study in Merlin-deficient conditions.

One of the negative regulators of STAT3 is STAT5. In Merlin-defective GBM cells, YAP/TEAD2 induced the expression of miR-296-3p that in turn silenced the STAT5 gene, favoring activation of STAT3 (18). In addition, the signaling elicited by PDGFR and EGFR pathways, in Merlin-deficient conditions, also activate STAT3 (59-61). Further, our investigations showed that STAT3 activates HK2 expression, indicating a novel mechanism contributing to aerobic glycolysis upon Merlin deficiency in breast cancer. HK2 converts glucose into G6P which is the first step in glucose catabolism (42). The increased expression of HK2 may be necessary to assist the higher influx of glucose promoted by increased expression of GLUT in *NF2*-silenced breast cancer cells. Additionally, increased expression of both, LDH and MCT, is likely induced to keep up with higher conversion rate of pyruvate into lactate and lactate efflux, respectively. Interestingly, the expression of all these genes, including HK2, are in part regulated by PI3K/AKT, Ras GTPase, and WNT/ $\beta$ -catenin (40), all of which are aberrantly activated upon Merlin deficiency. Therefore, lack of functional Merlin leading to enhancement of

multiple cell signaling pathways gives potential explanation for the reprogramming of glucose catabolism into aerobic glycolysis in breast cancer cells.

The oxidation of acetyl-CoA generating reducing agents NADH and FADH<sub>2</sub> in the TCA cycle is a crucial step prior to OXPHOS (42). The overall levels of TCA cycle intermediate metabolites were reduced in Merlin-deficient breast cancer cells, suggesting lower activity of the TCA cycle. This further supports the glycolytic switch upon Merlin deficiency, as it suggests less input of acetyl-CoA, the first substrate of the TCA cycle, and decreased feed of NADH and FADH<sub>2</sub> into OXPHOS.

Reduction of OXPHOS-dependent ATP generation is the immediate result of reduced mitochondrial processes. Extrapolated, this would imply that generation of mitochondrial ROS is downregulated. It is known that electrons can leak from complex I and complex III and partially reduce oxygen, forming ROS in the mitochondrial matrix (51). Therefore, this main mechanism of ROS generation is expected to be diminished in glycolytic cells due to less flow of electrons. However, despite low mitochondrial activity, increased levels of ROS were detected in *NF2*-deficient breast cancer cells, suggesting alternative mechanisms supporting higher accumulation of ROS.

The second source of intracellular ROS generation is the NADPH oxidase family of enzymes, which are commonly upregulated in tumor cells (52, 62). The expression of these professional ROS generators, specifically NOX4, DUOX1, and DUOX2, was enhanced upon Merlin-deficiency in breast cancer. Therefore, higher levels of ROS are likely supported by the upregulation of these enzymes, despite the low mitochondrial activity. Moreover, STAT3 signaling has been reported to positively regulate the expression of NOX/DUOX (63-66). Indeed, inhibition of STAT3 with the small molecule

inhibitor STAT3 downregulated the expression of NOX4, DUOX1, and DUOX2 in *NF2*-deficient cells (Fig. 5). Therefore, in addition to being involved in the upregulation of HK2, enhanced STAT3 also elevates the expression of selected NADPH oxidases, contributing to ROS generation.

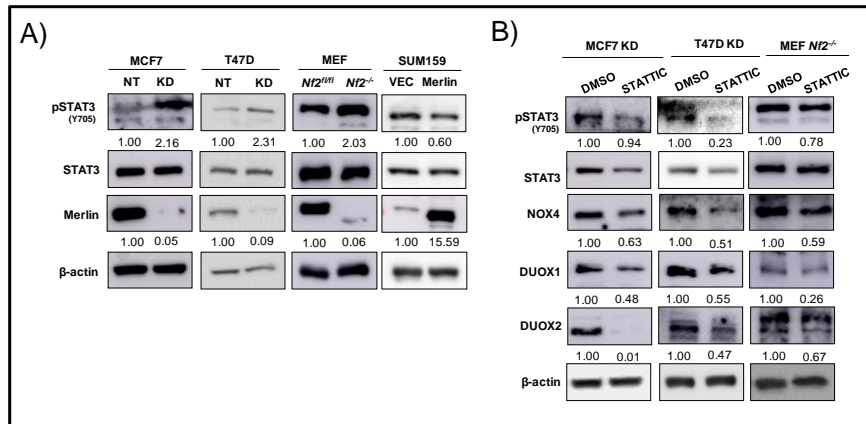


**Figure 5: STAT3 signaling upregulates the expression of NADPH oxidase enzymes in Merlin-deficient cells.** (A) Phosphorylation levels of Tyrosine 705 (Y705) of STAT3, a mark of activation, are increased upon Merlin deficiency; restoration of Merlin downregulated STAT3's Y705 phosphorylation. (B) STAT3 inhibition with STAT3IC diminished NOX4, DUOX1, and DUOX2 protein expression.

Interestingly, the NADPH oxidase enzymes have also been shown to contribute to aerobic glycolysis. In non-small cell lung cancer (NSCLC), genetic silencing and pharmacological inhibition of NOX4 downregulated transcript and protein levels of both, GLUT1 and LDHA. In addition, the expression of pyruvate kinase M2 (PKM2), that mediates the final enzymatic step of glycolysis, generating pyruvate, was also repressed. Indeed, glucose consumption and lactate production decreased in NOX4-inhibited NSCLC cells, evidencing attenuated aerobic glycolysis. Mechanistically, NOX4-derived H<sub>2</sub>O<sub>2</sub> activates PI3K/AKT pathway that in turn stabilizes c-Myc, an activator of many effectors that promotes glucose addiction in tumor cells (67). Another study showed that mitochondrial NOX4 is inhibited by allosterically binding OXPHOS-derived ATP.

Following the glycolytic switch, decreased mitochondrial ATP production attenuated NOX4 inhibition that in turn enhanced ROS generation and further contributed to aerobic glycolysis by preventing PKM2 degradation (68).

Defective mechanisms of ROS elimination also contribute to accumulation of ROS. We uncovered that Nrf2-related functions, such as GSH *de novo* synthesis and expression of SOD1, were negatively impacted in Merlin-deficient cells. In contrast, levels of Keap1 protein, the classical negative regulator of Nrf2, were upregulated. This finding indicates that the negative impact of Merlin deficiency in redox imbalance affects not only ROS-generating, but also ROS-quenching mechanisms. This further highlights the various functions Merlin performs to maintain a balanced ROS management system. Interestingly, silencing of NOX4 increased nuclear Nrf2 levels in lung fibroblasts, suggesting NOX4 as a negative regulator of Nrf2 activity (69). Therefore, it is possible that upregulated NOX4 contributes to glycolysis addiction and abolishment of ROS clearance in *NF2*-deficient breast cancer cells.

It should be noted that ROS oxidize Keap1, releasing their repression of Nrf2 nuclear translocation. Thus, ROS are actually known for activating Nrf2 signaling (70, 71). This poses a question of how increased levels of ROS generated by NOX4, for example, is concomitantly downregulating Nrf2 activity. It can be hypothesized that the positive effect of increased amounts of ROS on activation of Nrf2 is overcome by increased Keap1 expression in *NF2*-deficient cells. In addition, alternative inducers of Nrf2 protein degradation, such as Src subfamily A kinases and the GSK-3- $\beta$ -TrCP signaling (70), may also play a role in downregulating Nrf2 activation upon Merlin deficiency despite an oxidative environment.

ROS are known for acting as second messengers, oxidizing and changing the status of activation of many proteins (54, 55, 72). For instance, the oxidation and inhibition of protein tyrosine phosphatases (PTPs) by ROS result in the activation of MAPK and NF- $\kappa$ B pathways. This results in the expression of EMT-related and matrix metalloproteinase genes which enhance migration and invasion, respectively (73). Therefore, it is likely that increased levels of ROS play a role in the upregulation of *MM2*, *SNAIL2*, *TWIST1*, and *ZEB*. In addition, Merlin controls migration by direct inhibition of FAK phosphorylation or downregulation of FAK upstream regulators. One of the effects of ROS-dependent PTP inhibition is the activation of FAK (74), suggesting increased ROS levels promote the acquisition of migration ability by *NF2*-deficient cells. These analyses suggest that redox imbalance, triggered by silencing of *NF2*, enhances malignant features. This provides an explanation for the correlation between levels of Merlin and tumor grade found in breast cancer patient specimens, implicating loss of Merlin in tumor progression and metastasis

In conclusion, this body of work shows that deficiency of Merlin impinges upon multiple signals that can crosstalk and reprogram metabolic behaviors. This work characterized that glycolytic switch and a dysregulated redox management system are the most prominent effects in breast cancer cells.

## FUTURE DIRECTIONS

Merlin influences the activation of many signaling pathways which enable the exploitation of different mechanisms, such as those driving glycolysis and ROS accumulation. Further studies are needed to elucidate how Merlin-deficient function leads to increased phosphorylation and activation of STAT3 in breast cancer cells. The signaling induced by YAP/TEAD2/miR-296-3p, PDGFR, and EGFR are promising leads considering that Merlin negatively regulates these pathways. Moreover, pro-inflammatory cytokines, such as IL-6, IL-10, IFNs, and TNF- $\alpha$  also activate the STAT3 pathway (59). There are no studies showing modulation of cytokine production by Merlin yet. However, considering that Merlin deficiency enhances malignant characteristics, it should be investigated whether Merlin loss directly or indirectly affects the levels of tumor promoting cytokines. Indeed, the production and activity of many of these cytokines are stimulated in breast cancer (75). Another point of consideration is that NOX4 is also a transcriptional target of TGF- $\beta$  signaling (76-78), which is upregulated in Merlin-defective breast cancer cells. Indeed, inhibition of the TGF- $\beta$  pathway with A8301 inhibitor decreased NOX4 and DUOX1 protein levels in *NF2*-deficient breast cancer cells (Fig. 6). Therefore, co-inhibition of these pathways may further repress NOX4 and DUOX expression and downregulate glycolysis and ROS production.



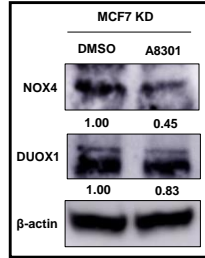


**Figure 6: Inhibition of TGF- $\beta$  reduces NADPH oxidase expression.** Inhibition of TGF- $\beta$  pathway with A8301 inhibitor downregulated expression of NOX4 and DUOX1 proteins. DMSO was used as vehicle control.  $\beta$ -actin was used as loading control. Band densitometry is shown.

Blockage of metabolic reprogramming is a promising therapeutic strategy in cancer since it disables the rewired metabolic network required to meet the energy demands of tumor cells. For being a classical metabolic characteristic of transformed cells, glucose uptake addiction is utilized as a powerful marker of tumorigenic cells by 18-FDG PET scan (40). Importantly, Merlin-deficient breast cancer cells exhibited increased 18-FDG uptake in *in vitro* experiments, further confirming increased glucose uptake upon *NF2* silencing (Fig. 7). Thus, it would be reasonable to perform an 18-FDG PET scan on the engineered mammary-specific *NF2* knockout mice to analyze the effect of Merlin deficiency and aerobic glycolysis at the organismal level. As a therapeutic approach, the glucose analog 2-deoxy-D-glucose (2-DG) competes with glucose for GLUT-dependent uptake, but it cannot be processed by HK2 into G6P and consequently cannot proceed into the glycolytic pathway (42). Thus, treatment with 2-DG is a key strategy to target aerobic glycolysis and could be used in both *in vitro* and *in vivo* Merlin-deficient breast cancer systems.

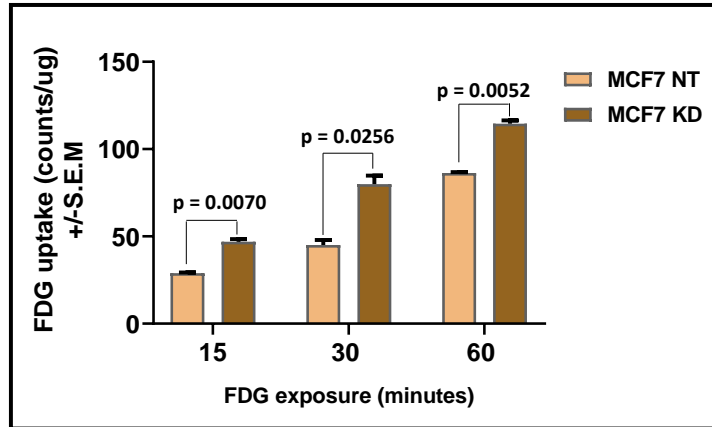


**Figure 7: Merlin-deficient breast cancer cells have increased 18-FDG uptake.**

Merlin-deficient breast cancer cell, MCF7 KD, displayed higher 18-FDG uptake compared to its control counterpart (MCF7 NT) in a course of 60 minutes. Statistical significance was determined for  $p < 0.05$ .

Glutamine addiction, the secondary energy source used by cancer cells, has also been associated with lack of Merlin function. An *NF2*-mutated renal cell carcinoma cell, SN12C, lost its ability to utilize glutamine when silenced for YAP/TAZ, becoming very sensitive to this amino acid withdrawal. This resulted in cell death, which was reversed by YAP/TAZ restoration (79). Another study also showed that human *NF2*-deficient Schwann cells are highly dependent on glutamine use (80). Although not analyzed in the context of *NF2*/Merlin, YAP/TAZ/TEAD was found to upregulate glutamine transporter SLC1A5 and glutaminase, the enzyme that converts glutamine into glutamate, in HER2+ breast cancer (81). The clinical relevance of abnormal glutamine consumption in cancer is translated by the use of radiolabeled glutamine in PET scan and also development of glutaminase inhibitors, such as the orally bioavailable inhibitor CB-839 (40, 82). Therefore, it would be prudent to investigate whether breast cancer cells also become dependent on glutamine upon Merlin deficiency.

Redox management in cancer has been challenging. In early stages, ROS clearance mitigates genomic instability and attenuates the activation of oncogenic pathways. However, in late stages, elimination of ROS actually benefits tumor cells by keeping ROS amounts at non-toxic levels (71, 83). A melanoma mouse model showed that although treatment with antioxidants decreased circulating cancer cells, they were more prone to metastasize, indicating limited ROS levels as an advantage to metastasis (84). N-acetyl-cysteine (NAC) is an antioxidant commonly used as a precursor of L-cysteine that generates GSH. NAC is often appointed as a ROS clearance-based treatment in cancer (85); however, considering controversial beneficial effects of ROS clearance, NAC should be administered with caution. Breast cancer patients treated with NAC showed significant reduction of both MCT4, a lactate transporter, in stromal cells and Ki67 proliferation marker in tumor cells. These results not only indicate the role of ROS clearance in tumor cells, but also in surrounding tissue. Importantly, the breast cancer specimens used in this study were from stages 0 and I (85). Thus, it is possible that NAC had a tumor suppressing effect, because it was applied in early stage disease.

Antioxidant supplementation in the diet has also become a therapeutic strategy to eradicate redox stress in cancer. Although the direct consumption of antioxidants sounds appears to be an effective intervention, unexpected effects have been observed. For instance, a trial to investigate whether diet supplementation with the antioxidant vitamin E could prevent men age 50 and older from developing prostate cancer showed increased risk of developing prostate cancer by 17%. For selenium-supplemented diet, increased risk was also registered, although it was not statistically significant (86). Another study showed that diet supplementation with vitamin E and NAC increased tumor progression

in a KRAS-BRAF-induced lung cancer mouse model (87). In order to block glucose addiction, adoption of a ketogenic diet, which is high in fat and low in carbohydrates, has shown promising therapeutic results. Endometrial and ovarian cancer patients presented lower insulin levels, which negatively affect glucose uptake, when under a ketogenic diet (88). Moreover, a ketogenic diet supplemented with NAC reduced tumor growth in a xenograft mouse model of anaplastic thyroid cancer (89).

Tissues from both, *Nf2*-deleted mammary glands and tumors, showed increased expression of 4-HNE, indicating higher oxidative stress. Considering that ROS clearance by GSH administration reduced cell migration and invasion of Merlin-deficient breast cancer cells *in vitro*, it is reasonable that interventions to reduce oxidative stress might be advantageous in *Nf2*-deficient mice. Therefore, a ketogenic diet supplemented with antioxidants, such as NAC, or administration of STAT3 inhibitors, such as the repurposed drug ponatinib (90), could be applied to analyze whether it decreases tumor latency and malignant characteristics in *Nf2*-deficient tumor-bearing mice.

## LIST OF REFERENCES

1. Cooper J, Giancotti FG. Molecular insights into NF2/Merlin tumor suppressor function. *FEBS Lett.* 2014;588(16):2743-52.
2. Petrilli AM, Fernández-Valle C. Role of Merlin/NF2 inactivation in tumor biology. *Oncogene.* 2016;35(5):537-48.
3. Li W, Cooper J, Karajannis MA, Giancotti FG. Merlin: a tumour suppressor with functions at the cell cortex and in the nucleus. *EMBO Rep.* 2012;13(3):204-15.
4. Trofatter JA, MacCollin MM, Rutter JL, Murrell JR, Duyao MP, Parry DM, et al. A novel moesin-, ezrin-, radixin-like gene is a candidate for the neurofibromatosis 2 tumor suppressor. *Cell.* 1993;72(5):791-800.
5. Evans DGR. Neurofibromatosis type 2 (NF2): a clinical and molecular review. *Orphanet J Rare Dis.* 2009;4:16-.
6. Bianchi AB, Mitsunaga SI, Cheng JQ, Klein WM, Jhanwar SC, Seizinger B, et al. High frequency of inactivating mutations in the neurofibromatosis type 2 gene (NF2) in primary malignant mesotheliomas. *Proc Natl Acad Sci U S A.* 1995;92(24):10854-8.
7. Luo ZL, Cheng SQ, Shi J, Zhang HL, Zhang CZ, Chen HY, et al. A splicing variant of Merlin promotes metastasis in hepatocellular carcinoma. *Nat Commun.* 2015;6:8457.
8. Sun J, Tian X, Zhang J, Huang Y, Lin X, Chen L, et al. Regulation of human glioma cell apoptosis and invasion by miR-152-3p through targeting DNMT1 and regulating NF2 : MiR-152-3p regulate glioma cell apoptosis and invasion. *J Exp Clin Cancer Res.* 2017;36(1):100.
9. Peng Y, Croce CM. The role of MicroRNAs in human cancer. *Signal Transduct Target Ther.* 2016;1:15004.
10. Yu C, Zhang L, Luo D, Yan F, Liu J, Shao S, et al. MicroRNA-146b-3p Promotes Cell Metastasis by Directly Targeting NF2 in Human Papillary Thyroid Cancer. *Thyroid.* 2018;28(12):1627-41.
11. Thurneysen C, Opitz I, Kurtz S, Weder W, Stahel RA, Felley-Bosco E. Functional inactivation of NF2/merlin in human mesothelioma. *Lung Cancer.* 2009;64(2):140-7.
12. Horiguchi A, Zheng R, Shen R, Nanus DM. Inactivation of the NF2 tumor suppressor protein merlin in DU145 prostate cancer cells. *Prostate.* 2008;68(9):975-84.

13. Zhang N, Bai H, David KK, Dong J, Zheng Y, Cai J, et al. The Merlin/NF2 tumor suppressor functions through the YAP oncoprotein to regulate tissue homeostasis in mammals. *Dev Cell*. 2010;19(1):27-38.
14. McClatchey AI, Saotome I, Ramesh V, Gusella JF, Jacks T. The Nf2 tumor suppressor gene product is essential for extraembryonic development immediately prior to gastrulation. *Genes Dev*. 1997;11(10):1253-65.
15. Sato T, Sekido Y. NF2/Merlin Inactivation and Potential Therapeutic Targets in Mesothelioma. *Int J Mol Sci*. 2018;19(4):988.
16. Xiao G-H, Gallagher R, Shetler J, Skele K, Altomare DA, Pestell RG, et al. The NF2 tumor suppressor gene product, merlin, inhibits cell proliferation and cell cycle progression by repressing cyclin D1 expression. *Mol Cell Biol*. 2005;25(6):2384-94.
17. Lau YK, Murray LB, Houshmandi SS, Xu Y, Gutmann DH, Yu Q. Merlin is a potent inhibitor of glioma growth. *Cancer Res*. 2008;68(14):5733-42.
18. Lee H, Hwang SJ, Kim HR, Shin CH, Choi KH, Joung JG, et al. Neurofibromatosis 2 (NF2) controls the invasiveness of glioblastoma through YAP-dependent expression of CYR61/CCN1 and miR-296-3p. *Biochim Biophys Acta*. 2016;1859(4):599-611.
19. Garcia-Rendueles ME, Ricarte-Filho JC, Untch BR, Landa I, Knauf JA, Voza F, et al. NF2 Loss Promotes Oncogenic RAS-Induced Thyroid Cancers via YAP-Dependent Transactivation of RAS Proteins and Sensitizes Them to MEK Inhibition. *Cancer Discov*. 2015;5(11):1178-93.
20. Cačev T, Aralica G, Lončar B, Kapitanović S. Loss of NF2/Merlin expression in advanced sporadic colorectal cancer. *Cell Oncol (Dordr)*. 2014;37(1):69-77.
21. Benhamouche S, Curto M, Saotome I, Gladden AB, Liu C-H, Giovannini M, et al. NF2/Merlin controls progenitor homeostasis and tumorigenesis in the liver. *Genes & development*. 2010;24(16):1718-30.
22. Quan M, Cui J, Xia T, Jia Z, Xie D, Wei D, et al. Merlin/NF2 Suppresses Pancreatic Tumor Growth and Metastasis by Attenuating the FOXM1-Mediated Wnt/ $\beta$ -Catenin Signaling. *Cancer research*. 2015;75(22):4778-89.
23. Murray LB, Lau YK, Yu Q. Merlin is a negative regulator of human melanoma growth. *PLoS One*. 2012;7(8):e43295.
24. Morrow KA, Das S, Metge BJ, Ye K, Mulekar MS, Tucker JA, et al. Loss of tumor suppressor Merlin in advanced breast cancer is due to post-translational regulation. *J Biol Chem*. 2011;286(46):40376-85.

25. Morrow KA, Das S, Meng E, Menezes ME, Bailey SK, Metge BJ, et al. Loss of tumor suppressor Merlin results in aberrant activation of Wnt/ $\beta$ -catenin signaling in cancer. *Oncotarget*. 2016;7(14):17991-8005.
26. Das S, Jackson WP, Prasain JK, Hanna A, Bailey SK, Tucker JA, et al. Loss of Merlin induces metabolomic adaptation that engages dependence on Hedgehog signaling. *Sci Rep*. 2017;7:40773.
27. Poulikakos PI, Xiao GH, Gallagher R, Jablonski S, Jhanwar SC, Testa JR. Re-expression of the tumor suppressor NF2/merlin inhibits invasiveness in mesothelioma cells and negatively regulates FAK. *Oncogene*. 2006;25(44):5960-8.
28. Shapiro IM, Kolev VN, Vidal CM, Kadariya Y, Ring JE, Wright Q, et al. Merlin deficiency predicts FAK inhibitor sensitivity: a synthetic lethal relationship. *Sci Transl Med*. 2014;6(237):237ra68.
29. Quesnelle KM, Boehm AL, Grandis JR. STAT-mediated EGFR signaling in cancer. *J Cell Biochem*. 2007;102(2):311-9.
30. Wu X, Tu X, Joeng KS, Hilton MJ, Williams DA, Long F. Rac1 activation controls nuclear localization of beta-catenin during canonical Wnt signaling. *Cell*. 2008;133(2):340-53.
31. Lallemand D, Manent J, Couvelard A, Watilliaux A, Siena M, Chareyre F, et al. Merlin regulates transmembrane receptor accumulation and signaling at the plasma membrane in primary mouse Schwann cells and in human schwannomas. *Oncogene*. 2009;28(6):854-65.
32. Meng JJ, Lowrie DJ, Sun H, Dorsey E, Pelton PD, Bashour AM, et al. Interaction between two isoforms of the NF2 tumor suppressor protein, merlin, and between merlin and ezrin, suggests modulation of ERM proteins by merlin. *J Neurosci Res*. 2000;62(4):491-502.
33. Clucas J, Valderrama F. ERM proteins in cancer progression. *J Cell Sci*. 2014;127(Pt 2):267-75.
34. Zhang N, Wei P, Gong A, Chiu WT, Lee HT, Colman H, et al. FoxM1 promotes  $\beta$ -catenin nuclear localization and controls Wnt target-gene expression and glioma tumorigenesis. *Cancer Cell*. 2011;20(4):427-42.
35. Arakawa H, Hayashi N, Nagase H, Ogawa M, Nakamura Y. Alternative splicing of the NF2 gene and its mutation analysis of breast and colorectal cancers. *Hum Mol Genet*. 1994;3(4):565-8.

36. Yaegashi S, Sachse R, Ohuchi N, Mori S, Sekiya T. Low incidence of a nucleotide sequence alteration of the neurofibromatosis 2 gene in human breast cancers. *Jpn J Cancer Res.* 1995;86(10):929-33.
37. Hanahan D, Weinberg RA. Hallmarks of cancer: the next generation. *Cell.* 2011;144(5):646-74.
38. Rong R, Tang X, Gutmann DH, Ye K. Neurofibromatosis 2 (NF2) tumor suppressor merlin inhibits phosphatidylinositol 3-kinase through binding to PIKE-L. *Proc Natl Acad Sci U S A.* 2004;101(52):18200-5.
39. DeBerardinis RJ, Chandel NS. Fundamentals of cancer metabolism. *Sci Adv.* 2016;2(5):e1600200.
40. Pavlova NN, Thompson CB. The Emerging Hallmarks of Cancer Metabolism. *Cell Metab.* 2016;23(1):27-47.
41. Shiraishi T, Verdone JE, Huang J, Kahlert UD, Hernandez JR, Torga G, et al. Glycolysis is the primary bioenergetic pathway for cell motility and cytoskeletal remodeling in human prostate and breast cancer cells. *Oncotarget.* 2015;6(1):130-43.
42. Kalyanaraman B. Teaching the basics of cancer metabolism: Developing antitumor strategies by exploiting the differences between normal and cancer cell metabolism. *Redox Biol.* 2017;12:833-42.
43. Sheng SL, Liu JJ, Dai YH, Sun XG, Xiong XP, Huang G. Knockdown of lactate dehydrogenase A suppresses tumor growth and metastasis of human hepatocellular carcinoma. *Febs j.* 2012;279(20):3898-910.
44. Panieri E, Santoro MM. ROS homeostasis and metabolism: a dangerous liason in cancer cells. *Cell Death & Disease.* 2016;7(6):e2253-e.
45. Doherty JR, Yang C, Scott KE, Cameron MD, Fallahi M, Li W, et al. Blocking lactate export by inhibiting the Myc target MCT1 Disables glycolysis and glutathione synthesis. *Cancer Res.* 2014;74(3):908-20.
46. Gorrini C, Harris IS, Mak TW. Modulation of oxidative stress as an anticancer strategy. *Nat Rev Drug Discov.* 2013;12(12):931-47.
47. Hurd TR, DeGennaro M, Lehmann R. Redox regulation of cell migration and adhesion. *Trends Cell Biol.* 2012;22(2):107-15.
48. Du S, Miao J, Zhu Z, Xu E, Shi L, Ai S, et al. NADPH oxidase 4 regulates anoikis resistance of gastric cancer cells through the generation of reactive oxygen species and the induction of EGFR. *Cell Death & Disease.* 2018;9(10):948.



49. Chio IIC, Tuveson DA. ROS in Cancer: The Burning Question. *Trends Mol Med.* 2017;23(5):411-29.
50. Weinberg F, Ramnath N, Nagrath D. Reactive Oxygen Species in the Tumor Microenvironment: An Overview. *Cancers (Basel).* 2019;11(8):1191.
51. Li X, Fang P, Mai J, Choi ET, Wang H, Yang X-f. Targeting mitochondrial reactive oxygen species as novel therapy for inflammatory diseases and cancers. *Journal of Hematology & Oncology.* 2013;6(1):19.
52. Skonieczna M, Hejmo T, Poterala-Hejmo A, Cieslar-Pobuda A, Buldak RJ. NADPH Oxidases: Insights into Selected Functions and Mechanisms of Action in Cancer and Stem Cells. *Oxidative Medicine and Cellular Longevity.* 2017;2017:9420539.
53. Perillo B, Di Donato M, Pezone A, Di Zazzo E, Giovannelli P, Galasso G, et al. ROS in cancer therapy: the bright side of the moon. *Exp Mol Med.* 2020;52(2):192-203.
54. Nishikawa M. Reactive oxygen species in tumor metastasis. *Cancer Lett.* 2008;266(1):53-9.
55. Liou G-Y, Storz P. Reactive oxygen species in cancer. *Free Radic Res.* 2010;44(5):479-96.
56. Mullarky E, Cantley LC, editors. *Diverting Glycolysis to Combat Oxidative Stress. Innovative Medicine; 2015 2015//; Tokyo: Springer Japan.*
57. Bosco EE, Nakai Y, Hennigan RF, Ratner N, Zheng Y. NF2-deficient cells depend on the Rac1-canonical Wnt signaling pathway to promote the loss of contact inhibition of proliferation. *Oncogene.* 2010;29(17):2540-9.
58. Li Z, Li X, Wu S, Xue M, Chen W. Long non-coding RNA UCA1 promotes glycolysis by upregulating hexokinase 2 through the mTOR-STAT3/microRNA143 pathway. *Cancer Sci.* 2014;105(8):951-5.
59. Huynh J, Chand A, Gough D, Ernst M. Therapeutically exploiting STAT3 activity in cancer — using tissue repair as a road map. *Nature Reviews Cancer.* 2019;19(2):82-96.
60. Fang B. Genetic Interactions of STAT3 and Anticancer Drug Development. *Cancers (Basel).* 2014;6(1):494-525.
61. Kim Y, Kim E, Wu Q, Guryanova O, Hitomi M, Lathia JD, et al. Platelet-derived growth factor receptors differentially inform intertumoral and intratumoral heterogeneity. *Genes Dev.* 2012;26(11):1247-62.
62. O'Leary DP, Wang JH, Cotter TG, Redmond HP. Less stress, more success? Oncological implications of surgery-induced oxidative stress. *Gut.* 2013;62(3):461-70.

63. Manea A, Tanase LI, Raicu M, Simionescu M. Jak/STAT signaling pathway regulates nox1 and nox4-based NADPH oxidase in human aortic smooth muscle cells. *Arterioscler Thromb Vasc Biol.* 2010;30(1):105-12.
64. Li J, Lan T, Zhang C, Zeng C, Hou J, Yang Z, et al. Reciprocal activation between IL-6/STAT3 and NOX4/Akt signalings promotes proliferation and survival of non-small cell lung cancer cells. *Oncotarget.* 2015;6(2):1031-48.
65. Roy K, Wu Y, Meitzler JL, Juhasz A, Liu H, Jiang G, et al. NADPH oxidases and cancer. *Clin Sci (Lond).* 2015;128(12):863-75.
66. Corzo CA, Cotter MJ, Cheng P, Cheng F, Kusmartsev S, Sotomayor E, et al. Mechanism regulating reactive oxygen species in tumor-induced myeloid-derived suppressor cells. *J Immunol.* 2009;182(9):5693-701.
67. Zeng C, Wu Q, Wang J, Yao B, Ma L, Yang Z, et al. NOX4 supports glycolysis and promotes glutamine metabolism in non-small cell lung cancer cells. *Free Radic Biol Med.* 2016;101:236-48.
68. Shanmugasundaram K, Nayak BK, Friedrichs WE, Kaushik D, Rodriguez R, Block K. NOX4 functions as a mitochondrial energetic sensor coupling cancer metabolic reprogramming to drug resistance. *Nat Commun.* 2017;8(1):997.
69. Bernard K, Logsdon NJ, Miguel V, Benavides GA, Zhang J, Carter AB, et al. NADPH Oxidase 4 (Nox4) Suppresses Mitochondrial Biogenesis and Bioenergetics in Lung Fibroblasts via a Nuclear Factor Erythroid-derived 2-like 2 (Nrf2)-dependent Pathway. *J Biol Chem.* 2017;292(7):3029-38.
70. Niture SK, Khatri R, Jaiswal AK. Regulation of Nrf2-an update. *Free Radic Biol Med.* 2014;66:36-44.
71. Pandey P, Singh AK, Singh M, Tewari M, Shukla HS, Gambhir IS. The see-saw of Keap1-Nrf2 pathway in cancer. *Crit Rev Oncol Hematol.* 2017;116:89-98.
72. Wang K, Jiang J, Lei Y, Zhou S, Wei Y, Huang C. Targeting Metabolic-Redox Circuits for Cancer Therapy. *Trends Biochem Sci.* 2019;44(5):401-14.
73. Tothhawn L, Deng S, Pervaiz S, Yap CT. Redox regulation of cancer cell migration and invasion. *Mitochondrion.* 2013;13(3):246-53.
74. Tamborindeguy MT, Matte BF, Ramos GO, Alves AM, Bernardi L, Lamers ML. NADPH-oxidase-derived ROS alters cell migration by modulating adhesions dynamics. *Biol Cell.* 2018;110(10):225-36.

75. Esquivel-Velázquez M, Ostoa-Saloma P, Palacios-Arreola MI, Nava-Castro KE, Castro JI, Morales-Montor J. The role of cytokines in breast cancer development and progression. *J Interferon Cytokine Res.* 2015;35(1):1-16.
76. Jain M, Rivera S, Monclus EA, Synenki L, Zirk A, Eisenbart J, et al. Mitochondrial reactive oxygen species regulate transforming growth factor- $\beta$  signaling. *J Biol Chem.* 2013;288(2):770-7.
77. Jiang F, Liu GS, Dusing GJ, Chan EC. NADPH oxidase-dependent redox signaling in TGF- $\beta$ -mediated fibrotic responses. *Redox Biol.* 2014;2:267-72.
78. Krstić J, Trivanović D, Mojsilović S, Santibanez JF. Transforming Growth Factor-Beta and Oxidative Stress Interplay: Implications in Tumorigenesis and Cancer Progression. *Oxid Med Cell Longev.* 2015;2015:654594.
79. White SM, Avantaggiati ML, Nemazanyy I, Di Poto C, Yang Y, Pende M, et al. YAP/TAZ Inhibition Induces Metabolic and Signaling Rewiring Resulting in Targetable Vulnerabilities in NF2-Deficient Tumor Cells. *Dev Cell.* 2019;49(3):425-43.e9.
80. Pestoni JC, Klingeman Plati S, Valdivia Camacho OD, Fuse MA, Onatunde M, Sparrow NA, et al. Peroxynitrite supports a metabolic reprogramming in merlin-deficient Schwann cells and promotes cell survival. *J Biol Chem.* 2019;294(30):11354-68.
81. Edwards DN, Ngwa VM, Wang S, Shiuan E, Brantley-Sieders DM, Kim LC, et al. The receptor tyrosine kinase EphA2 promotes glutamine metabolism in tumors by activating the transcriptional coactivators YAP and TAZ. *Sci Signal.* 2017;10(508):eaan4667.
82. Gross MI, Demo SD, Dennison JB, Chen L, Chernov-Rogan T, Goyal B, et al. Antitumor activity of the glutaminase inhibitor CB-839 in triple-negative breast cancer. *Mol Cancer Ther.* 2014;13(4):890-901.
83. Harris IS, Treloar AE, Inoue S, Sasaki M, Gorrini C, Lee KC, et al. Glutathione and thioredoxin antioxidant pathways synergize to drive cancer initiation and progression. *Cancer Cell.* 2015;27(2):211-22.
84. Piskounova E, Agathocleous M, Murphy MM, Hu Z, Huddlestun SE, Zhao Z, et al. Oxidative stress inhibits distant metastasis by human melanoma cells. *Nature.* 2015;527(7577):186-91.
85. Monti D, Sotgia F, Whitaker-Menezes D, Tuluc M, Birbe R, Berger A, et al. Pilot study demonstrating metabolic and anti-proliferative effects of in vivo anti-oxidant supplementation with N-Acetylcysteine in Breast Cancer. *Semin Oncol.* 2017;44(3):226-32.

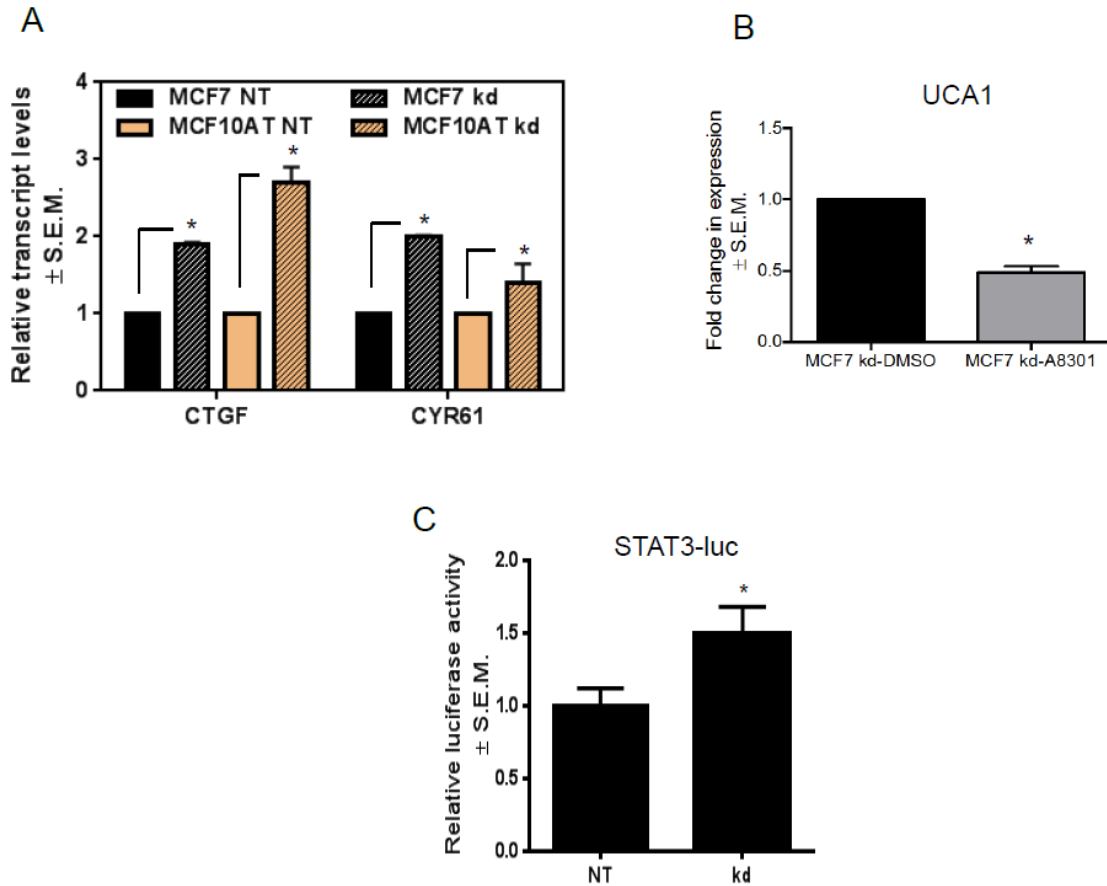
86. Klein EA, Thompson IM, Jr., Tangen CM, Crowley JJ, Lucia MS, Goodman PJ, et al. Vitamin E and the risk of prostate cancer: the Selenium and Vitamin E Cancer Prevention Trial (SELECT). *JAMA*. 2011;306(14):1549-56.
87. Sayin VI, Ibrahim MX, Larsson E, Nilsson JA, Lindahl P, Bergo MO. Antioxidants accelerate lung cancer progression in mice. *Sci Transl Med*. 2014;6(221):221ra15.
88. Cohen CW, Fontaine KR, Arend RC, Alvarez RD, Leath CA, III, Huh WK, et al. A Ketogenic Diet Reduces Central Obesity and Serum Insulin in Women with Ovarian or Endometrial Cancer. *J Nutr*. 2018;148(8):1253-60.
89. Aggarwal A, Yuan Z, Barletta JA, Lorch JH, Nehs MA. Ketogenic diet combined with antioxidant N-acetylcysteine inhibits tumor growth in a mouse model of anaplastic thyroid cancer. *Surgery*. 2020;167(1):87-93.
90. Tan FH, Putoczki TL, Lou J, Hinde E, Hollande F, Giraud J, et al. Ponatinib Inhibits Multiple Signaling Pathways Involved in STAT3 Signaling and Attenuates Colorectal Tumor Growth. *Cancers (Basel)*. 2018;10(12):526.

## **APPENDIX A**

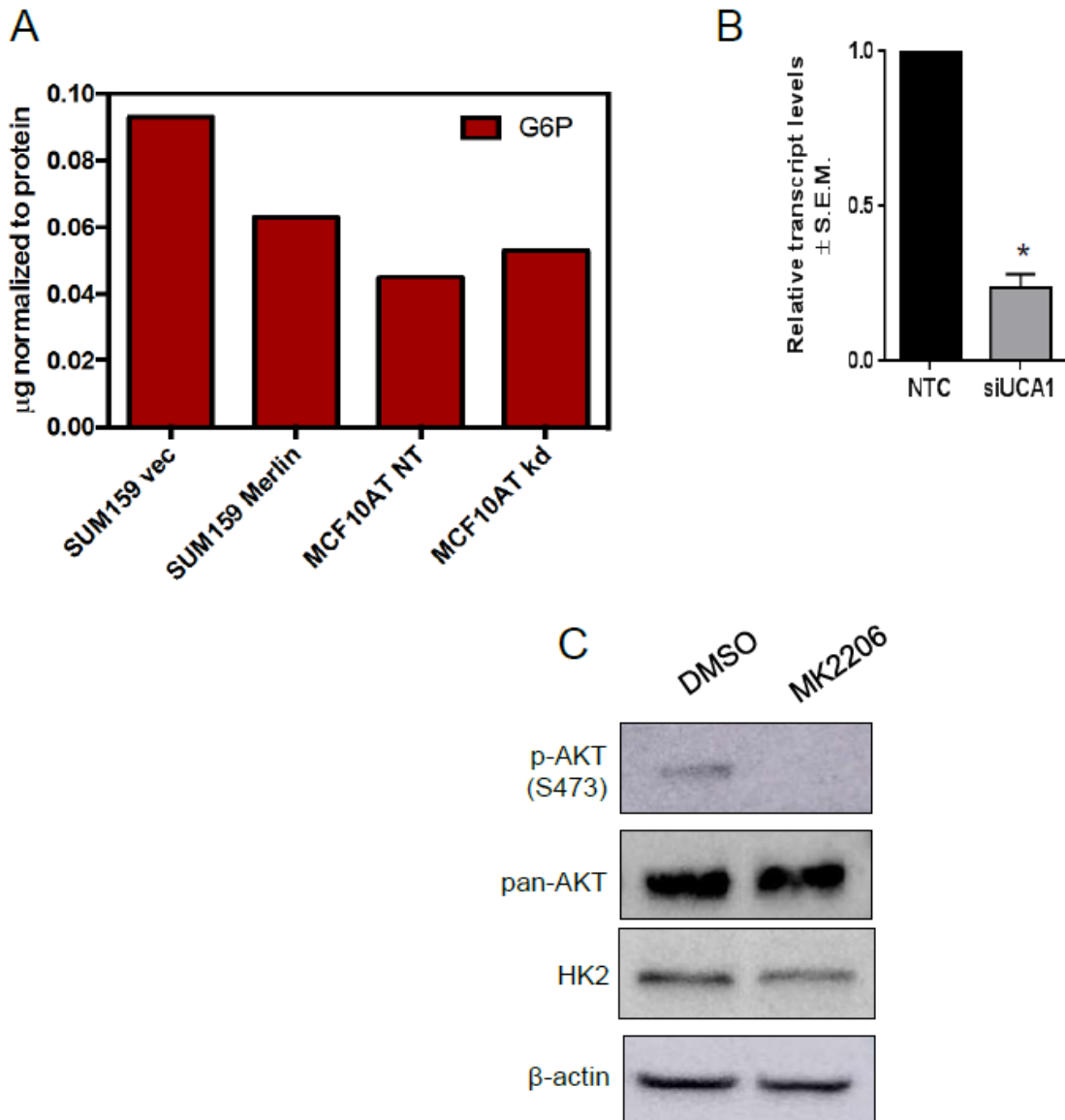
**DEFICIENCY OF TUMOR SUPPRESSOR MERLIN FACILITATES METABOLIC  
ADAPTATION BY CO-OPERATIVE ENGAGEMENT OF SMAD-HIPPO  
SIGNALING IN BREAST CANCER - Supplementary material**

Details	n	Merlin IHC score				n	SMAD7 IHC score			
		Mean	S.D.	S.E.M	p-value (Dunnett's)		Mean	S.D.	S.E.M	p-value (Dunnett's)
<b>Normal breast</b>	45	59.8533	38.4928	5.7382		28	7.15670	0.95948	0.18133	
<b>Grade</b>										
I	34	23.9412	23.9366	4.1051	<0.0001	29	6.08791	1.49800	0.27817	0.0553
II	97	20.3763	23.9497	2.4317	<0.0001	84	5.17070	1.95229	0.21301	<0.0001
III	77	20.5844	21.7855	2.4827	<0.0001	67	4.92308	1.86810	0.22822	<0.0001
<b>Nodal involvement</b>										
N0	87	29.9264	28.0837	3.0109	<0.0001	78	5.28726	1.66358	0.18836	<0.0001
N1	91	16.8549	19.7476	2.0701	<0.0001	75	5.16398	2.04610	0.23626	<0.0001
N2	10	16.8300	17.7738	5.6206	<0.0001	8	3.86480	2.01799	0.71347	<0.0001
<b>Metastasis</b>										
M0	156	24.5026	25.5069	2.0422	<0.0001	128	7.15670	0.95948	0.18133	
M1	71	15.3704	18.0757	2.1452	<0.0001	68	5.37289	1.72479	0.15245	<0.0001
<b>Stage</b>										
0	18	39.6667	31.5510	7.4366	0.0325	17	5.88423	1.67917	0.40726	0.0841
I	43	26.3000	27.0798	4.1296	<.0001	40	5.29567	1.66267	0.26289	0.0002
II	83	23.2157	24.3558	2.6734	0.0000	68	5.43511	1.78033	0.21590	0.0001
III	7	18.3000	15.9132	6.0146	0.0008	5	5.11715	2.23406	0.99910	0.0773
IV	64	14.9094	17.3477	2.1685	0.0000	65	4.88447	2.09569	0.25994	<.0001

**Table 1:** Details of the tissues analyzed with immunohistochemistry scores for Merlin and SMAD7.



**Supplementary figure 1:** (A) The expression of YAP/TAZ/SMAD transcriptional target genes, connective tissue growth factor (CTGF) and cysteine-rich angiogenic inducer 61 (CYR61), are increased in MCF7 and MCF10AT cells silenced for NF2 (MCF7 kd and MCF10AT kd) relative to control cells (MCF7 NT and MCF10AT NT) when analyzed by quantitative RT-PCR (qRT-PCR). (B) MCF7 kd cells were treated with 4 $\mu$ M of TGF- $\beta$  type I receptor inhibitor A8301 or DMSO (vehicle control) for 24h. The transcript levels of UCA1 were attenuated in A8301-treated cells. (C) MCF7 NT and MCF7 kd cells were transfected with a STAT3 Luciferase reporter vector to measure the STAT3 binding activity. The luciferase reporter activity was increased in Merlin-deficient cells.  $\beta$ -actin was used as control gene for the qRT-PCR and relative gene expression was measured by 2- $\Delta\Delta$ Ct method. \* =  $p < 0.05$ .

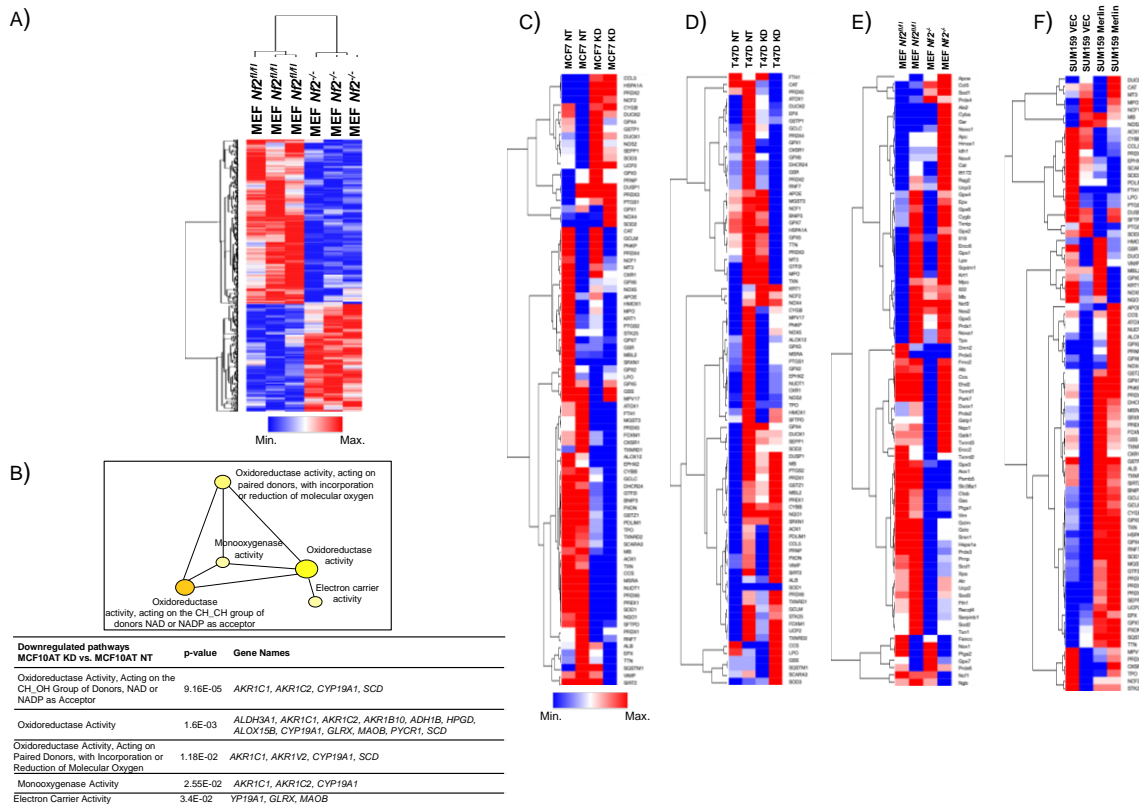


**Supplementary figure 2:** (A) Metabolomics analysis of NF2-restored (Merlin) and control (vec) SUM159 cells and NF2-silenced (kd) and control (NT) MCF10AT cells indicated decreased glucose-6-phosphate (G6P) metabolite upon Merlin restoration and slight increase upon Merlin deficiency. Metabolite concentration was normalized to protein concentration. (B) Quantitative RT-PCR depicting the level of UCA1 achieved in MCF7 cells silenced for Merlin and silenced for UCA1. (C) NF2-silenced MCF7 cells were treated with 1μM of the phosphorylated AKT inhibitor MK2206 or DMSO for 48h and immunoblotting analysis showed a reduction in the HK2 protein levels. β-actin was used as a loading control.



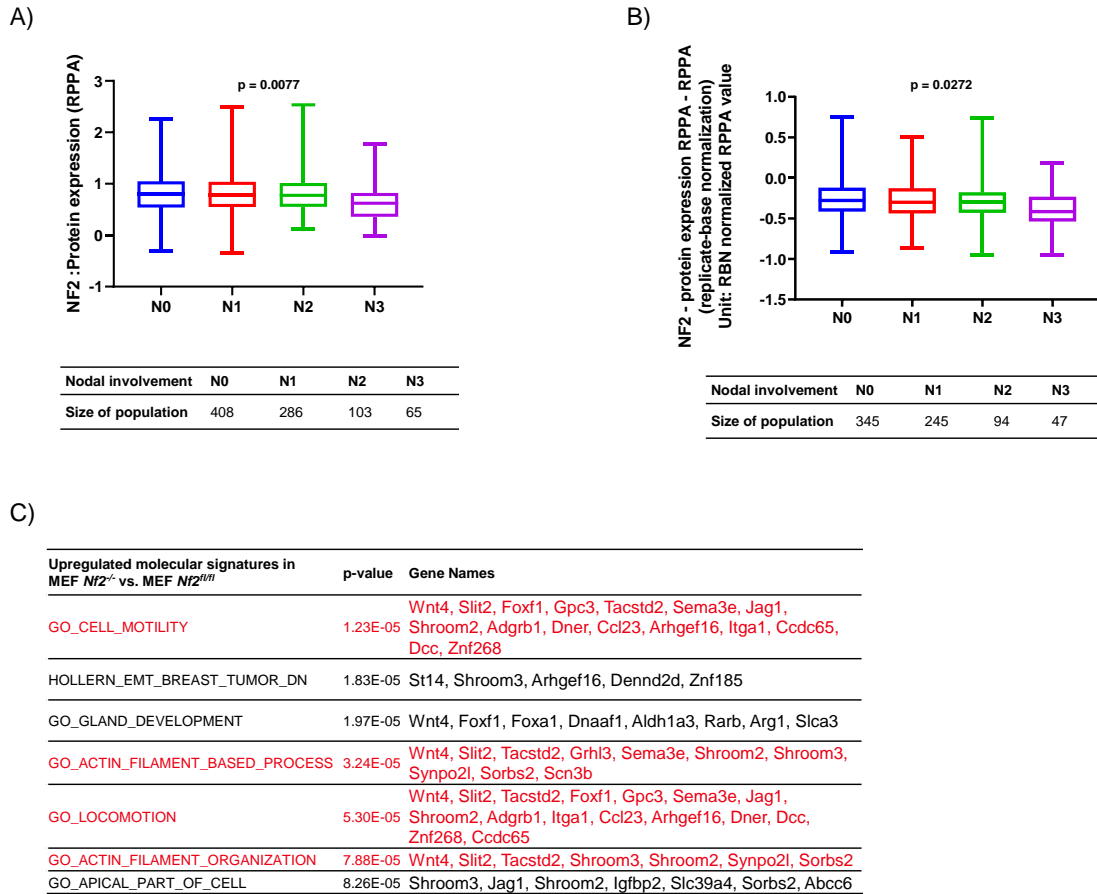
## **APPENDIX B**

### **MERLIN DEFICIENCY ALTERS THE REDOX MANAGEMENT PROGRAM IN BREAST CANCER - Supplementary material**

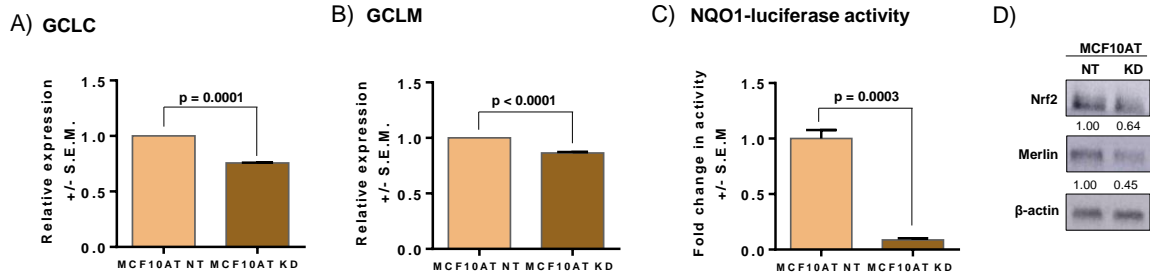


**Supplementary figure 1 : Merlin deficiency modulates a redox signaling signature.**

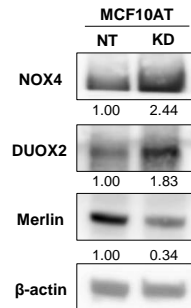
(A) The whole RNA sequencing data of MEF *Nf2<sup>fl/fl</sup>* and MEF *Nf2<sup>-/-</sup>* was plotted as a heatmap ( $n = 3$  for each group). (B) The analysis of RNA sequencing data by the Network Analyst platform detected downregulated redox-associated pathways in *NF2*-silenced MCF10AT (MCF10AT KD) compared to control (MCF10AT NT). Student's *t* test was applied for statistical analysis. Heatmap of the whole gene list assessed by the redox-associated gene expression array ( $n = 2$  for each group) was plotted for (C) MCF7 NT and MCF7 KD, (D) control and *NF2*-silenced T47D (T47D NT and T47D KD, respectively), (E) MEF *Nf2<sup>fl/fl</sup>* x MEF *Nf2<sup>-/-</sup>*, and (F) SUM159 VEC and SUM159 Merlin.



**Supplementary figure 2: ROS clearance attenuates migratory and invasion phenotypes in *NF2*-deficient cells.** (A) The Merlin protein expression of the Invasive Carcinoma TCGA, Firehouse Legacy cohort was significantly decreased ( $p = 0.0077$ ) when analyzed in correlation to the Neoplasm Disease Lymph Node Stage American Joint Committee on Cancer Code; (B) The Merlin protein expression of the TCGA Breast Cancer - BRCA cohort was also significantly decreased ( $p = 0.0272$ ) when analyzed in correlation to the auxiliary lymph node stage (Pathological\_N); (One-way ANOVA technique was applied for statistical analysis for both comparisons); (C) Analysis of the RNA sequencing data by MSigDB database showed significant upregulation of molecular signatures associated with migration and invasion (in red bold) in MEF *Nf2*<sup>-/-</sup> compared to MEF *Nf2*<sup>fl/fl</sup> ( $n = 3$  for each group). Student's *t* test was applied for statistical analysis.

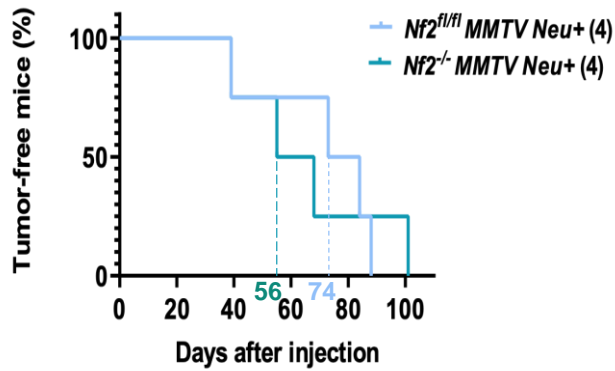


**Supplementary figure 3: Merlin-deficient breast cancer cells display a dysfunctional anti-oxidant system.** Expression levels of *GCLC* and *GCLM* were decreased in MCF10AT KD (A and B, respectively) ( $p = 0.0001$  and  $p < 0.0001$ , respectively) compared to MCF10AT NT. (C) Nrf2 activity ( $p = 0.0003$ ) ( $n = 3$  for each group) and (D) protein levels of Nrf2 were decreased in MCF10AT KD cells compared to MCF10AT NT. Error bars represent  $\pm$  S.E.M. Student's *t* test was applied for statistical analysis.  $\beta$ -actin was used as loading control. Representative immunoblot band densitometry is shown.

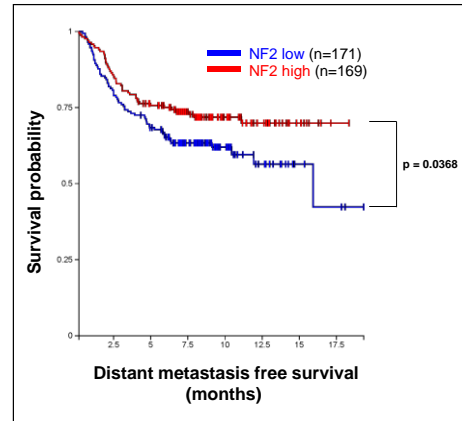


**Supplementary figure 4: Merlin deficiency upregulates proteins from the pro-oxidative NOX family.** Protein expression of NOX4 and DUOX2 was increased in MCF10AT KD compared to MCF10AT NT.  $\beta$ -actin was used as loading control. Representative immunoblot band densitometry is shown.

A)



B)



**Supplementary figure 5: Genetically-engineered oncogene-driven Merlin deficient mammary tumors harbor elevated oxidative stress.** (A) Tumor-free survival curve showing tumor latency. *Nf2<sup>-/-</sup>* MMTV Neu+ group had 50% tumor-free mice at day 56 while the *Nf2<sup>fl/fl</sup>* MMTV Neu+ group hit that mark at day 74 ( $n = 4$  for each group). (B) Microarray data analysis from breast cancer patients showed higher distant metastasis free survival for patients with high Merlin expression compared to low ( $p = 0.0368$ ). Log-rank test was applied for statistical analysis.

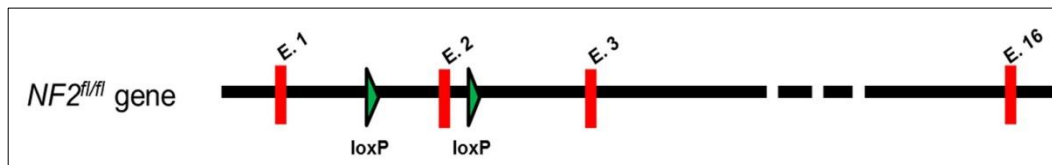
## **APPENDIX C**

Extended animal material and methods

## EXTENDED ANIMAL MATERIAL AND METHODS

### Acquisition of *Nf2* floxed mouse

Mouse strain FVB.129P2-*Nf2*<tm2Gth> (RBRC 02344) (developed by Marco Giovannini and Gilles Thomas - strain of origin: 129P2/OlaHsd-Hprt1<b-m3> via HM-1 ES cell line) was purchased from Riken BioResource Research Center (Japan). These mice carried *Nf2* alleles with phage P1 loxP sites inserted in the intronic region of genomic DNA flanking exon 2 (*Nf2*<sup>fl/fl</sup>):

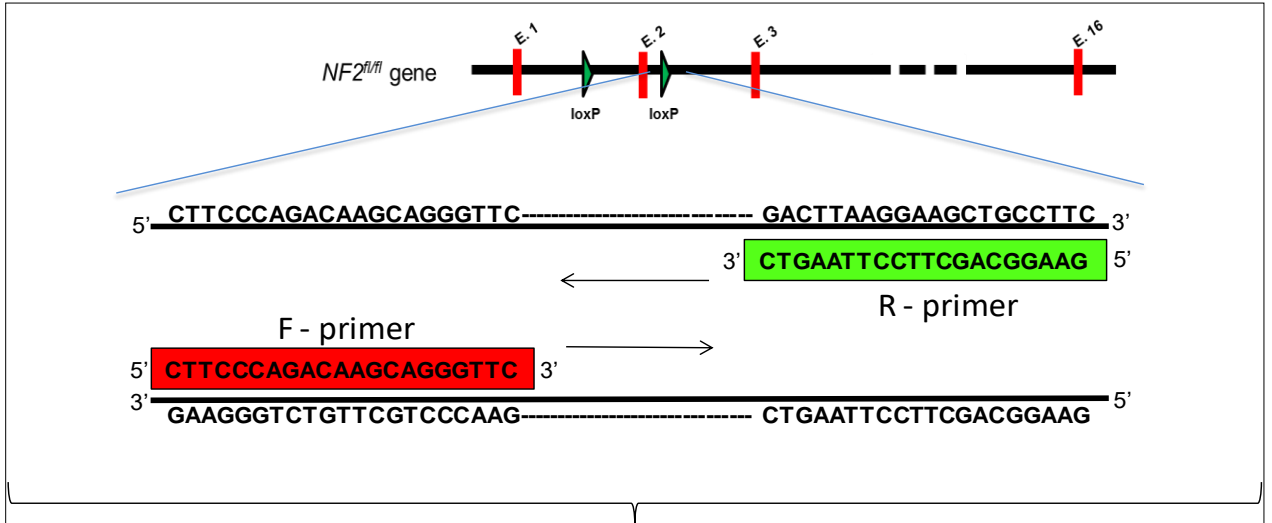


In accordance with the guidelines of the IACUC, these mice were quarantined in the Research Support Building of the University of Alabama at Birmingham (UAB) and then transferred to the animal facility of the Wallace Tumor Institute (WTI) at UAB. To confirm the *Nf2* floxed genotype, tail clips were collected and incubated with 6.25ul of Extraction Solution (Sigma #E7526) and 25ul of Tissue Preparation solution (Sigma #T3073) for 10 minutes at room temperature followed by an additional 3-minute incubation at 95°C. To neutralize DNA-damaging compounds in the extracted genomic DNA, 25ul of Neutralization solution B (Sigma #N3910) was added. Amplification of genomic DNA to detect the loxP sites by PCR was performed using the following pair of primers as previously described by [Giovannini et al., 2000](#):

**Primers:**

**Forward (F)** 5' CTT CCC AGA CAA GCA GGG TTC 3'

**Reverse (R)** 5' GAA GGC AGC TTC CTT AAG TC 3'



**Transcript ID:** ENSMUST00000109910.8 (Ensembl)

>Nf2-205 intron 2:protein\_coding

```
GTTGGGCTAGATCTCAGGGAACCGGTGGGGGAGGCTTGTGCTTTCTGGGTTTGTGGTT
TGTTTGTGGTTTGTGGTTTCCCGAGCAGCAGCACTTAGCTTCACTTATCTTATTTGCTCATTG
TTGAGGTGTCACAGGGACATGGCAAAAAGGGAACAATTTTTTAAATGAAGTCATGTATG
TAGAAAGCAGATCCTATAGTCAGGCATTCTAGCCTCCACAGA CTCCCAGACAAGCAG
GTTCCAGGACATTTCCACTATCTTTGTATACTTCAGAACAAACAACAACAACAACA
ACAACGGTGTACATCTGTGAGAGATTTTCTAGGCCTCATATTCTTTAGAGTTGGTTTTT
GTTTTTTAACTAGCCTTTGAGAACATGAGGATCCAAGTACTTAACCATTGCTAAGGAAT
AAAGAGCTGGCGATGACGGAGGCTTTTCTCCTCCTCAGGGTTCTAAAGCACATGGAATCTAG
GTTTCTAGCAAATTGAAGATTTGAAATGGATAT GACTTAAGGAAGCTGCCTTCTAAGGG
GTTTCATATCCTCACAAAAGACATGCCCATCCATTTTCTGGCCACCTGACACTGAAGAC
AGCTGGAGAACAAAGCCCAAGGACCCTGATTCCCAAAGTTAGTTCACATCTAACGCTGA
CCCTAAATGTTGTTTCCCCTATCAATGTTACCCCTGAAGTTATCTACCGCATAATATGAT
GACCAACAAAAGTCTCTTGTCTTACTAAGTAAGGTATTCAAATTTGTTTACAGCATGTA
```

F-primer binding location on the 3' → 5' strand

R-primer binding location

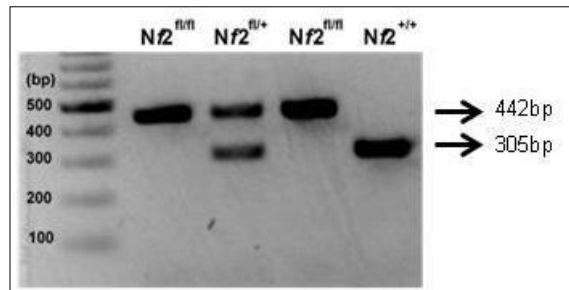
**PCR cycling conditions:**

95°C – 3 minutes  
 95°C – 30 seconds  
 55°C – 30 seconds  
 72°C – 1 minute  
 72°C – 7 minutes

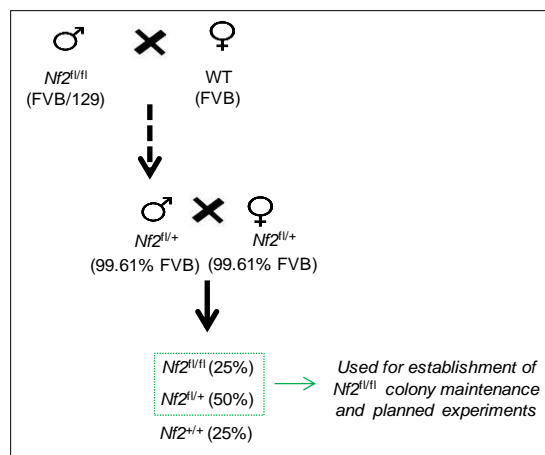
35 cycles



The size of the PCR product of WT *Nf2* allele (*Nf2*<sup>+/+</sup>) is 305 base pair (bp); heterozygous *Nf2* floxed (*Nf2*<sup>fl/+</sup>) produces a 305 bp and 442 bp sized amplicons; and homozygous *Nf2* floxed (*Nf2*<sup>fl/fl</sup>) lends a single 442 bp sized product as shown in the examples below:



The hybrid FVB/129 founder mice were backcrossed to generate offspring of a pure FVB genetic background. The male pups from the backcross breeding between mixed background male *Nf2*<sup>fl/fl</sup> and FVB females (FVB/NJ, stock no: 001800) had their *Nf2*<sup>fl/+</sup> genotype confirmed and tail clip sent to the Jackson Laboratory (Bar Harbor, ME) for FVB background-specific single nucleotide polymorphism (SNP) genome scanning. The males with the highest percentage of FVB genetic background were used for subsequent breeding. 99.61% pure FVB *Nf2*<sup>fl/+</sup> males were crossed with *Nf2*<sup>fl/+</sup> females to generate full FVB *Nf2*<sup>fl/fl</sup> mice:



## **GENERATION OF *Nf2*-KNOCKOUT MOUSE EMBRYONIC FIBROBLAST CELL LINE**

### **1 - Harvesting and isolation of embryos**

Pregnant *Nf2<sup>fl/fl</sup>* females mouse were euthanized, at embryonic day 14, and the uterine horns with embryos were removed. The embryos were individually separated with forceps followed by removal and discard of the yolk sac and head. A superficial opening was cut from the neck to the tail and all the internal organs were removed and discarded. The remaining carcass was kept in DMEM 1X culture media supplemented with 10% heat inactivated FBS, 1% sodium pyruvate, 1% nonessential amino acids, and 1% Penicillin/streptomycin before fibroblast isolation.

### **2 - Isolation of fibroblast**

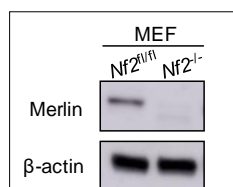
The embryo carcass was washed four times with sterile 1x PBS and all remaining liquid was aspirated off the plate. With a scalpel (#21 blade), the embryos were chopped and 450ul of sterile 1x PBS was added. The tissue was pipetted up and down several times with a P1000 pipette (end of tip cut off) to further dissociation. The embryonic tissue suspension was transferred to a 1.5mL microcentrifuge tube and 110ul of 0.05% trypsin-EDTA was added. The tube was shaken up and down five times and incubated in a water bath (37°C) for 20 minutes with shaking by hand every 2 minutes. After incubation, mouse embryonic cells were passed in a 3mL syringe (18 gauge needle) three times, placed into a T25 flask with media, and incubated in 9% CO<sub>2</sub> incubator for 24h. After 24h of incubation, old media was replaced by fresh media with the attached cells being the *Nf2<sup>fl/fl</sup>* mouse embryonic fibroblasts (MEFs). The *Nf2<sup>fl/fl</sup>* MEFs were passaged as the culture reached confluence.

### 3 - Immortalization of MEF

Primary *Nf2<sup>fl/fl</sup>* MEFs were transduced with SV40 large T antigen Purified Lentifect Lentiviral Particles (GeneCopoeia, Rockville, MD) at multiplicity of infection (MOI) = 10. After 16h of transduction, lentiviral particle-containing media was replaced with fresh media. Immortalization was confirmed by culturing *Nf2<sup>fl/fl</sup>* MEFs with puromycin (resistance marker)-containing media and multiple cell passaging.

### 4 - Knockout of *Nf2* gene

Immortalized *Nf2<sup>fl/fl</sup>* MEFs were transduced with CMV-Cre GFP lentivirus (puro) (Cellomics Technology, Halethorpe, MD) at MOI =10 to excise *Nf2* by Cre-loxP recombination, generating MEF *Nf2<sup>-/-</sup>*. A separate group of *Nf2<sup>fl/fl</sup>* MEFs was transduced with vector-control CMV-GFP lentivirus (Cellomics Technology), generating control MEF *Nf2<sup>fl/fl</sup>*. Both cell lines were then sorted based on GFP expression by flow cytometry. The high-GFP population was selected and validated for Merlin expression by immunoblotting with an antibody against Merlin (Cell signaling #6995) before use in planned experiments:

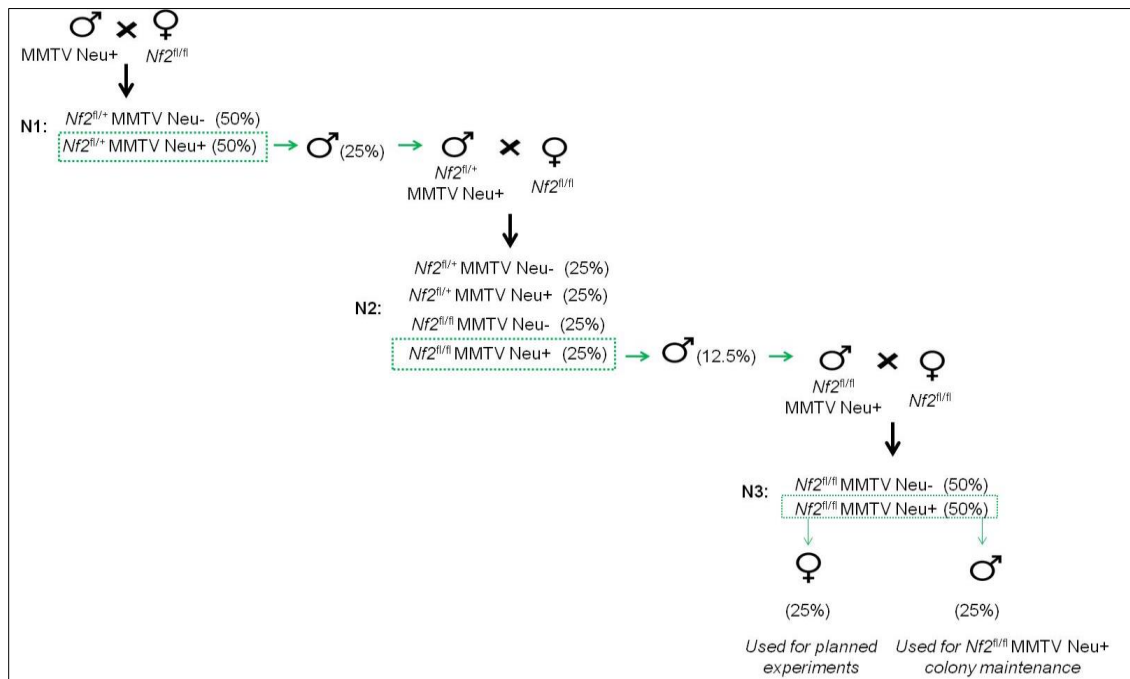


## GENERATION OF MAMMARY-SPECIFIC *Nf2* KNOCKOUT BREAST CANCER MOUSE MODEL

The transgenic mouse mammary tumor virus (MMTV) Neu mouse expresses inactivated Neu (the murine version of *ErbB2*) under the transcriptional regulation of the MMTV promoter. In order to simulate the impact of *NF2* deficiency in breast cancer, a mammary-specific *Nf2* MMTV Neu+ mouse model was generated according to the following steps:

### 1 - Breeding strategy to generate *Nf2<sup>fl/fl</sup>* MMTV Neu+

*Nf2<sup>fl/fl</sup>* mice and MMTV Neu (FVB/N-Tg(MMTVneu)202Mul/J, stock no: 002376) mice, purchased from Jackson Laboratory, were maintained and crossed to generate *Nf2<sup>fl/fl</sup>* MMTV Neu+ mice in the Animal Facility of WTI at UAB according to the following breeding scheme:



## 2 - Induction of mammary-specific *Nf2* knockout

In order to silence *NF2* in the mammary gland of *Nf2<sup>fl/fl</sup>* MMTV Neu+ female mice, CMV-Cre GFP lentivirus (Cellomics Technology) was intraductally injected in the 4<sup>th</sup> inguinal mammary glands based on the technique of [Krause et al., 2013](#). The nipples of non-parous mice are very narrow and embedded in the mammary fat pad. Thus, in order to have a wider and protruded nipple structure, 6-week old mice went through one round of pregnancy, nursed the pups for 7 days only, and after additional 7 days of post-early weaning, intraductal injection was performed.

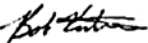
Prior to intraductal injection, stereoscope, light source and oxygen/isoflurane flow were set up in the animal procedure room of WTI. To better expose the nipples on the mouse, hair was removed from the 4<sup>th</sup> inguinal mammary glands by applying hair removal lotion; remaining lotion was removed with wet paper towel. Mouse was anesthetized in a sealable container with constant oxygen/isoflurane flow for a few minutes. When completely anesthetized, mouse was placed on the illuminated stereoscope making sure the snout was fully positioned into the oxygen/isoflurane flow tube. For injection of each gland, 21ul of lentiviral particles ( $3.6 \times 10^7$  TU) with 0.2% Evans blue dye solution was loaded into a 50 $\mu$ l syringe with a 33 G metal hub needle affixed. Then, after removing the keratin plug, the nipple was held vertically with forceps and injected. (Note: 1ul can leak out of the nipple upon pulling out the needle thus 21ul was injected; the blue color of the dye solution enables the visualization of the injection into the ductal tree).

## **APPENDIX D**

Institutional Animal Care and Use Committee (IACUC) notice of approval



MEMORANDUM

DATE: 01-Nov-2017  
TO: Samant, Lalita R  
FROM:   
Robert A. Kesterson, Ph.D., Chair  
Institutional Animal Care and Use Committee (IACUC)  
SUBJECT: NOTICE OF APPROVAL

The following application was approved by the University of Alabama at Birmingham Institutional Animal Care and Use Committee (IACUC) on 01-Nov-2017.

Protocol PI: Samant, Lalita R  
Title: Molecular Determinants of Breast Cancer Malignancy  
Sponsor: UAB DEPARTMENT  
Animal Project Number (APN): IACUC-09719

This institution has an Animal Welfare Assurance on file with the Office of Laboratory Animal Welfare (OLAW), is registered as a Research Facility with the USDA, and is accredited by the Association for Assessment and Accreditation of Laboratory Animal Care International (AAALAC).

This protocol is due for full review by 31-Oct-2020.

Institutional Animal Care and Use Committee (IACUC) | Mailing Address:  
CH19 Suite 403 | CH19 Suite 403  
933 19th Street South | 1530 3rd Ave S  
(205) 934-7692 | Birmingham, AL 35294-0019  
Fax (205) 934-1188 |

## **APPENDIX E**

Reprints approval forms



**DEFICIENCY OF TUMOR SUPPRESSOR MERLIN FACILITATES  
METABOLIC ADAPTATION BY CO-OPERATIVE ENGAGEMENT OF SMAD-  
HIPPO SIGNALING IN BREAST CANCER**

**OXFORD UNIVERSITY PRESS LICENSE  
TERMS AND CONDITIONS**

Oct 16, 2020

---

---

This Agreement between Mateus Mota ("You") and Oxford University Press ("Oxford University Press") consists of your license details and the terms and conditions provided by Oxford University Press and Copyright Clearance Center.

License Number

4926250936507

License date

Oct 11, 2020

Licensed Content Publisher

Oxford University Press

Licensed Content Publication

Carcinogenesis

Licensed Content Title

Deficiency of tumor suppressor Merlin facilitates metabolic adaptation by co-operative engagement of SMAD-Hippo signaling in breast cancer

Licensed Content Author

Mota, Mateus S V; Jackson, William P

Licensed Content Date

Jun 9, 2018

Type of Use

Thesis/Dissertation

Institution name

Title of your work

Deficiency of tumor suppressor Merlin facilitates metabolic adaptation by co-operative engagement of SMAD-Hippo signaling in breast cancer

Publisher of your work

University of Alabama at Birmingham

Expected publication date

Nov 2020

Permissions cost

0.00 USD

Value added tax

0.00 USD

**Total**

**0.00 USD**

Title

Deficiency of tumor suppressor Merlin facilitates metabolic adaptation by co-operative engagement of SMAD-Hippo signaling in breast cancer

Institution name

University of Alabama at Birmingham

Expected presentation date

Nov 2020

Order reference number

10.1093/carcin/bgy078

Portions

All the article contents.

Requestor Location

Mateus Mota  
2133 16th Ave. S. apt W

BIRMINGHAM, AL 35205  
United States  
Attn: Mateus Mota

Publisher Tax ID

GB125506730

Total

**0.00 USD**

Terms and Conditions

**STANDARD TERMS AND CONDITIONS FOR REPRODUCTION OF MATERIAL FROM AN OXFORD  
UNIVERSITY PRESS JOURNAL**

1. Use of the material is restricted to the type of use specified in your order details.
2. This permission covers the use of the material in the English language in the following territory: world. If you have requested additional permission to translate this material, the terms and conditions of this reuse will be set out in clause 12.
3. This permission is limited to the particular use authorized in (1) above and does not allow you to sanction its use elsewhere in any other format other than specified above, nor does it apply to quotations, images, artistic works etc that have been reproduced from other sources which may be part of the material to be used.
4. No alteration, omission or addition is made to the material without our written consent. Permission must be re-cleared with Oxford University Press if/when you decide to reprint.
5. The following credit line appears wherever the material is used: author, title, journal, year, volume, issue number, pagination, by permission of Oxford University Press or the sponsoring society if the journal is a society journal. Where a journal is being published on behalf of a learned society, the details of that society must be included in the credit line.
6. For the reproduction of a full article from an Oxford University Press journal for whatever purpose, the corresponding author of the material concerned should be informed of the proposed use. Contact details for the corresponding authors of all Oxford University Press journal contact can be found alongside either the abstract or full text of the article concerned, accessible from [www.oxfordjournals.org](http://www.oxfordjournals.org) Should there be a problem clearing these rights, please contact [journals.permissions@oup.com](mailto:journals.permissions@oup.com)

7. If the credit line or acknowledgement in our publication indicates that any of the figures, images or photos was reproduced, drawn or modified from an earlier source it will be necessary for you to clear this permission with the original publisher as well. If this permission has not been obtained, please note that this material cannot be included in your publication/photocopies.

8. While you may exercise the rights licensed immediately upon issuance of the license at the end of the licensing process for the transaction, provided that you have disclosed complete and accurate details of your proposed use, no license is finally effective unless and until full payment is received from you (either by Oxford University Press or by Copyright Clearance Center (CCC)) as provided in CCC's Billing and Payment terms and conditions. If full payment is not received on a timely basis, then any license preliminarily granted shall be deemed automatically revoked and shall be void as if never granted. Further, in the event that you breach any of these terms and conditions or any of CCC's Billing and Payment terms and conditions, the license is automatically revoked and shall be void as if never granted. Use of materials as described in a revoked license, as well as any use of the materials beyond the scope of an unrevoked license, may constitute copyright infringement and Oxford University Press reserves the right to take any and all action to protect its copyright in the materials.

9. This license is personal to you and may not be sublicensed, assigned or transferred by you to any other person without Oxford University Press's written permission.

10. Oxford University Press reserves all rights not specifically granted in the combination of (i) the license details provided by you and accepted in the course of this licensing transaction, (ii) these terms and conditions and (iii) CCC's Billing and Payment terms and conditions.

11. You hereby indemnify and agree to hold harmless Oxford University Press and CCC, and their respective officers, directors, employees and agents, from and against any and all claims arising out of your use of the licensed material other than as specifically authorized pursuant to this license.

12. Other Terms and Conditions:

v1.4

Questions? [customercare@copyright.com](mailto:customercare@copyright.com) or +1-855-239-3415 (toll free in the US) or +1-978-646-2777.

---

---

## **MERLIN REGULATES SIGNALING EVENTS AT THE NEXUS OF DEVELOPMENT AND CANCER**

© The Author(s). 2020 Open Access This article is licensed under a Creative Commons Attribution 4.0 International License, which permits use, sharing, adaptation, distribution and reproduction in any medium or format, as long as you give appropriate credit to the original author(s) and the source, provide a link to the Creative Commons licence, and indicate if changes were made. The images or other third party material in this article are included in the article's Creative Commons licence, unless indicated otherwise in a credit line to the material. If material is not included in the article's Creative Commons licence and your intended use is not permitted by statutory regulation or exceeds the permitted use, you will need to obtain permission directly from the copyright holder. To view a copy of this licence, visit <http://creativecommons.org/licenses/by/4.0/>. The Creative Commons Public Domain Dedication waiver (<http://creativecommons.org/publicdomain/zero/1.0/>) applies to the data made available in this article, unless otherwise stated in a credit line to the data.

## Creative Commons Legal Code

---

### Attribution 4.0 International

Official translations of this license are available [in other languages](#).

Creative Commons Corporation ("Creative Commons") is not a law firm and does not provide legal services or legal advice. Distribution of Creative Commons public licenses does not create a lawyer-client or other relationship. Creative Commons makes its licenses and related information available on an "as-is" basis. Creative Commons gives no warranties regarding its licenses, any material licensed under their terms and conditions, or any related information. Creative Commons disclaims all liability for damages resulting from their use to the fullest extent possible.

#### **Using Creative Commons Public Licenses**

Creative Commons public licenses provide a standard set of terms and conditions that creators and other rights holders may use to share original works of authorship and other material subject to copyright and certain other rights specified in the public license below. The following considerations are for informational purposes only, are not exhaustive, and do not form part of our licenses.

**Considerations for licensors:** Our public licenses are intended for use by those authorized to give the public permission to use material in ways otherwise restricted by copyright and certain other rights. Our licenses are irrevocable. Licensors should read and understand the terms and conditions of the license they choose before applying it. Licensors should also secure all rights necessary before applying our licenses so that the public can reuse the material as expected. Licensors should clearly mark any material not subject to the license. This includes other CC-licensed material, or material used under an exception or limitation to copyright.

**Considerations for the public:** By using one of our public licenses, a licensor grants the public permission to use the licensed material under specified terms and conditions. If the licensor's permission is not necessary for any reason—for example, because of any applicable exception or limitation to copyright—then that use is not regulated by the license. Our licenses grant only permissions under copyright and certain other rights that a licensor has authority to grant. Use of the licensed material may still be restricted for other reasons, including because others have copyright or other rights in the material. A licensor may make special requests, such as asking that all changes be marked or described. Although not required by our licenses, you are encouraged to respect those requests where reasonable.

### Creative Commons Attribution 4.0 International Public License

By exercising the Licensed Rights (defined below), You accept and agree to be bound by the terms and conditions of this Creative Commons Attribution 4.0 International Public License ("Public License"). To the extent this Public License may be interpreted as a contract, You are granted the Licensed Rights in consideration of Your acceptance of these terms and conditions, and the Licensor grants You such rights in consideration of benefits the Licensor receives from making the Licensed Material available under these terms and conditions.

#### Section 1 – Definitions.

- a. **Adapted Material** means material subject to Copyright and Similar Rights that is derived from or based upon the Licensed Material and in which the Licensed Material is translated, altered, arranged, transformed, or otherwise modified in a manner requiring permission under the Copyright and Similar Rights held by the Licensor. For purposes of this Public License, where the Licensed Material is a musical work, performance, or sound recording, Adapted Material is always produced where the Licensed Material is synched in timed relation with a moving image.
- b. **Adapter's License** means the license You apply to Your Copyright and Similar Rights in Your contributions to Adapted Material in accordance with the terms and conditions of this Public License.
- c. **Copyright and Similar Rights** means copyright and/or similar rights closely related to copyright including, without limitation, performance, broadcast, sound recording, and Sui Generis Database Rights, without regard to how the rights are labeled or categorized. For purposes of this Public License, the rights specified in Section 2(b)(1)-(2) are not Copyright and Similar Rights.
- d. **Effective Technological Measures** means those measures that, in the absence of proper authority, may not be circumvented under laws fulfilling obligations under Article 11 of the WIPO Copyright Treaty adopted on December 20, 1996, and/or similar international agreements.
- e. **Exceptions and Limitations** means fair use, fair dealing, and/or any other exception or limitation to Copyright and Similar Rights that applies to Your use of the Licensed Material.
- f. **Licensed Material** means the artistic or literary work, database, or other material to which the Licensor applied this Public License.
- g. **Licensed Rights** means the rights granted to You subject to the terms and conditions of this Public License, which are limited to all Copyright and Similar Rights that apply to Your use of the Licensed Material and that the Licensor has authority to license.
- h. **Licensor** means the individual(s) or entity(ies) granting rights under this Public License.
- i. **Share** means to provide material to the public by any means or process that requires permission under the Licensed Rights, such as reproduction, public display, public performance, distribution, dissemination, communication, or importation, and to make material available to the public including in ways that members of the public may access the material from a place and at a time individually chosen by them.
- j. **Sui Generis Database Rights** means rights other than copyright resulting from Directive 96/9/EC of the European Parliament and of the Council of 11 March 1996 on the legal protection of databases, as

amended and/or succeeded, as well as other essentially equivalent rights anywhere in the world.

- k. **You** means the individual or entity exercising the Licensed Rights under this Public License. **Your** has a corresponding meaning.

## Section 2 – Scope.

### a. License grant.

1. Subject to the terms and conditions of this Public License, the Licensor hereby grants You a worldwide, royalty-free, non-sublicensable, non-exclusive, irrevocable license to exercise the Licensed Rights in the Licensed Material to:
  - A. reproduce and Share the Licensed Material, in whole or in part; and
  - B. produce, reproduce, and Share Adapted Material.
2. Exceptions and Limitations. For the avoidance of doubt, where Exceptions and Limitations apply to Your use, this Public License does not apply, and You do not need to comply with its terms and conditions.
3. Term. The term of this Public License is specified in Section 6(a).
4. Media and formats: technical modifications allowed. The Licensor authorizes You to exercise the Licensed Rights in all media and formats whether now known or hereafter created, and to make technical modifications necessary to do so. The Licensor waives and/or agrees not to assert any right or authority to forbid You from making technical modifications necessary to exercise the Licensed Rights, including technical modifications necessary to circumvent Effective Technological Measures. For purposes of this Public License, simply making modifications authorized by this Section 2(a)(4) never produces Adapted Material.
5. Downstream recipients.
  - A. Offer from the Licensor – Licensed Material. Every recipient of the Licensed Material automatically receives an offer from the Licensor to exercise the Licensed Rights under the terms and conditions of this Public License.
  - B. No downstream restrictions. You may not offer or impose any additional or different terms or conditions on, or apply any Effective Technological Measures to, the Licensed Material if doing so restricts exercise of the Licensed Rights by any recipient of the Licensed Material.
6. No endorsement. Nothing in this Public License constitutes or may be construed as permission to assert or imply that You are, or that Your use of the Licensed Material is, connected with, or sponsored, endorsed, or granted official status by, the Licensor or others designated to receive attribution as provided in Section 3(a)(1)(A)(i).

### b. Other rights.

1. Moral rights, such as the right of integrity, are not licensed under this Public License, nor are publicity, privacy, and/or other similar personality rights; however, to the extent possible, the Licensor



waives and/or agrees not to assert any such rights held by the Licensor to the limited extent necessary to allow You to exercise the Licensed Rights, but not otherwise.

2. Patent and trademark rights are not licensed under this Public License.
3. To the extent possible, the Licensor waives any right to collect royalties from You for the exercise of the Licensed Rights, whether directly or through a collecting society under any voluntary or waivable statutory or compulsory licensing scheme. In all other cases the Licensor expressly reserves any right to collect such royalties.

### Section 3 – License Conditions.

Your exercise of the Licensed Rights is expressly made subject to the following conditions.

#### a. Attribution.

1. If You Share the Licensed Material (including in modified form), You must:
  - A. retain the following if it is supplied by the Licensor with the Licensed Material:
    - i. identification of the creator(s) of the Licensed Material and any others designated to receive attribution, in any reasonable manner requested by the Licensor (including by pseudonym if designated);
    - ii. a copyright notice;
    - iii. a notice that refers to this Public License;
    - iv. a notice that refers to the disclaimer of warranties;
    - v. a URI or hyperlink to the Licensed Material to the extent reasonably practicable;
  - B. indicate if You modified the Licensed Material and retain an indication of any previous modifications; and
  - C. indicate the Licensed Material is licensed under this Public License, and include the text of, or the URI or hyperlink to, this Public License.
2. You may satisfy the conditions in Section 3(a)(1) in any reasonable manner based on the medium, means, and context in which You Share the Licensed Material. For example, it may be reasonable to satisfy the conditions by providing a URI or hyperlink to a resource that includes the required information.
3. If requested by the Licensor, You must remove any of the information required by Section 3(a)(1)(A) to the extent reasonably practicable.
4. If You Share Adapted Material You produce, the Adapter's License You apply must not prevent recipients of the Adapted Material from complying with this Public License.

### Section 4 – Sui Generis Database Rights.

Where the Licensed Rights include Sui Generis Database Rights that apply to Your use of the Licensed Material:

- a. for the avoidance of doubt, Section 2(a)(1) grants You the right to extract, reuse, reproduce, and Share all or a substantial portion of the contents of the database;
- b. if You include all or a substantial portion of the database contents in a database in which You have Sui Generis Database Rights, then the database in which You have Sui Generis Database Rights (but not its individual contents) is Adapted Material; and
- c. You must comply with the conditions in Section 3(a) if You Share all or a substantial portion of the contents of the database.

For the avoidance of doubt, this Section 4 supplements and does not replace Your obligations under this Public License where the Licensed Rights include other Copyright and Similar Rights.

#### Section 5 – Disclaimer of Warranties and Limitation of Liability.

- a. Unless otherwise separately undertaken by the Licensor, to the extent possible, the Licensor offers the Licensed Material as-is and as-available, and makes no representations or warranties of any kind concerning the Licensed Material, whether express, implied, statutory, or other. This includes, without limitation, warranties of title, merchantability, fitness for a particular purpose, non-infringement, absence of latent or other defects, accuracy, or the presence or absence of errors, whether or not known or discoverable. Where disclaimers of warranties are not allowed in full or in part, this disclaimer may not apply to You.
- b. To the extent possible, in no event will the Licensor be liable to You on any legal theory (including, without limitation, negligence) or otherwise for any direct, special, indirect, incidental, consequential, punitive, exemplary, or other losses, costs, expenses, or damages arising out of this Public License or use of the Licensed Material, even if the Licensor has been advised of the possibility of such losses, costs, expenses, or damages. Where a limitation of liability is not allowed in full or in part, this limitation may not apply to You.
- c. The disclaimer of warranties and limitation of liability provided above shall be interpreted in a manner that, to the extent possible, most closely approximates an absolute disclaimer and waiver of all liability.

#### Section 6 – Term and Termination.

- a. This Public License applies for the term of the Copyright and Similar Rights licensed here. However, if You fail to comply with this Public License, then Your rights under this Public License terminate automatically.
- b. Where Your right to use the Licensed Material has terminated under Section 6(a), it reinstates:

1. automatically as of the date the violation is cured, provided it is cured within 30 days of Your discovery of the violation; or
2. upon express reinstatement by the Licensor.

For the avoidance of doubt, this Section 8(b) does not affect any right the Licensor may have to seek remedies for Your violations of this Public License.

- c. For the avoidance of doubt, the Licensor may also offer the Licensed Material under separate terms or conditions or stop distributing the Licensed Material at any time; however, doing so will not terminate this Public License.
- d. Sections 1, 5, 6, 7, and 8 survive termination of this Public License.

#### **Section 7 – Other Terms and Conditions.**

- a. The Licensor shall not be bound by any additional or different terms or conditions communicated by You unless expressly agreed.
- b. Any arrangements, understandings, or agreements regarding the Licensed Material not stated herein are separate from and independent of the terms and conditions of this Public License.

#### **Section 8 – Interpretation.**

- a. For the avoidance of doubt, this Public License does not, and shall not be interpreted to, reduce, limit, restrict, or impose conditions on any use of the Licensed Material that could lawfully be made without permission under this Public License.
- b. To the extent possible, if any provision of this Public License is deemed unenforceable, it shall be automatically reformed to the minimum extent necessary to make it enforceable. If the provision cannot be reformed, it shall be severed from this Public License without affecting the enforceability of the remaining terms and conditions.
- c. No term or condition of this Public License will be waived and no failure to comply consented to unless expressly agreed to by the Licensor.
- d. Nothing in this Public License constitutes or may be interpreted as a limitation upon, or waiver of, any privileges and immunities that apply to the Licensor or You, including from the legal processes of any jurisdiction or authority.

Creative Commons is not a party to its public licenses. Notwithstanding, Creative Commons may elect to apply one of its public licenses to material it publishes and in those instances will be considered the "Licensor." The text of the Creative Commons public licenses is dedicated to the public domain under the [CC0 Public Domain Dedication](#). Except for the limited purpose of indicating that material is shared under a Creative Commons public license or as otherwise permitted by the Creative Commons policies published at [creativecommons.org/policies](https://creativecommons.org/policies), Creative Commons does not authorize the use of the trademark "Creative Commons" or any other trademark or logo of Creative Commons without its prior written consent including, without limitation, in connection with any unauthorized modifications to any of its public licenses or any other

arrangements, understandings, or agreements concerning use of licensed material. For the avoidance of doubt, this paragraph does not form part of the public licenses.

Creative Commons may be contacted at [creativecommons.org](https://creativecommons.org).

Additional languages available: العربية, čeština, Deutsch, Ελληνικά, Español, euskara, suomeksi, français, hrvatski, Bahasa Indonesia, italiano, 日本語, 한국어, Lietuvių, latviski, te reo Māori, Nederlands, norsk, polski, português, română, русский, Slovenščina, svenska, Türkçe, українська, 中文, 華語. Please read the [FAQ](#) for more information about official translations.